



UNIVERSITÀ DEGLI STUDI DI PADOVA

Sede amministrativa: Università degli Studi di Padova

Dipartimento Territorio e Sistemi Agro-Forestali

DOTTORATO DI RICERCA IN "IDRONOMIA AMBIENTALE"

XX CICLO

**SOIL MOISTURE DISTRIBUTION AND RUNOFF RESPONSE
AT THE HILLSLOPE SCALE: EXPERIMENTAL ANALYSIS
IN AN ALPINE ENVIRONMENT**

Coordinatore: Ch.mo prof. MARIO ARISTIDE LENZI

Supervisore: Ch.mo prof. GIANCARLO DALLA FONTANA

Co-supervisore: Ch.mo prof. MARCO BORGA

Dottorando: DANIELE PENNA

31 Gennaio 2008

ABSTRACT

This work focuses on the analysis of hydrological data collected at the hillslope scale during three summer field campaigns carried out in a small mountain catchment (1.9 km²) in the Dolomites (central-eastern Italian Alps). The thesis is partitioned in three main sections regarding i) the analysis of spatial distribution of water content over three soil depths, ii) the assessment of its temporal stability, iii) the study of runoff and water table variations.

Soil moisture is one of the most important hydrological variables: it has a critical influences on several processes at different spatial scales, plays an important role in hydrological modelling and flood forecasting and represents one of the main factors in infiltration of water, surface and subsurface runoff generation. Soil moisture data were collected during summers season in 2005, 2006 and 2007 at 0-6, 0-12 and 0-20 cm depth over three hillslopes with steep relief and shallow soil depth. Volumetric water content values were collected at several points over the three hillslopes by means of an impedance and a TDR probe. Soil moisture data were used to analyse the statistical moments and their interrelationships, the relationships between data collected at various soil depths, and time stability. Results showed that the surface layer was usually wetter than deeper soil layers, particularly during dry-down. This was attributed to the effect of dew, which was observed in the field and might have contributed to the increase in the surface soil moisture. For all depths and over the three hillslopes, the spatial variability patterns were well represented by negative exponential functions between the mean and the coefficient of variation of soil moisture. Vertical water content variability was mainly attributed to the increase of soil properties heterogeneity with depth. The degree of correlation between the data collected at the three depths was relatively high, as also confirmed by the visual comparison of interpolated water content maps.

Temporal stability of soil moisture patterns was investigated applying a multiple approach: i) ranking stability analysis; ii) slope-intercept analysis of linear regression; iii) autocorrelation analysis; (iv) evolution of correlation against mean soil moisture over time and relationship with piezometric increase. Results show that spatial patterns of sampling points were reasonably well preserved at the three depths. The highest degree of temporal stability was

associated to wet conditions and the decline of correlation occurred at times of transition from a dry to a wetter state; such behaviour is more evident for the surface layers, more quickly affected by precipitation inputs. Less correlated patterns were found in 2006 owing to a different distribution of precipitation: this observation was confirmed by less sloping correlograms in 2005 and 2007. Temporal stability of surface measurements could be considered as good indicator of subsurface time stability; identification of these temporally stable sites within the experimental basin will assist to provide data sets for watershed hydrologic modelling of subsurface soil water content.

Overland flow is recognized as an important contributor to the total stream discharge and to the determination of the size and the shape of flood peaks; nevertheless, it has hardly ever been observed through direct measurements. In this study, occurrence of overland flow was measured by special detectors installed over a small subcatchment (3.3 ha) of the main basin and stream discharge, soil moisture at 0-30 cm depth (by means of a water content reflectometer) and groundwater variations were monitored continuously. Generation of overland flow was identified in mechanisms of saturation from above and in return flows of water along preferential flow paths. At the rainfall scale, a clear interconnection among several hydrological variables was found, suggesting a strong consistency between subsurface and surface runoff, which respond with similar spatial and temporal dynamics to precipitation inputs both at the rainstorm scale and over a longer period. Water table was found to be highly correlated with stream discharge independently of the topographical localization of piezometric wells across the site. The steady state assumption for the whole hillslope was tested by applying a reformulation of Topmodel at the single rainfall scale. The linear model proved to be a fine predictor of the groundwater level with small overall errors although often the maximum rise of water table was underestimated, especially for significant variations. These deviations were attributed to the hysteresis effect of the relationship between discharge and groundwater, whose non linear behaviour prevented the linear model from accurate predictions of groundwater levels during noticeable fluctuations.

Il presente lavoro è basato sull'analisi di dati idro-meteorologici raccolti sul campo a scala di versante in un piccolo bacino (1.9km²) delle Dolomiti venete. La tesi è suddivisa in tre parti principali che riguardano i) l'analisi della distribuzione spaziale dell'umidità del suolo a tre profondità, ii) la valutazione della sua stabilità temporale, iii) lo studio dei processi di generazione di deflusso e delle variazioni del livello di falda idrica.

L'umidità del suolo è una delle più importanti variabili idrologiche a diverse scale spaziali: ha una diretta influenza su numerosi processi quali piene, fenomeni erosivi, mobilitazione di sedimenti e innesco di frane, ricopre un ruolo fondamentale nella modellistica idrologica ai fini previsionali di piena e rappresenta uno dei principali fattori nelle dinamiche di infiltrazione dell'acqua e nella generazione di deflusso superficiale e sottosuperficiale. Durante il programma di dottorato, nelle estati del 2005, 2006 e 2007 sono state svolte tre campagne di misura che hanno permesso il prelievo di misure di umidità del terreno alla profondità di 0-6, 0-12 e 0-20 cm su tre versanti sperimentali caratterizzati da pendenze elevate e bassa profondità del suolo. I valori volumetrici di contenuto idrico sono stati raccolti su numerosi punti dislocati sui tre versanti di studio tramite l'utilizzo di sonde ad impedenza e TDR. I dati raccolti sono stati utilizzati per analizzare i momenti statistici dell'umidità del suolo e le loro interrelazioni, la relazione tra valori di contenuto idrico a diversa profondità e la stabilità temporale dei campi di umidità. I risultati ottenuti evidenziano come gli strati superficiali su tutti e tre i versanti siano caratterizzati da valori più elevati di umidità rispetto agli strati più profondi. Alti valori di contenuto idrico a livello superficiale permangono anche durante i periodi asciutti e questo comportamento è stato attribuito all'influenza della rugiada, osservata spesso sul campo, che potrebbe aver contribuito significativamente all'aumento di umidità dello strato superficiale del terreno. Per tutte le profondità ed i versanti analizzati, i campi di variabilità spaziale sono ben rappresentati da funzioni esponenziali negative tra valor medio dell'umidità su tutto il sito e corrispondente coefficiente di variazione. La variabilità verticale del contenuto idrico è stata attribuita principalmente all'aumento dell'eterogeneità delle caratteristiche del suolo col variare della profondità. La correlazione tra campi a diversa profondità risulta alta ed è confermata anche dal confronto visivo di mappe di umidità interpolata.

La stabilità temporale dei campi di contenuto idrico del suolo è stata studiata tramite diversi approcci: i) l'analisi della stabilità per ranghi; ii) l'analisi

dei parametri di intercetta e pendenza angolare della retta di regressione lineare; iii) l'analisi di autocorrelazione; iv) lo studio dell'evoluzione della correlazione confrontata con l'andamento dell'umidità media nel tempo e la relazione con l'incremento del livello di falda. I risultati dimostrano che i campi spaziali di contenuto idrico del terreno vengono preservati alle tre profondità indagate. Il maggior grado di correlazione si osserva in condizioni di elevata umidità dei siti e la flessione di correlazione avviene nella fase di transizione da stato asciutto a stato bagnato; tale comportamento risulta maggiormente evidente per gli strati superficiali, influenzati più velocemente dalle precipitazioni rispetto a quelli più profondi. Correlazioni più basse si osservano nei dati raccolti nel 2006 e tale differenza è stata attribuita ad una diversa distribuzione delle precipitazioni nel corso delle tre stagioni analizzate; ciò è stato anche confermato dalla minore pendenza dei correlogrammi di umidità per gli anni 2005 e 2007. La stabilità nel tempo dei campi di umidità nei primi centimetri di suolo può infine essere considerata come indicatrice della stabilità temporale anche degli strati sottosuperficiali; quindi, l'identificazione di punti maggiormente stabili sui versanti di studio consente di ottenere informazioni utili ai fini della modellistica idrologica dell'umidità del suolo nell'intero bacino.

Il deflusso superficiale non incanalato riveste una notevole importanza nel contribuire alla portata totale nel torrente e nella determinazione della forma e della intensità dei picchi di piena; nonostante la sua significatività idrologica, misure dirette sono difficili da attuare e quindi infrequenti. In questo lavoro, il verificarsi del deflusso superficiale non incanalato è stato valutato tramite l'installazione di appositi rivelatori su un piccolo sottobacino (3.3 ha) sotteso da un effimero tributario del torrente principale. Sono inoltre state monitorate in continuo altre variabili idrologiche quali portata, livello di falda e umidità del suolo a 0-30 cm di profondità per mezzo di un riflettometro. I processi alla base della formazione di deflusso superficiale sono stati individuati in meccanismi di saturazione dall'alto e di flusso di ritorno attraverso percorsi preferenziali. A scala di evento piovoso è stata trovata una forte interazione tra i diversi processi idrologici: ciò suggerisce la consistenza tra deflusso superficiale e sottosuperficiale che rispondono alle precipitazioni con simili dinamiche spaziali e temporali sia a scala di singola pioggia che su periodi più lunghi. È stata individuata una correlazione altamente significativa tra le variazioni di portata nel rio e quelle del livello della falda acquifera, indipendentemente

dalla posizione topografica dei pozzi piezometrici nel bacino. La validità del presupposto dello stato stazionario per l'intero versante considerato è stata analizzata tramite una riformulazione del modello Topmodel a scala di singolo evento piovoso. Il modello lineare utilizzato si è dimostrato un fine predittore dell'andamento della falda idrica con lievi errori tra osservato e simulato; in qualche caso, però, il picco piezometrico è stato sottostimato dal modello, specialmente durante marcate fluttuazioni di livello. Tali discrepanze sono state attribuite ad un comportamento ad isteresi della relazione tra portata e falda a scala di evento piovoso, il cui comportamento ciclico e dunque non lineare non permette al modello lineare di simulare accuratamente variazioni di falda durante marcate fluttuazioni di livello.

Summary

ABSTRACT	3
Summary	9
Figure index	10
Table index	12
Equation index	13
CHAPTER 1: INTRODUCTION	15
1.1 Study area	15
Piramide	21
Emme	21
Vallecola	21
CHAPTER 2: MATERIALS AND METHODS	27
2.1 Instrumentation	27
Calibration of soil moisture probes	35
2.2 Data collection	40
CHAPTER 3: DISTRIBUTION OF SOIL MOISTURE OVER DIFFERENT DEPTHS	43
Introduction	43
Results and discussion	45
3.1 Summary statistical analysis	47
3.2 Data distribution	49
3.3 Relationship between mean and standard deviation	52
3.4 Relationship between mean and coefficient of variation	52
3.5 Correlation between point measurements at different depths	56
Distribution of soil moisture over different depths: concluding remarks ..	65
CHAPTER 4: TIME STABILITY OF SOIL MOISTURE	67
Introduction	67
Results and discussion	69
4.1 Ranking stability analysis	69
4.2 Slope-intercept analysis of linear regression	76
4.3 Autocorrelation analysis	77
4.4 Mean soil moisture, correlation between successive days and piezometric increase	85
Time stability of soil moisture: concluding remarks	92
CHAPTER 5: WATER TABLE VARIATIONS AND RUNOFF RESPONSE	95
Introduction	95
Results and discussion	98
5.1 Runoff response and interaction of processes	98
5.2 Water table variations and assessment of the steady state assumption	105
Water table variations and runoff response: concluding remarks	116
REFERENCES	119
Web references	127
CURRICULUM VITAE	129

Figure index

Figure 1 (left): aerial photograph of Rio Vauz catchment and its position in the country. Figure 2 (right): average climatic conditions in the study area	15
Figure 3 (left): elevation and hydrographic network of the Cordevole catchment; the Rio Vauz catchment is highlighted. Figure 4 (right): geological map of the Cordevole catchment (Gardi, 2003)	17
Figure 5: digital elevation model and main hydrographic network of Rio Vauz catchment.....	20
Figure 6: experimental hillslopes and lower part of Rio Vauz catchment, south-eastward (above); the three hillslopes after a late snowfall, at the end of May 2006.....	22
Figure 7: representation of the three hillslopes within the hillslope similarity diagram.....	24
Figure 8: overall view of Rio Larici subcatchment (left) and of the central part of the site (right).....	25
Figure 9: position of Rio Larici micro-catchment and of the three experimental hillslopes within Rio Vauz basin.....	25
Figure 10: position of rain gauges and water level loggers within the study area	27
Figure 11: position of piezometric wells over Piramide (left) and Emme (right).	28
Figure 12: Overland Flow Detector after construction (left) and in place in the field; the cap was removed to show the device filled with surface runoff after a storm event.....	30
Figure 13: experimental grid drawn over the study area in Rio Larici subcatchment.	30
Figure 14: water content reflectometer (left); probe and stainless steel rods (right).....	32
Figure 15: Theta Probe: data logger and probe	34
Figure 16: TDR300: the instrument (left) and the data logger display (right)	35
Figure 17: split tube soil sampler	37
Figure 18: regression between gravimetric values and probe outputs for the three instruments over the experimental site.....	38
Figure 19: localization of sampling points over the three experimental hillslopes	42
Figure 20: time series of hillslope-averaged soil moisture over different depths for 2005.....	45
Figure 21: time series of hillslope-averaged soil moisture over different depths for 2006	46
Figure 22: time series of hillslope-averaged soil moisture over different depths for 2007	46
Figure 23: plots of probability density functions according to PPCC test	51
Figure 24: relationship between mean and standard deviation for 2005, 2006 and 2007 data as a whole	54

Figure 25: relationship between mean and coefficient of variation for 2005, 2006 and 2007 data as a whole	55
Figure 26: scatter plots for 2005, 2006 and 2007 soil moisture data in total at different depths	57
Figure 27: maps of mean soil moisture at Piramide site at different depths over three years	60
Figure 28: maps of mean soil moisture at Emme site at different depths over three years	62
Figure 29: maps of mean soil moisture at Vallecola site at different depths for 2005	63
Figure 30: ranked ordered mean relative difference with standard deviation error bars for Piramide.....	74
Figure 31: ranked ordered mean relative difference with standard deviation error bars for Emme.....	75
Figure 32: ranked ordered mean relative difference with standard deviation error bars for Vallecola.....	76
Figure 33: autocorrelation matrices for 2005 soil moisture data.....	80
Figure 34: autocorrelation matrices for 2006 soil moisture data.....	82
Figure 35: autocorrelation matrices for 2007 soil moisture data.....	84
Figure 36: correlograms for soil moisture values at three soil depths	86
Figure 37: time series over different depths of hillslope-averaged soil moisture and Spearman rank correlation coefficient computed between values of a given day with respect to the values of the previous day	90
Figure 38: river network developed during rain storm number 22-07 and recorded by the OFD response	99
Figure 39: relationship between percentage of Rio Larici active network and peak discharge (a), maximum rise of water table (b), maximum water content (c) and antecedent moisture conditions (d).....	100
Figure 40: relationship between runoff coefficient and maximum water content (a), maximum rise of water table (b) and active stream network (c).....	101
Figure 41: relationship between maximum rise of water table and peak discharge (a), pre-event discharge (b), maximum water content (c) and antecedent moisture conditions (d).....	102
Figure 43: regression between Rio Larici stream discharge and soil moisture at 0-30 cm depth for the whole 2006 (hourly from June 26 to October 16) and 2007 (hourly from May 16 to October 15) datasets	103
Figure 44: water table level recorded by four piezometric wells within Rio Larici subcatchment in 2007 compared to stream discharge and precipitation	106
Figure 45: Spearman rank correlation between water table levels and discharge against distance of each piezometric well from the stream.....	107
Figure 46: RMSE for the model $z_{i,t} = a_0 + b_i + c_t + \varepsilon$ for each rainfall plotted against maximum value of soil moisture at 0-30 cm depth (a), piezometric peak (b) and active stream network (c).....	110
Figure 47: RMSE of every piezometric well averaged over all storms and plotted against the distance from the stream	112

Figure 48: examples of differences between measured and modelled values of water table recorded by four piezometric wells compared to stream discharge for storms number 19-2007 (a) and 22-2007 (b).....	113
Figure 49: examples of hysteretic behaviour of relationship between water table height and stream discharge at the rainstorm scale.....	115

Table index

Table 1: morphological properties of the Cordevole catchment	16
Table 2: main hydrological processes in reference to geological units (Gardi, 2003, modified)	19
Table 3: morphological properties of the Rio Vauz catchment	20
Table 4: number of soil samples taken at the experimental sites for calibration of moisture sensors	36
Table 5: standard deviation and RMSE for calibration curves of the soil moisture probes.....	38
Table 6: number of soil moisture measurements for 2005.....	40
Table 7: number of soil moisture measurements for 2006.....	41
Table 8: number of soil moisture measurements for 2007.....	41
Table 9: summary of soil moisture statistics over the three experimental sites for the various depths for 2005 (only common sampling times are considered).....	48
Table 10: summary of soil moisture statistics over the three experimental sites for the various depths for 2006.....	49
Table 11: summary of soil moisture statistics over the three experimental sites for the various depths for 2007.....	49
Table 12: spearman rank correlation coefficient for the complete soil moisture dataset 2005, 2006 and 2007	58
Table 13: Spearman rank coefficients reported for MRD, for the three different depths and the three years (two layers and one year for Vallecola): a) Piramide; b) Emme; c) Vallecola.....	72
Table 14: four time stability conditions according to the slope-intercept analysis of linear regression (from Grant et al., 2004, modified).....	77
Table 15: Spearman rank correlation coefficients for the 2006 monitoring period from June 26 to July 10; all values are statistically significant ($p < 0.01$)	105
Table 16: Spearman rank correlation coefficients for the whole 2007 monitoring period; all values are statistically significant ($p < 0.01$) except the one marked with *	105
Table 17: errors and R^2 values obtained by the analysis of variance for the model $z_{i,t} = a_0 + b_i + c_t + \varepsilon$ for single rainfalls in 2006 and 2007	109
Table 18: RMSE for the model $z_{i,t} = a_0 + b_i + c_t + \varepsilon$ for each piezometric well at the rainstorm scale.....	111

Equation index

	$\alpha = aL$	
(1)	$\psi = \ln\left(\frac{2\gamma L}{\beta} + 1\right)$	23
(2)	$\theta_v = \frac{V_w}{V_s}$	31
(3)	$\theta_v = \frac{\sqrt{\varepsilon} - \alpha_0}{\alpha_1}$	33
(4)	$\theta_v = \frac{M_{wet} - M_{dry}}{\rho_w * V_s}$	37
(5)	$\theta_g = \frac{M_w}{M_s} = \frac{M_{wet} - M_{dry}}{M_{dry}}$	37
(6)	$\rho_s = \frac{M_{dry}}{V_s}$	37
(7)	$\theta_v = \theta_g \frac{\rho_b}{\rho_w}$	38
(8)	$\varphi = \frac{V_a + V_w}{V_s}$	38
(9)	$CV = C \exp(B\mu)$	53
(10)	$\delta_{i,j} = \frac{S_{i,j} - \bar{S}_j}{\bar{S}_j}$	69
(11)	$\bar{S}_j = \frac{1}{n} \sum_{i=1}^n S_{i,j}$	69
(12)	$MRD_i = \frac{1}{m} \sum_{j=1}^m \delta_{i,j}$	69
(13)	$\sigma_i = \sqrt{\frac{\sum (\delta_{i,j} - DRM_i)^2}{m}}$	70
(14)	$\rho = 1 - 6 \sum \frac{d^2}{N(N^2 - 1)}$	71
(15)	$\theta_{t_2}(i) = a_{t_2-t_1} \theta_{t_1}(i) + b_{t_2-t_1} + \varepsilon_{t_2-t_1}$	76
(16)	$z_{i,t} = \bar{z}_t - \frac{1}{f} (I_i - \bar{I})$	108

- (17) $z_{i,t} = \frac{\bar{I}}{f} - \frac{I_i}{f} + \bar{z}_t$ 108
- (18) $z_{i,t} = a_0 + b_i + c_t + \varepsilon$ 108

CHAPTER 1: INTRODUCTION

1.1 Study area

Hydro-meteorological data were collected in a small alpine basin (Rio Vauz catchment, 1.9 km²) in the Northern Italian Dolomites, between the village of Arabba (1601 m a.s.l.) and Pordoi Pass (2240 m a.s.l.); the study area is a subcatchment of the Torrente Cordevole basin, an area of about 7 km², whose outlet is located approximately 3 km west of Arabba. The average annual precipitation is 1160 mm/year, 40% of which falls as snow. The maximum peak is recorded in early summer and a second one in fall (Figure 2). In the lower parts of the catchment the snow cover period typically lasts from November to April, reaching maximum snow depths of about 1.5m in April. The upper parts of the basin are bare only for three months from July to September and maximum annual snow depths are on the order of 3 m. Runoff is usually dominated by snowmelt in May and June but summer and early autumn floods represent an important contribution to the flow regime. The average monthly temperature varies from -5.7°C in January to 14.1°C in July.

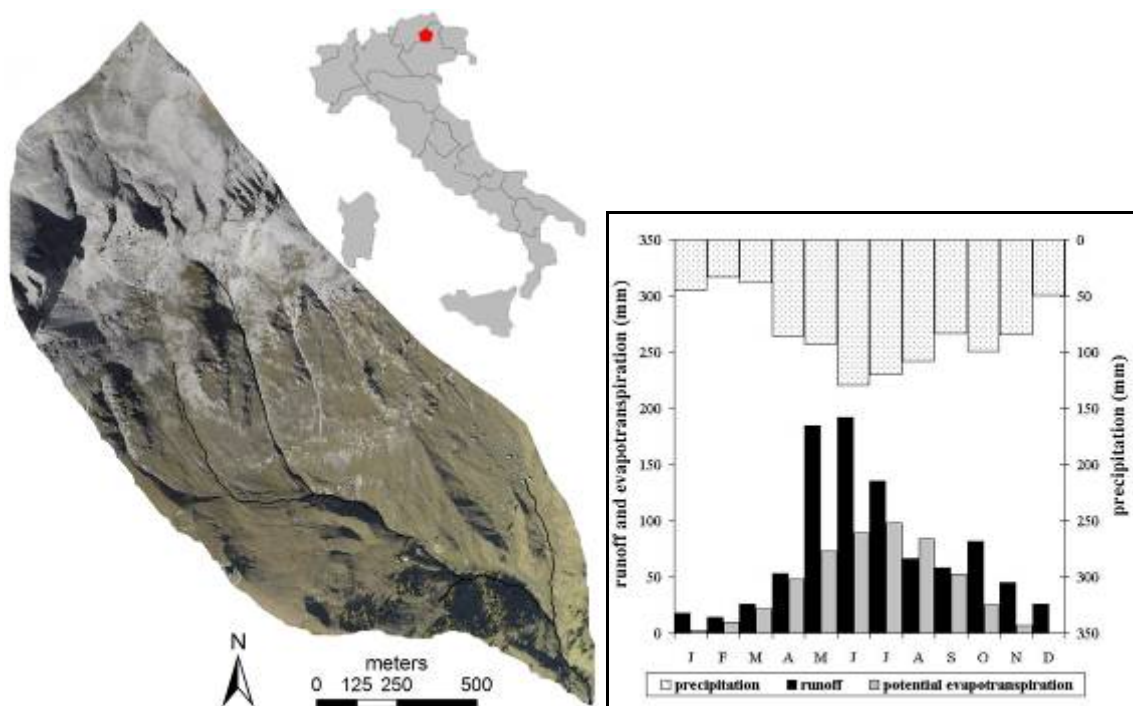


Figure 1 (left): aerial photograph of Rio Vauz catchment and its position in the country. Figure 2 (right): average climatic conditions in the study area

The Cordevole catchment (Figure 3) can be divided into three topographic units:

- a gently rising upland plateau which is located in the northern part and lies above 2000 m;
- steep slopes and cliffs almost above 2200 m in both northern and southern parts of the catchment;
- a relatively wide valley in which the main stream flows.

The basin is almost undisturbed by human activity: neither roads nor urban areas are present and most of vegetated basin slopes are pasture lands, which represent the traditional land use in alpine basins above the timberline. The main morphological properties of Cordevole catchment are summarized in Table 1.

Table 1: morphological properties of the Cordevole catchment

Surface	7.1 km ²
Maximum altitude	3152 m a.s.l.
Minimum altitude	1810 m a.s.l.
Mean altitude	2274 m a.s.l.
Mean slope	24.4°

The upper part of the catchment is geologically formed by Sciliar dolomite and Haupt dolomite leaning on the San Cassiano formation, while the lower unit is characterized by conglomerate lava (La Valle formation). The substratum is constituted by layers of fractured limestone alternating with deposits of volcanic ash. In the lower part of the catchment there are several steep hillslopes where flow of water cuts deep gullies; on the contrary, at the bottom of hillslopes many areas partly filled in alluvial sediments can be found. Soil depth varies from 0.2 m along the hillslopes to 1.2 m at the bottom. Generally, where the soil is deeper, the first 20 cm are composed of organic and mineral components; while the layers underneath are basically mineral. The organic-mineral components decrease where flow of water is particularly important (Gardi, 2003, van Beusekom, 2004). The geological formations are:

- Marine deposits (Quaternary): bad to moderately rounded, highly unsorted glacial deposits. It contains material from all the formations and consists of slightly permeable or impermeable material.

- Haupt dolomite (Upper Triassic, Norian) formation: this formation consists of regularly stratified, massive, white, orange and grey-black dolomite. It forms the high tops of the northern part of the catchment.

- Sciliar dolomite formation (Upper Triassic): it is a massive, brown to grey and sometimes rose coloured dolomite, originally a coral reef. It forms steep slopes and cliffs in the northern part of the basin. The rocks are fractured and they form the central large aquifer in the catchment.

- San Cassiano formation (Upper Triassic): the upper part of the such formation consists of a thin fine-grained volcanic tuffs with fauna of Raibliana and the rest are mostly marl, marly-limestone and marly-dolomite with Crinoides, Brachipoda and small Ammonites. It is a very low permeable or impermeable formation.

- La Valle (Wengen) formation (Upper Triassic): it contains mainly fine-grained volcanic tuffs and tuffaceous-calcareous shales. In some places, porphyric lava, coarse tuff conglomerates and coarse lava conglomerates can be found. The last is a hard and dark rock which forms the southern tops of the catchment. The fine-grained volcanic tuffs are mostly impervious or low pervious layers but the coarse-grained tuffs can provide small aquifers.

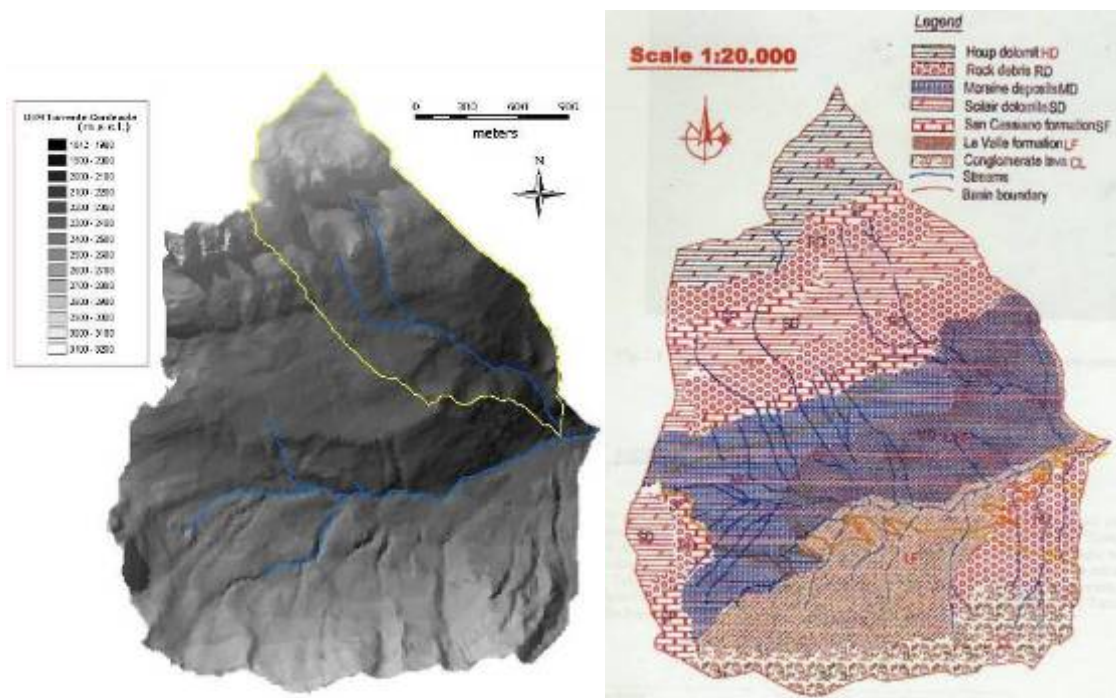


Figure 3 (left): elevation and hydrographic network of the Cordevole catchment; the Rio Vauz catchment is highlighted. Figure 4 (right): geological map of the Cordevole catchment (Gardi, 2003)

From a geomorphologic point of view, the Cordevole catchment is characterized by a strong effect of glacial erosion and deposition. There are differences in resistance to erosion between the massive dolomite at the top of the northern part and coarse lava conglomerate in the southern one. La Valle formation was partly glacially eroded at the end of ice-age and resulted in several small, deep, narrow valleys, especially in the southern part of the catchment while glacial deposits (moraine) formed a gently rising upland plateau in the northern part.

In the Cordevole basin, response to precipitation is strongly affected by topography, geology and local climate factors. Usually, base flow at the outlet varies from 0.14 to 0.35 m³s⁻¹, while the highest discharge ever recorded was 2.3 m³s⁻¹, mainly caused by intense precipitation. Ground water is discharged through various springs over the catchment. Precipitation felt as snow sometimes accumulates as temporary surface storage; the maximum snow reserve is usually reached in January or early February and strong snowmelt processes usually occur in April and early May.

In the following table the main hydrogeological processes are summarized in reference to the four major hydrogeological units into which the catchment can be divided. The tops of the northern part of the catchment are formed by dolomite, very resistant to erosion; it is a very pervious rock and water infiltrates easily generating important aquifers. There are good surface reservoirs due to snow accumulation. Volcanic tuffs are very complex and consist mainly of pyroclastic material. Layers finely fractured are impervious while the coarser ones have many cracks and consequently a better permeability. Alluvium contains basically rock debris with coarse fragments which allow the formation of good infiltration zones and aquifers. Impermeability of moraine deposits depends on the state of consolidation and grain size distribution; sometimes moraine deposits have a good ground water storage capacity. Soils in the Cordevole catchment seem to be strictly associated with the basin topographical structure and geology. La Valle and San Cassiano formations developed brown and grey thin layers, variations of lithosols, rendzinas, rankers and brown calcareous. As long as the lithology changes from a fine-grained volcanic tuffs of La Valle formation to San Cassiano formation (which contains more marls and limestones and less volcanic components) the soil type changes too. The soil contains weathered rock fragments in all soil horizons (Gardi, 2003, van Beusekom, 2004).

Table 2: main hydrological processes in reference to geological units (Gardi, 2003, modified)

Hydrogeological processes	Dolomite	Volcanic tuffs	Alluvium	Morain deposits
Interception	0	X	0	0
Transpiration	0	X	0	0
Surface storage	0	X	0	0
Ground water storage	X	0	XX	0
Ground water flow	X	0	XX	0
Surface runoff	0	XX	0	XX
Evaporation	0	X	0	0
Infiltration	X	X	XX	0
Interflow	0	XX	0	X

Legend: 0: no effect; X: positive effect; XX: significant positive effect

Vegetation is dominated by grass. It covers the major part of the catchment, except for the steep slopes and cliffs on both sides of the valley. In the southern part, beside the grass, there is a great presence of shrubs, particularly alpine roses (gen. *Rosa*), junipers (gen. *Juniperus*), willows (gen. *Salix*) and alders (*Alnus viridis*). Due to intense logging in the fifties and sixties, trees only exist in the small area near the catchment outlet, mostly larches (*Larix decidua*) and spruces (*Picea abies*). Forest soils have a several times higher water intake compared to bare soils; moreover, trees intercept more water than grasses and this may result in a slower catchment response to precipitation and a greater lag between precipitation and stream discharge. Usually, the catchment area is used as a grazing field for cows from middle June to middle September; nowadays, only few peasants still use this land for scything (Gardi, 2003, van Beusekom, 2004).

The Rio Vauz subcatchment (Figure 5) is located in the northern part of the Cordevole basin; it can be divided into three morphological units:

- an upper part (3152-2200 m a.s.l.) entirely formed by rock cliffs;
- a middle part (2200-2000 m a.s.l.) composed by an almost flat plateau;
- a lower part (2000-1835 m a.s.l.) where steep slopes are.

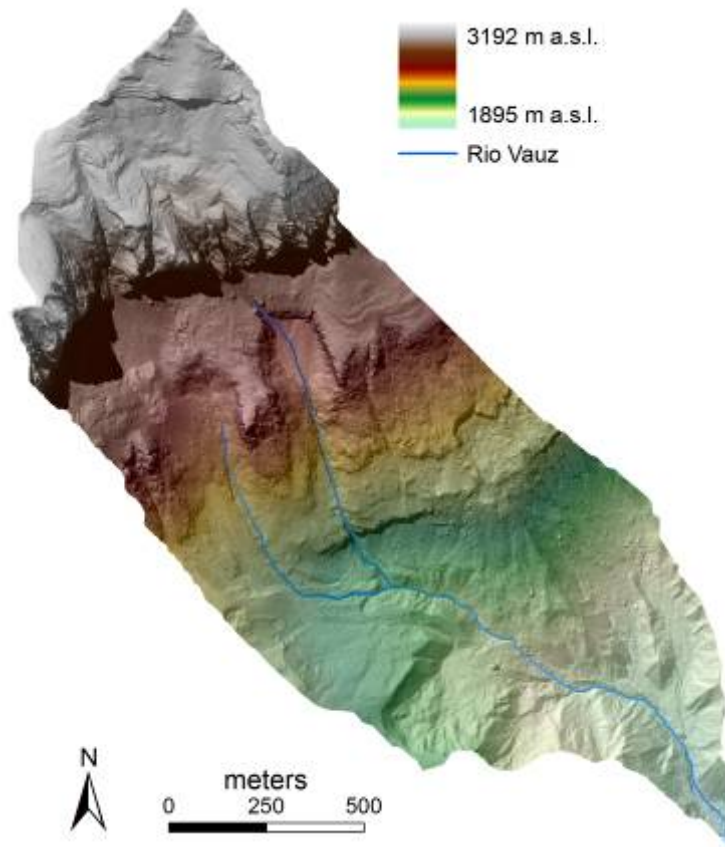


Figure 5: digital elevation model and main hydrographic network of Rio Vauz catchment

The main morphological properties of Rio Vauz catchment are summarized in Table 3.

Table 3: morphological properties of the Rio Vauz catchment

Surface	1.9 km ²
Maximum altitude	3152 m a.s.l.
Minimum altitude	1835 m a.s.l.
Mean altitude	2401 m a.s.l.
Mean slope	27.4 °

Within the Rio Vauz catchment three hillslopes were chosen in order to collect detailed soil moisture data; the hillslopes are constituted by moraine deposits covered by soil of variable thickness. The experimental sites have been named “Piramide”, “Emme” and “Vallecola” after their morphological properties.

Piramide

Piramide comprises one largely divergent hillslope covering an area of approximately 0.46 ha. The hillslope has a predominantly south-east aspect, although almost all aspects comprised between east and west are represented. Elevation ranges from around 1930 to 1975 m a.s.l.. Gradients range between around 1:5 to 1:1,2. The soil profile consists of an organic-rich horizon (in the first 10 cm), overlying mineral subsoil, which is turn is underlain by weathered till and bedrock. Mineral soil is predominantly silty clay (55% clay, 25% silt, 10–40 cm depth). Depth of soil above compact till and bedrock ranges from 60 cm on the ridge to more than 100 cm at the base of the hillslope. No permanent watercourse exists on this hillslope.

Emme

Emme is a hillslope with a dominant west aspect covering an area of 0.47 ha. Elevation varies from 1935 m a.s.l. to 1996 m a.s.l., at the top of the ridge. At the bottom, near a left tributary of Rio Vauz arbitrary named Rio Ponte , the hillslope is characterized by low values of slope and after a small and almost flat plateau the slope rises abruptly, reaching values of 45° and more. The soil profile is basically similar to that in Piramide, with a thin organic horizon and a massive thickness of soil, whose main mineral component is clay. Depth of soil is quite different according to the positions in the site: low depth is found at the bottom of the hillslopes, near the stream, where soil saturation is reached quite easily during storm events. The hillslope exhibits no permanent watercourses but on several occasions, during and after storm events, even not particularly intense, water was observed to be heavily flowing from various pipe holes at the bottom of the hillslope, before the slope interruption.

Vallecola

Vallecola is a convergent hillslope site which comprises an area of approximately 0.56 ha; the dominant aspect of the field site is south-west. Elevation ranges from 1915 to 1985 m ASL, with hillslope gradients of typically

1:1.5, with lower gradients around 1:4 and steeper gradients up to 1:1. As for Piramide, an organic-rich horizon overlies mineral silty clay subsoil (45% clay, 35 % silt, 10-40 cm depth) with intermixed cobbles. Both clay and coarse fragments tend to increase with soil depth towards fractured bedrock. Depth of soil above compact till and bedrock ranges from 30 cm on the hillslope to more than 100 cm at the base of the hillslope. No permanent watercourse exists at Vallecola, though an eroded landslide scar exists in the central portion of the sampling area. Exposed walls of this gully reveal a light coloured clay soil and evidence of pipe erosion. On several occasions, water was seen to be freely discharging from pipe holes in the wall of this eroded gully.



Figure 6: experimental hillslopes and lower part of Rio Vauz catchment, south-eastward (above); the three hillslopes after a late snowfall, at the end of May 2006

The topographic structure of the three hillslopes has been characterised by using the hillslope similarity parameters introduced by Norbiato and Borga (2007). The authors adopted a second order polynomial function to describe the bedrock slope and an exponential function to explain the width variation of the hillslope with hillslope distance. Thus, they defined two hillslope similarity parameters α and ψ as:

$$\begin{aligned} \alpha &= aL \\ \psi &= \ln\left(\frac{2\gamma L}{\beta} + 1\right) \end{aligned} \quad (1)$$

where L defines the length of the hillslope in the horizontal direction, a represents the degree of convergence of the planar shape, γ and β are parameters of the quadratic profile curvature fitted to the topographic data. As a result, parameter ψ characterises the convexity of the curvature profile of hillslope: values of $\psi < 0$ define concave profiles, $\psi > 0$ define convex profiles, and for $\psi = 0$ the profile is linear. Parameter α characterises the divergence of the plan shape of the hillslope: values of $\alpha > 0$ define divergent shapes, $\alpha < 0$ define convergent shapes, and for $\alpha = 0$ the shape is rectangular. The two geometric parameters α and ψ thus define the hydrological similarity between hillslopes with respect to their characteristic response as described by the subsurface flow kinematic wave. The geometric parameters α and ψ are reported in Figure 7 for the three hillslopes. Both similarity parameters are positive for Piramide, with the α divergence parameter larger than the ψ convexity parameter. This indicates that for this relief form divergence dominates over convexity. Emme is shown to be a relatively planar hillslope, with slightly negative values for both similarity parameters. Negative and relatively similar parameter values are reported for Vallecòla, which is therefore identified as a convergent and concave hillslope, as expected from field observation.

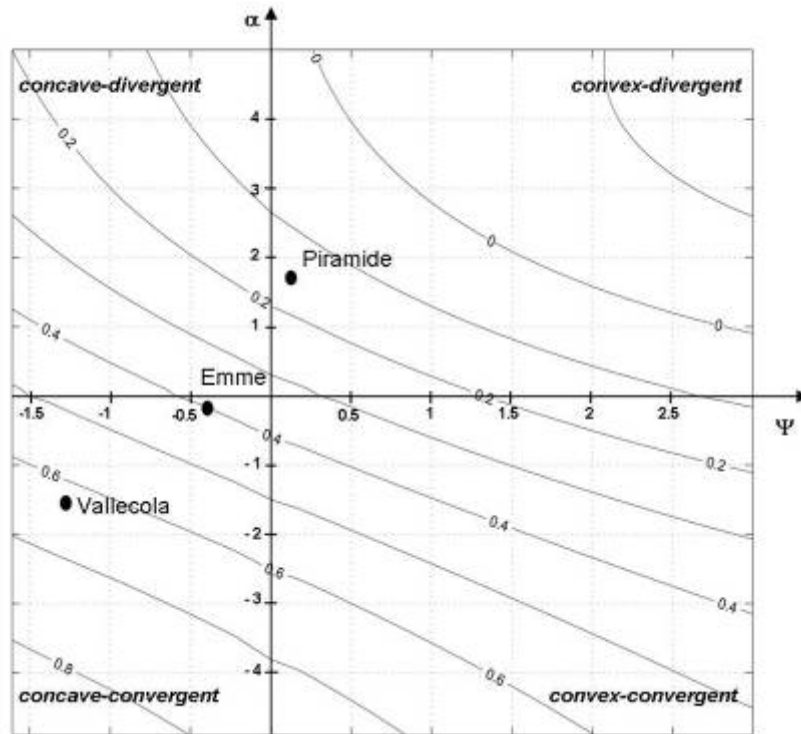


Figure 7: representation of the three hillslopes within the hillslope similarity diagram

Since 2006, a subcatchment of Rio Vauz basin, named Rio Larici, was selected in order to extend the sites for hydro-meteorological data collection. The micro-catchment is localized in the lower south-western part of the study area (Figure 9) and is defined by a ephemeral small right tributary of the main stream. The experimental watershed is 0.033 km² large and its elevations range from 1970 m a.s.l. at the confluence with Rio Vauz up to 2110 m a.s.l. on top of the divide. The upper part of the site presents the highest inclinations (up to 48°) while the central part is characterised by low slopes which tend to decrease to an almost flat area; during the late spring snow is usually still present in this sector of the watershed and in the summer months water tends to be stored: therefore, this area can be considered a sort of small reservoir being able to affect the hydrologic behaviour of the whole watershed. Soils are similar to those found in the surrounding area with clay or silty-clay layers underlying a deep organic matter portion. Rio Larici subcatchment is densely vegetated: alpine grassland, scattered shrubs, larches (*Larix decidua*) and spruces (*Picea abies*) are the most common species; particularly, the noticeable presence of trees make the site absolutely different from the rest of the study area where trees were intensively cut at the beginning of the last century (Figure 8). Finally, the presence of various erosion phenomena over the whole Rio Vauz catchment

has to be mentioned; among them the most important landslide is by a right tributary of Rio Vauz, occurred after an intense precipitation on October 7th, 1998.



Figure 8: overall view of Rio Larici subcatchment (left) and of the central part of the site (right)

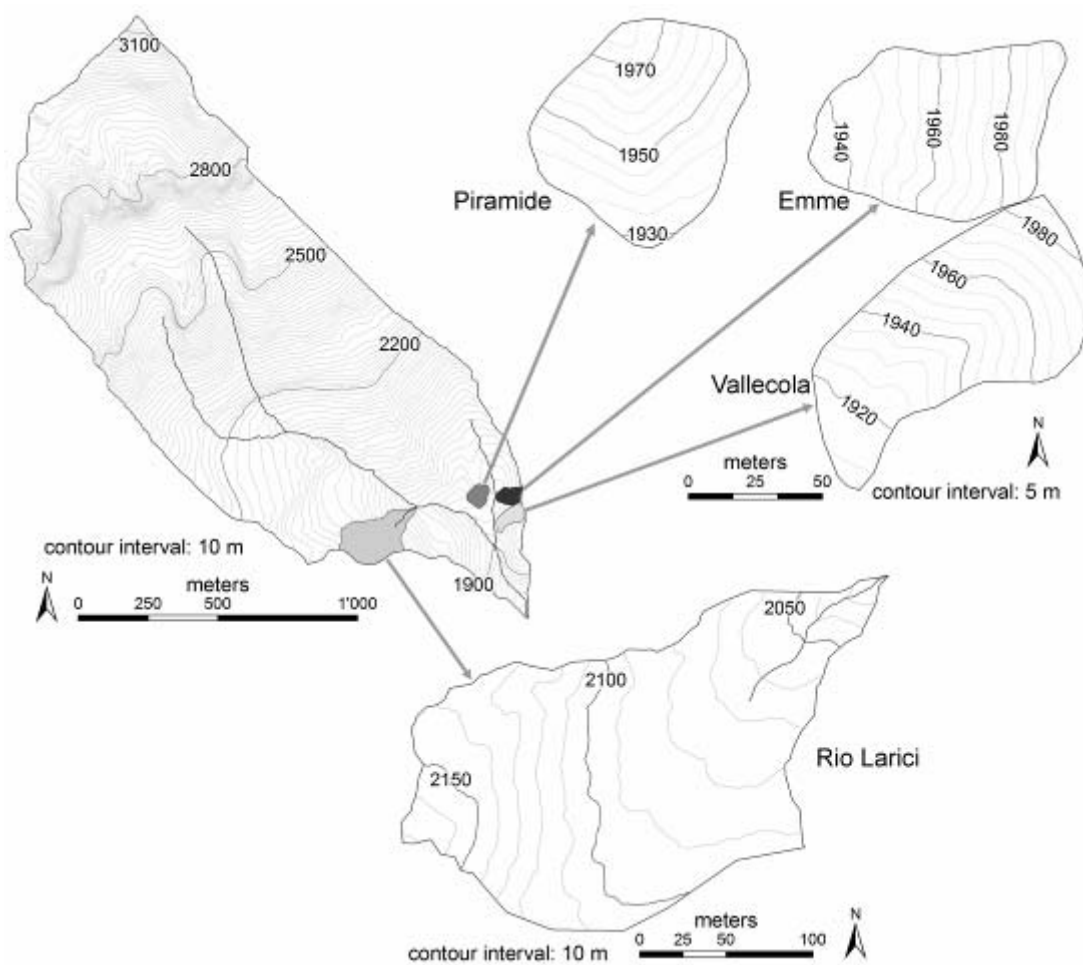


Figure 9: position of Rio Larici micro-catchment and of the three experimental hillslopes within Rio Vauz basin

CHAPTER 2: MATERIALS AND METHODS

2.1 Instrumentation

During the field works carried out over summers 2005, 2006 and 2007, several devices were installed in the study area. Precipitation data were collected by means of two tipping bucket rain gauges: one was located at 1923 m a.s.l., equipped with one thermometer and close to the sampled hillslopes, the other one was placed in the middle part of Rio Larici subcatchment, at 2022 m a.s.l. Two pressure transmitters, manufactured by the Swiss company Keller Druck (www.keller-druck.ch) were used to record stage at 15-minute interval; the sensors were installed by two V-notch sharp-crested weirs positioned on a small colluvial stream named Rio Ponte, a left tributary of the main stream, and on Rio Larici, few meters away from the confluence with Rio Vauz. A map showing the position of rain gauges and weirs is depicted in Figure 10.

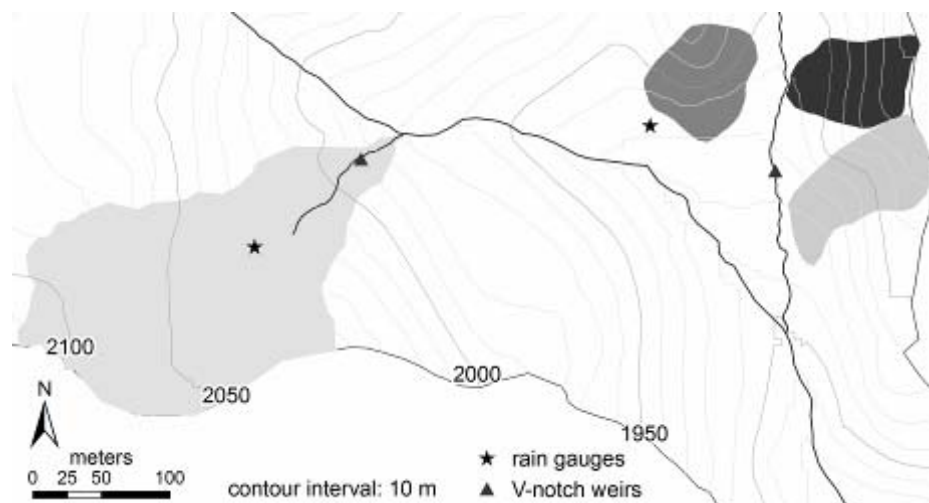


Figure 10: position of rain gauges and water level loggers within the study area

Pressure transducers determine fluid levels by measuring the prevailing pressure at a lower depth and comparing it with the pressure at the surface; this enables a calculation based on the density of the liquid. Level measurement by hydrostatic pressure is based on the principle that the hydrostatic pressure difference between the top and bottom of a column of liquid is related to the density of the liquid and the height of the column. The instruments used in the campaigns (DCX-22 AA) utilize an absolute pressure sensor: one body is placed

in the water upstream the weir, another one is positioned on the ground surface acting as a barometer and the air pressure characteristic is recorded. The water level is then calculated as the difference between the two measured values (Keller AG, 2004). Piramide and Emme comprise a net of 16 and 25 piezometric wells respectively, equipped with capacitance probes (www.trutrack.com) of different length (0.5 m and 1 m) installed to monitor the variations of the water table during and after rain events (Figure 11). The recording interval was set at 5 minutes to be able to intercept the possible rapid arise and decrease of the water table even at the short duration or weak intensity storm scale. Capacitance level transmitters operate on the principle that a capacitive circuit can be formed between a probe and a vessel wall, or between two rods of a probe. The capacitance of the circuit will change with a change in fluid level because all common liquids have dielectric constant higher than that of air. This change is then related proportionally to an analogic signal. The capacitance level probe therefore consists of a conducting, cylindrical probe, which acts as the first capacitor plate; this probe is covered by a suitable dielectric material. The second capacitor plate is formed by the chamber wall together with the water contained in the chamber. The capacitance increases as more of the plate area is immersed in the liquid, therefore, by changing the water level, the area of the second capacitor plate changes and this affects the overall capacitance of the system.

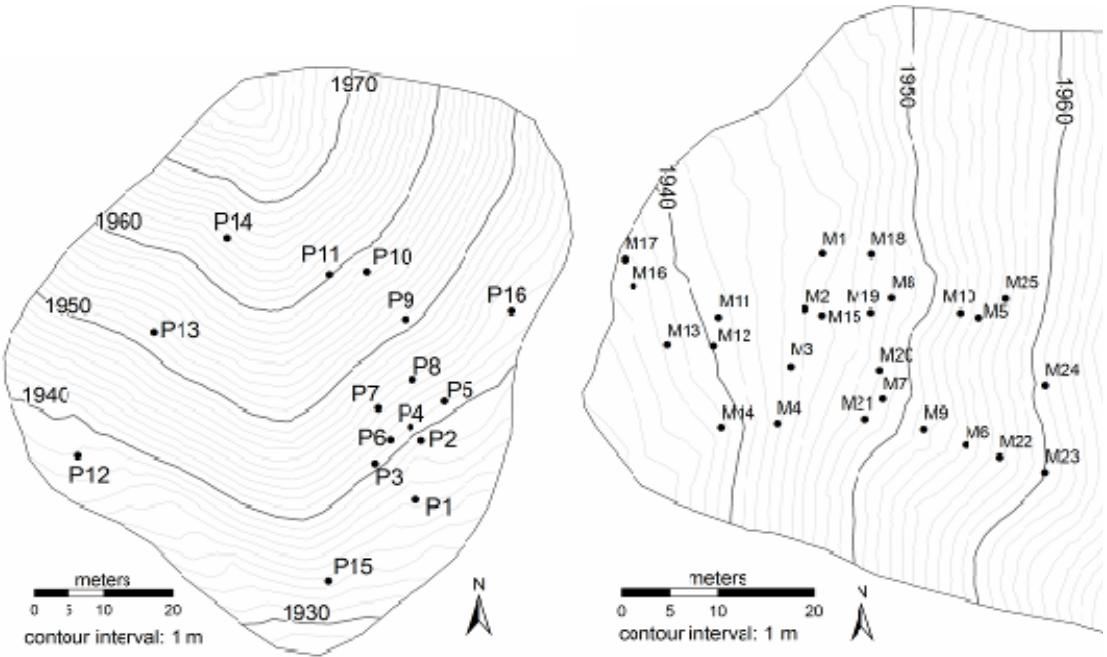


Figure 11: position of piezometric wells over Piramide (left) and Emme (right).

Within the Rio Larici subcatchment, an area approximately 0.1 ha large was selected and an experimental regular grid was drawn; the basic module is a square 10X10 m in size and every vertex represents a soil moisture sampling point. Volumetric water content was monitored for the first time during the 2007 field campaign at two soil depths (0-6 cm and 0-20 cm) by means of two portable sensors described later in this chapter. The experimental grid also includes twelve capacitance rods installed in 2006.

All the water level loggers were calibrated before every field campaign by means of a graduated barrel filled with water. TruTrack capacitive probes are provided with a software that allows the sensor calibration by setting two points of known water height. First, the level loggers were lowered into the water to the first index mark (at the bottom of the probe) and a 0 value was set in the software; then, the sensors were lowered into the water to the second index mark (at the top of the probe) entering the corresponding height. The remaining levels, automatically obtained by software interpolation, were later manually checked. The barrel was also used for testing the sensor response to water level fluctuations: the recording time of every probe was set to 1 minute and the barrel was gradually filled and then emptied at a constant rate; data were downloaded from all sensors and checked by looking at possible irregularities in the arising and decreasing curves, which were expected to be even in time and shape.

In order to identify the dynamics of the ephemeral river network in the Rio Larici micro-catchment, 25 overland flow detectors (OFDs, Figure 12) were built and installed in 2006 and 2007 in those portions where overland flow was expected to occur. These instruments are formed by an horizontal PVC pipe bearing around 200 small holes (1 mm in diameter) linked to a vertical pipe inserted into the soil; the horizontal portion lies on the soil and is supposed to intercept the overland flow, collected in the vertical chamber of the instrument (Vertessey et al., 2000). The OFDs were installed in concave zones interested by evidence of possible flows of water during or after rain events. The response provided by these instruments is a binary information (presence/absence of surface runoff) and out of 25 OFDs installed all over the micro-watershed, four are included in the experimental grid.

All the soil moisture sampling points and devices installed over the experimental grid are shown in Figure 13.



Figure 12: Overland Flow Detector after construction (left) and in place in the field; the cap was removed to show the device filled with surface runoff after a storm event.

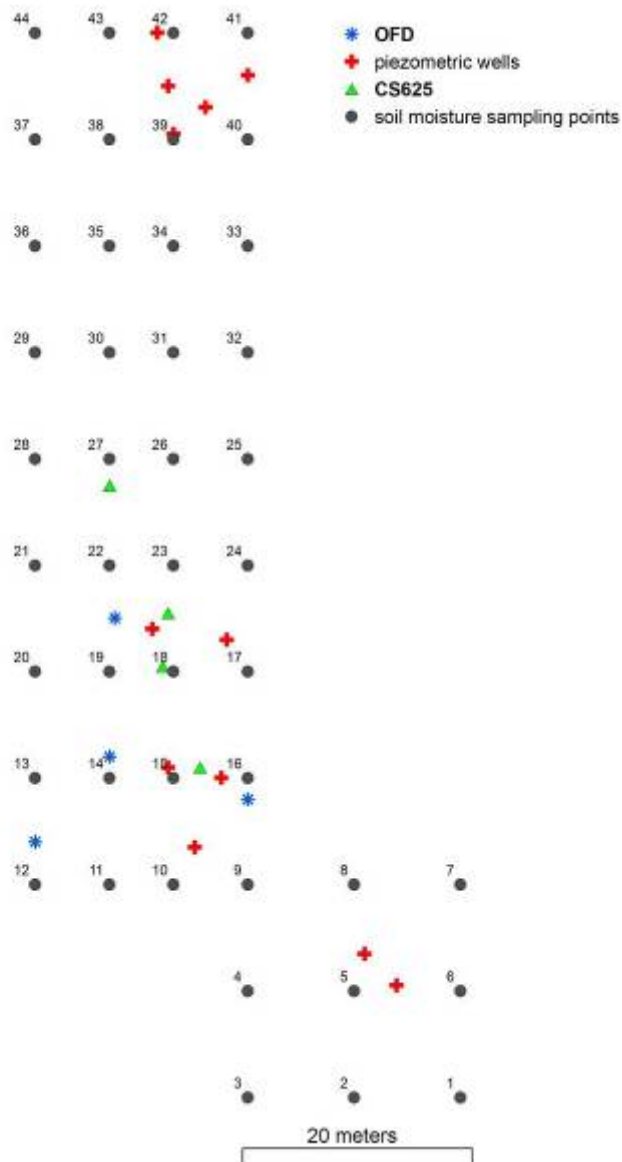


Figure 13: experimental grid drawn over the study area in Rio Larici subcatchment

Volumetric water content of soils at different depth both over Piramide, Emme, Vallecola hillslopes and within Rio Larici subcatchment was measured by means of three different tools; these instruments estimate soil moisture by using the dielectric characteristics of soil and water and require a conversion between dielectric constant and volumetric soil moisture (Topp and Ferre, 2002). Volumetric soil water content (θ_v) is the ratio between the volume of water present in the soil (V_w) and the total volume of the sample (V_s) and is therefore expressed as:

$$\theta_v = \frac{V_w}{V_s} \quad (2)$$

This is a dimensionless parameter, expressed either as a percentage (% volume) or as a ratio (m^3m^{-3}). Thus a completely dry soil corresponds to $0 \text{ m}^3\text{m}^{-3}$ whereas pure water gives a reading of $1.0 \text{ m}^3\text{m}^{-3}$. The volumetric water content of a wet mineral soil and a wet very organic soil could approach $0.5 \text{ m}^3\text{m}^{-3}$ and $0.8 \text{ m}^3\text{m}^{-3}$ respectively. At saturation the volumetric water content will equal the percent pore space of the soil.

Soil moisture measurements at 0-30 cm depth were continuously recorded by means of a CS 625 water content reflectometer (WCR) which was installed in the study area; the sensor was placed on hillslope Emme for the 2005 and 2006 field campaigns while in 2007 it was positioned in the experimental grid over Rio Larici subcatchment. The instrument, manufactured by Campbell Scientific Inc. (www.campbellsci.com) is formed by a data logger with battery lodged in a water proof box, a solar panel providing electricity supply, 4 probes (Figure 14, right) to be inserted in the soil with stainless steel rods 30 cm long, 1 temperature probe.; the latter is important because soil moisture is also depending on soil temperature and acquiring such data allows to apply a correction to the raw water content values.



Figure 14: water content reflectometer (left); probe and stainless steel rods (right).

The probe rods are connected to a printed circuit board whose electronic components are configured as a bistable multivibrator. The output of the multivibrator is connected to the probe rods. The method for measuring soil water content is an indirect measurement that is sensitive to the dielectric permittivity of the material surrounding the probe rods. Since water is the only soil constituent that (i) has a high value for dielectric permittivity and (ii) is the only component other than air that changes in concentration, a device sensitive to dielectric permittivity can be used to estimate volumetric water content. The fundamental principle for CS 625 operation is that an electromagnetic pulse will propagate along the probe rods at a velocity that is dependent on the dielectric permittivity of the material surrounding the line. As water content increases, the propagation velocity decreases because polarization of water molecules takes time. The travel time of the applied signal along 2 times the rod length is essentially measured. The applied signal travels the length of the probe rods and is reflected from the rod ends travelling back to the probe head. A part of the circuit detects the reflection and triggers the next pulse. The frequency of pulsing with the probe rods in free air is about 70 MHz. This frequency is scaled down in the water content reflectometer circuit output stages to a frequency easily measured by a data logger. The probe output frequency or period is empirically related to water content using a calibration equation (Campbell Scientific, Inc., 2002-2003).

Soil moisture values at 0-6 cm depth, both over the study hillslopes and within the experimental grid in Rio Larici subcatchment, were sampled by means of a hand-held impedance probe known as Theta Probe (Figure 15), manufactured by Delta-T Devices Ltd. (www.delta-t.co.uk). Soil moisture impedance probes have been proven to be an accurate means of quickly and efficiently measurement of volumetric water content in soil (Walker et al., 2004, Cosh et al., 2005); water content is inferred measuring the dielectric permittivity of the soil solution phase (Topp et al., 1980, Topp and Ferre, 2002, Cosh et al., 2005). The probe, a portable and user-friendly instrument, consists of a waterproof housing which contains the electronic, and, attached to it at one end, four sharpened stainless steel rods that are inserted into the soil. The probe generates a 100 MHz sinusoidal signal whose frequency has been chosen to minimise the effect of ionic conductivity; thus, changes in the transmission line impedance are dependent almost solely on the soil's apparent dielectric constant. Because the dielectric of water (~81) is very much higher than soil (typically 3 to 5) and air (1), the dielectric constant of soil is determined primarily by its water content (Delta-T Devices Ltd, 2004, Gaskin and Miller, 1996, Miller and Gaskin, 1999, Walker et al., 2004). Theta Probe measure volumetric soil water content by determination of the apparent dielectric constant using the following equation:

$$\theta_v = \frac{\sqrt{\varepsilon} - \alpha_0}{\alpha_1} \quad (3)$$

where ε is the apparent dielectric constant and α_0 and α_1 are constants dependent on soil type (Delta-T Devices Ltd, 2004).

The two Theta Probe sensors used in the field were different in age and were provided with an old and a newer version of firmware; in order to compare the behaviour of the two devices under different moisture conditions and to check possible discrepancies between their readings, a simple statistical analysis was performed. Since our major interest concerned the average value of measurements (usually five) taken by the two devices during the field surveys, a statistical test for comparing means was performed. 30 sites, characterized by different soil water contents, were selected and sampled five times by the two sensors; the truncated mean was then computed rejecting the highest and lowest values and averaging the others. Data distribution (both raw

values expressed in mV and values converted in percentage volumetric water content were considered) was evaluated by Shapiro-Wilk test which revealed a non-normal distribution of the samples (p value: 0.003, alpha: 0.05 for both devices). Thus, a non parametric approach was followed using Mann-Witney test for comparing medians. U value was converted in z value, which is smaller than 1.96: this means that a significant difference between the readings of the two sensor cannot be found and that the probes can be used without distinction in moisture sampling under the same soil conditions.



Figure 15: Theta Probe: data logger and probe

Soil moisture at 0-12 and 0-20 cm depth was evaluated by means of a TDR portable probe defined TDR300 (Figure 16), manufactured by Spectrum Technologies Inc. (www.specmeters.com) and operating on the basis of Time Domain Reflectometry technology, a highly accurate method, nowadays a standard for determining water content in soils (Blonquist et al. 2005, Hansson and Lundin, 2006, Jones et al., 2002, Moret et al., 2006, Serrarens et al., 2000, Stark et al., 2006, Western and Seyfried, 2005). TDR probes are quite easy to use and reduce cost of licensing and training when compared to other techniques. TDR300 probe is provided with two pairs of interchangeable rods of 12 cm and 20 cm length; the rods act as a wave guide and the electronics embedded in the probe body send a wave down the rods. This signal travels the length of the rods and is partially reflected when it reaches the interface between the rod tips and the soil. This signal is transformed into a square wave output with a frequency proportional to volumetric water content. The measurement volume for the TDR300 is an elliptical cylinder extending, radially, 3 cm from the rods

with a height equal to the length of the rods. The measured volumetric water content is the average over this entire volume (Spectrum Technologies, Inc. 2003).



Figure 16: TDR300: the instrument (left) and the data logger display (right)

Calibration of soil moisture probes

Soil moisture probes were calibrated for the specific local soil conditions; a specific calibration can noticeably improve the measure accuracy, especially for soils with a high clay content (Chandler et al., 2004, Fares et al., 2004, Kaleita et al., 2005, Kelleners et al., 2004, Morgan et al., 1999, Western et al., 2001). Particularly, a user-calibration can achieve an accuracy of $\pm 0.02 \text{ m}^3\text{m}^{-3}$ for the Theta Probe (Gaskin and Miller, 1996, Miller et al., 1997, Miller and Gaskin, 1999) decreasing errors and reducing significantly the bias (Cosh et al., 2005). Standard calibration equations provided by the manufacturer of the TDR300 and the water content reflectometer CS625 ensure accuracy of $\pm 3\%$ and $\pm 2\%$ volumetric soil moisture, respectively (Campbell Scientific, 2002-2003, Spectrum Technologies, 2003). Soil specific calibration of WCR usually gives significantly lower root mean squared errors compared to the manufacturer's standard calibration (Stenger et al., 2005) and each kind of soil requires a specific calibration (Seyfried and Murdock, 2001). Moreover, particularly for clay soils, a specific calibration is strongly recommended (Chandler et al., 2004, Western et al., 2001), leading to a greater accuracy of measurements (Stenger et al., 2005, Roth et al., 1990, Walker et al., 2004). The amount of organic matter and clay in a soil can alter the response of dielectric-dependent methods to changes in water content; particularly, high clay contents cause underestimation of soil water content in the low moisture range and overestimation of soil water content in the high moisture range (Gong et al., 2003). Indeed, the electromagnetic energy introduced by the probe acts to re-orientate or polarize

the water molecules. If other forces are acting on the polar water molecules, the force exerted by the applied signal will be less likely to polarize the molecules. This has the net effect of 'hiding' some of the water from the probe. Additionally, some clays absorb water interstitially and thus inhibit polarization by the applied field (Campbell Scientific, 2002-2003).

In the field, water content was measured by each probe in representative points within the study area and corresponding soil samples were collected at the investigated depths; sampling was carried out so that the collected samples were characterized by different water contents, necessary to calibrate every monitoring instrument with soil conditions varying from a dry to a wet status. A split tube soil sampler (www.eijkelkamp.com, Figure 17) was used in order to obtain rapid and undisturbed samples 6, 12, or 20 cm long; it consists of two stainless steel tube halves with a working length of 40 cm and a diameter of 5.3 cm when joined; once inserted into the soil, the sampler can be removed by means of a steel lifting jack with lever and chain and both parts can be easily separated. PVC pipes with air tight caps to reduce evaporation were used to store and transport the sample. Unfortunately, collection of good and undisturbed soil samples at 0-30 cm depth for calibration of CS625 proved to be very difficult due to the high density of clay soil: in order to get a 30 cm long sample, in fact, the soil sampler had to be pushed in the soil profile for almost 40 cm, denoting a likely compaction of the core and a subsequent change in porosity. Thus, a calibration equation for clay soils suggested by the manufacturer was used. However, for further studies and applications of this probe, another soil sampling method should be considered. The known volume of each sample was 132, 265 and 441 cm³ respectively for Theta Probe and TDR 300 equipped with rods 12 or 20 cm long. The samples were taken in an area representative of the soil conditions of the entire site; the number of samples is summarized in Table 4.

Table 4: number of soil samples taken at the experimental sites for calibration of moisture sensors

0-6 cm	0-12 cm	0-20 cm
55	45	40



Figure 17: split tube soil sampler

Soil samples were submitted to laboratory analysis in order to measure accurately the water content by gravimetric method; the undisturbed core taken in the field is weighted, oven-dried at 105°C for 24 hours and weighted again. The volumetric water content is calculated as follows:

$$\theta_v = \frac{M_{wet} - M_{dry}}{\rho_w * V_s} \quad (4)$$

where M_{wet} and M_{dry} are the mass of wet and dry soil respectively (grams), V_s is the total soil volume (ml) and ρ_w is the density of water (1g/ml). An alternate, but equivalent, calculation can be obtained from the gravimetric water content (θ_g):

$$\theta_g = \frac{M_w}{M_s} = \frac{M_{wet} - M_{dry}}{M_{dry}} \quad (5)$$

where M_w is the mass of water in the soil sample and M_s is the total mass of the dry sample. The bulk density of the soil sample (ρ_b) is expressed as:

$$\rho_s = \frac{M_{dry}}{V_s} \quad (6)$$

and thus volumetric soil moisture is:

$$\theta_v = \theta_g \frac{\rho_b}{\rho_w} \quad (7)$$

Regression between values of water content evaluated by gravimetric method and the raw values obtained by the probes allowed us to compute a calibration equation for each instrument (Figure 18), subsequently applied to the raw data collected in the field. For TDR 300, samples of both lengths (12 and 20cm) were gathered and used together since they appeared to fit the same relationship. Standard deviation of errors and root mean squared errors of calibration curves respect to gravimetric values are presented in Table 5.

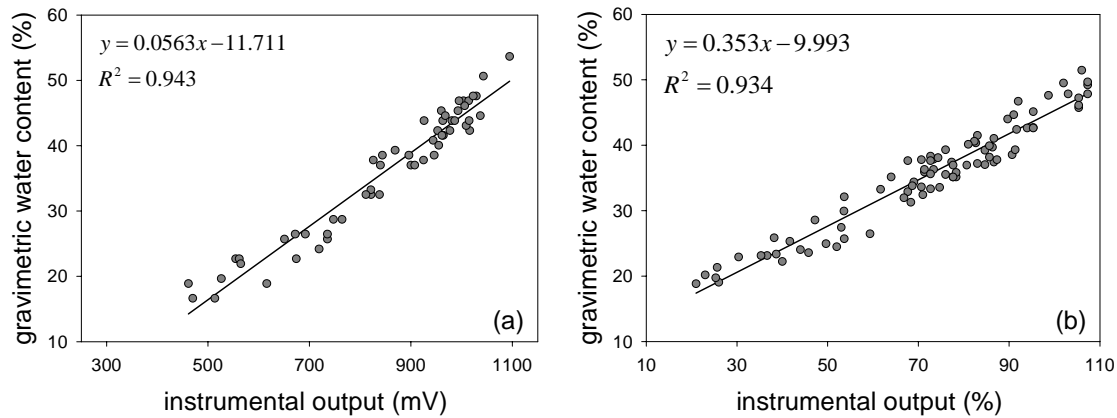


Figure 18: regression between gravimetric values and probe outputs for the three instruments over the experimental site. a) Theta Probe; b) TDR300

Table 5: standard deviation and RMSE for calibration curves of the soil moisture probes

	TP	TDR300
standard deviation of errors (%)	2.37	2.10
root mean squared error (%)	2.35	2.09

In order to know the porosity (ϕ) of soil at different layers, i.e. the proportion of pore space in a volume of soils and thus the maximum water content that can be reached, 67 samples were completely imbibed and oven dried; porosity was calculated by equation :

$$\phi = \frac{V_a + V_w}{V_s} \quad (8)$$

where V_a and V_w are the volumes of the air and liquid water in the soil and V_s is the total volume of the soil sample. The volume of pores, corresponding to the maximum quantity of water which can be store in a certain volume of soil, was determined as the weight difference between the wet and dry sample. Porosity values, quite similar among the sampling sites, obtained for 0-6 cm-long samples range from 48% to 75% with a mean of 59%; samples collected at 0-12 cm depth exhibit values between 45% to 57.5% and an average porosity of 50%; the minimum porosity shown by 0-20 cm long soil samples is 40%, the maximum is 61% and the mean value is 50%.

2.2 Data collection

Soil moisture data were manually collected at 0-6, 0-12 and 0-20 cm depth over Piramide, Emme and Vallecola during three field campaigns: from 28 June to 21 July, 2005, from 21 June to 16 July 2006 and from 28 August to 22 September 2007. Data were collected over Vallecola only during the 2005 field campaign: difficulties with deeper sampling, due to presence of cobbles, prevented measurement at 0-20 cm depth over this site. In 2007 field work, water content measurements were also taken in the experimental grid within Rio Larici subcatchment but data are still being analysed and results are not presented in this thesis. Water content measurements at 0-30 cm depths were automatically taken by means of CS625 reflectometer with 1 hour recording interval, placed at the foot of Emme hillslope from June to the beginning of October 2005 and 2006 and at Rio Larici site from the middle of May to the middle of October 2007. Number of sampling sites and times for the three hillslopes and the three depths sampled manually are reported in Table 6, Table 7 and Table 8 for 2005, 2006 and 2007, respectively. Measurements were generally carried out between 0900 and 1100 local time, to avoid showers which were likely to occur on the afternoon. Cumulated estimated rainfall amounts to 130 mm, 99.6 mm and 56.6 mm, for 2005, 2006 and 2007, respectively, while the climatological average for the period is 120 mm.

Table 6: number of soil moisture measurements for 2005

	Piramide			Emme			Vallecola	
	0-6 cm	0-12 cm	0-20 cm	0-6 cm	0-12 cm	0-20 cm	0-6 cm	0-12 cm
number of sampling points	26	26	26	26	26	26	16	16
number of sampling times	24	24	8	25	25	16	24	24
total number of measurements	624	624	208	624	624	416	384	384

Table 7: number of soil moisture measurements for 2006

	Piramide			Emme			Vallecola	
	0-6 cm	0-12 cm	0-20 cm	0-6 cm	0-12 cm	0-20 cm	0-6 cm	0-12 cm
number of sampling points	26	26	26	26	26	26	0	0
number of sampling times	23	23	23	23	23	23	0	0
total number of measurements	598	598	598	598	598	598	0	0

Table 8: number of soil moisture measurements for 2007

	Piramide			Emme			Vallecola	
	0-6 cm	0-12 cm	0-20 cm	0-6 cm	0-12 cm	0-20 cm	0-6 cm	0-12 cm
number of sampling points	26	26	26	26	26	26	0	0
number of sampling times	24	24	24	24	24	24	0	0
total number of measurements	624	624	624	624	624	624	0	0

Volumetric soil moisture was measured at 26 sites over Piramide and Emme, and at 16 sites over Vallecola (Figure 19). At the sampling points, the first few centimetres of grass cover were removed in order to reduce the influence of roots on the measure, otherwise strongly affected by the presence of pores and discontinuity zones (Walker et al., 2004). At each sampling point, five measures were collected in order to ascertain the repeatability of the results and instrument errors; the highest and lowest values were rejected and the truncated mean was calculated over the three remaining values. The measurements at the three depths were taken almost concurrently at each site to reduce the effect of temporal variability on the comparison of results. The temporal gap between the acquisition of soil moisture values at the first and the last point was around 45 minutes: during such a short time and for no-rain periods, no measurable variations of water content among the sampling points occurred, as checked in the field by repeating at the end of the sampling program the measurement at the first sampled point. Measurements can be therefore considered as instantaneous. Points were sampled in the same order on each occasion. A refined DEM with a 1 m resolution was delineated for the study area based on data obtained from a LIDAR topographical survey. The spatial distribution of soil depth was measured directly by using an iron pole at

each corresponding survey point. Soil samples were collected for particle size analysis.

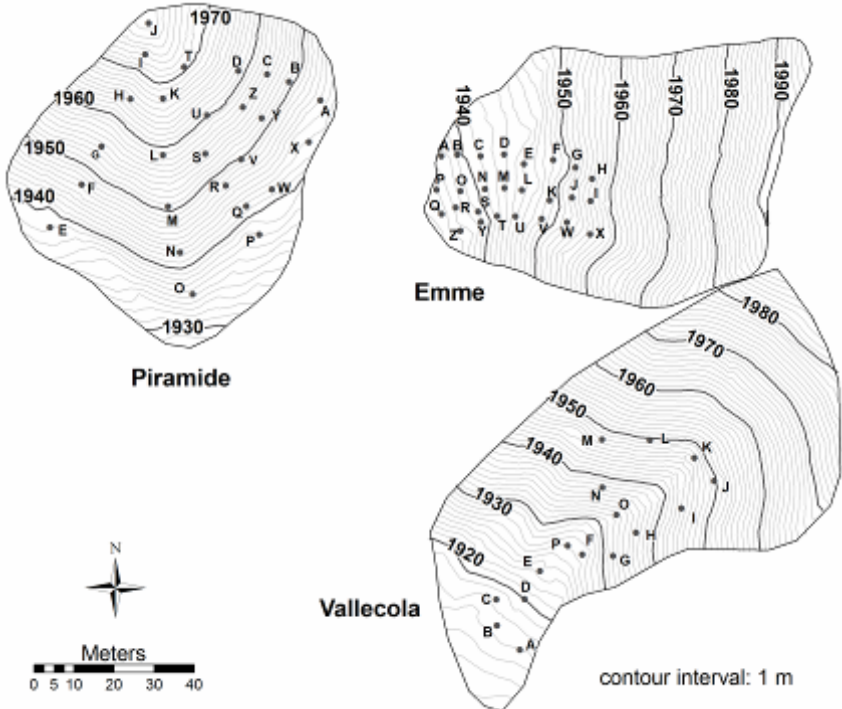


Figure 19: localization of sampling points over the three experimental hillslopes

CHAPTER 3: DISTRIBUTION OF SOIL MOISTURE OVER DIFFERENT DEPTHS

Introduction

Soil moisture is one of the most important hydrological variables. It has critical influence on several hydrological processes, such as floods, erosion of hillslopes, landslide triggering, on pedogenetic processes, migration of chemicals to aquifers, separation of net radiation between sensible and latent heat and also on land use, water and natural resources management. Near-surface soil moisture plays a central role in the global water cycle by controlling the partitioning of water and energy fluxes at the earth's surface and constitutes the physical linkage between soil, climate and vegetation (Pan et al., 2003; Albertson and Montaldo, 2003; Rodriguez-Iturbe and Porporato, 2004). Space-time variability of soil moisture influences many different processes acting at various scales ranging from point to hillslope to regional scale. At the point scale, for instance, soil moisture is crucial for the infiltration process (Raats, 2001; Bronstert and Bardossy, 1999) and plant dynamics (Porporato and Rodriguez-Iturbe, 2004). At the hillslope scale, soil moisture represents a controlling factor in the hydrological and mechanical processes responsible for slope instability and shallow landsliding (Borga et al., 2002a, Borga et al, 2002b). At the regional and continental scale, soil moisture controls water distribution through land-surface atmosphere feedback mechanisms (Koster et al., 2004). Space-time variability of soil moisture is a challenging topic for hydrologists. Information characterizing space-time variability of soil moisture across various scales can provide a blueprint to design ground-based experiments and networks and to efficiently use remote sensing estimates. The hillslope scale, however, is the basic building block for landscapes and for catchment models (Sivapalan 2003). Recent research has received significant input through experimental campaigns aimed at gathering extended samples of ground-based in-situ samples and comparing them to other hydrological variables. Examples are provided by the Tarrawarra and Mahurangi experiments (Western et al. 1999; Western et al., 2004; Western and Grayson, 1998, Western and Grayson, 2000; Wilson et al., 2003; Wilson et al., 2004), Panola Mountain Research

Watershed (Tromp-van Meerveld and McDonnell, 2005, Tromp-van Meerveld and McDonnell, 2006, Tromp-van Meerveld et al., 2007) and SGP97, SGP99, SMEX02 and SMEX03 (Mohanty and Skaggs, 2001; Cosh et al., 2003, Choi and Jacobs, 2007). These experiments have increased our understanding of temporal variability and of spatial structure of soil moisture fields and of their inherent hydrological and topographic controls. Some investigations aimed at elucidating the terrain controls on soil moisture have shown that topography becomes increasingly important in wet periods, but during dry periods soil moisture patterns depend primarily on soil properties, with topography having a limited effect (e.g., Grayson et al., 1997, Meyles et al., 2003). However, other studies were unable to show any significant control of topography on soil moisture patterns (Hebrard et al., 2006; Tromp-van Meerveld and McDonnell, 2006) even during wet conditions.

The main objective of this study is to better understand field scale soil moisture spatial distribution at different soil depths for three hillslopes in a small alpine catchment.

Results and discussion

Plots depicted in Figure 20, Figure 21 and Figure 22 show the time series of the hillslope-averaged water content at different soil depths over the three years, respectively. Precipitation has clearly a strong influence on soil water content: dry periods are characterized by relatively low values which rapidly increase after rain events; the time series generally display comparable dynamics over the three hillslopes.

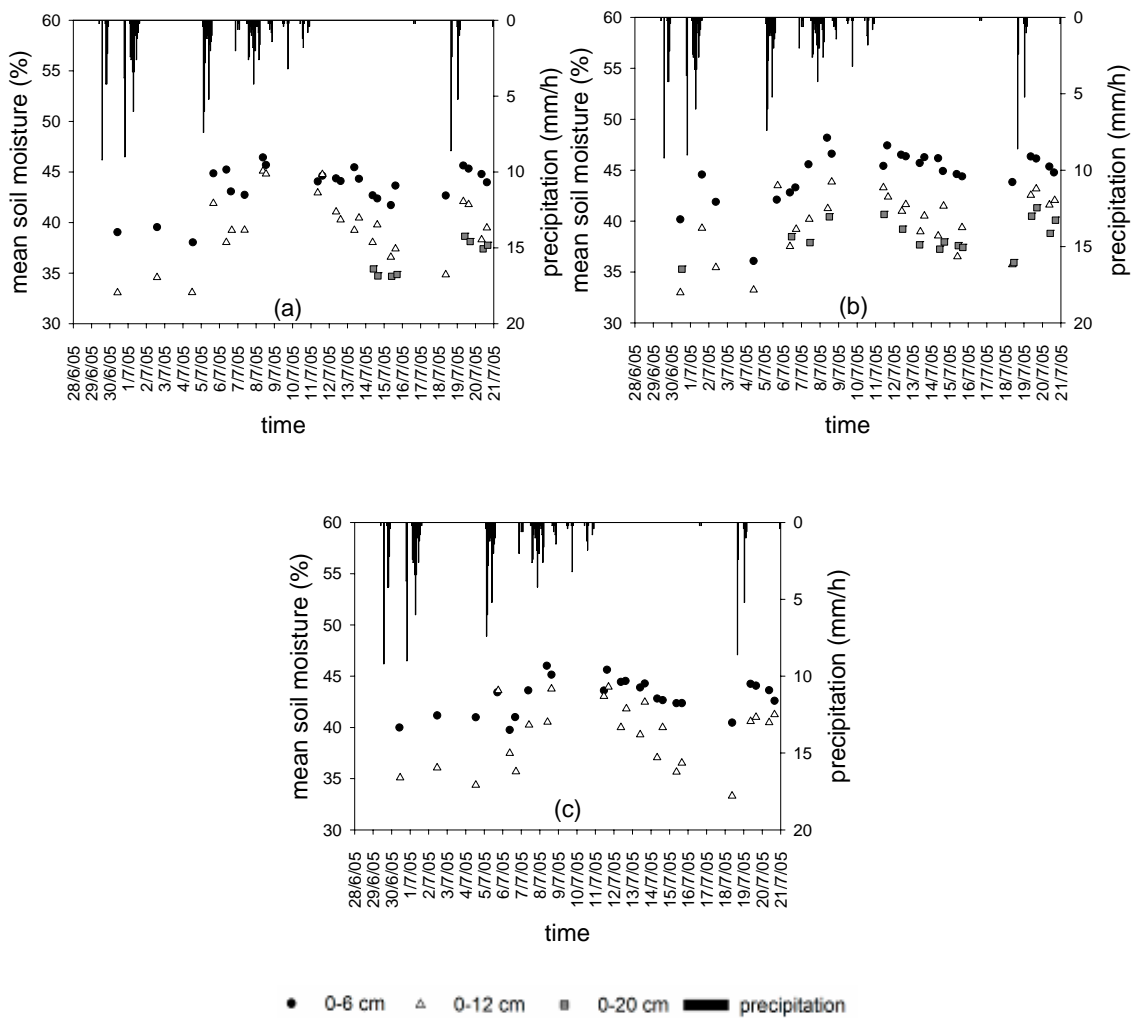


Figure 20: time series of hillslope-averaged soil moisture over different depths for 2005 for: a) Piramide; b) Emme; c) Vallecola

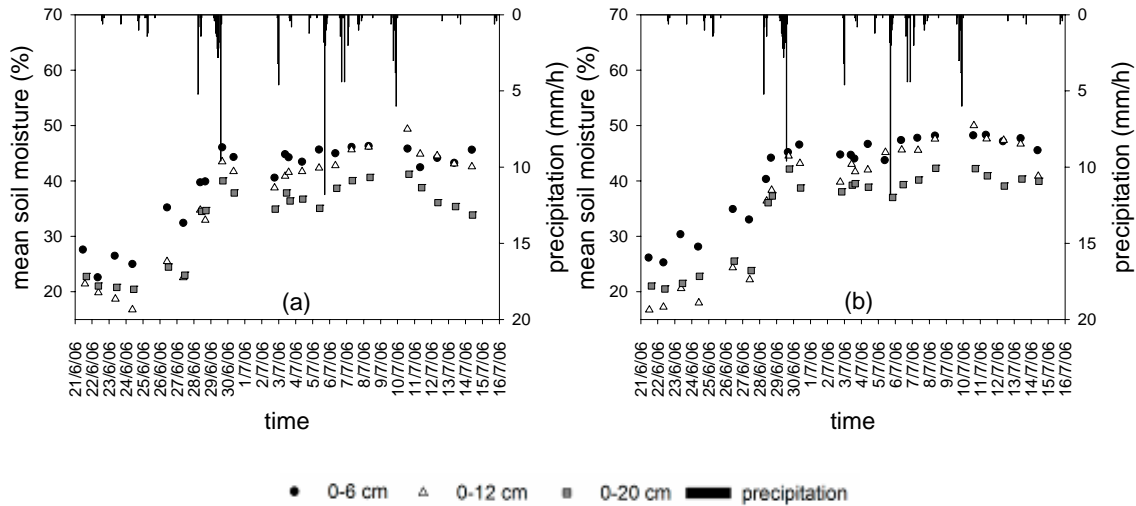


Figure 21: time series of hillslope-averaged soil moisture over different depths for 2006 for: a) Piramide; b) Emme

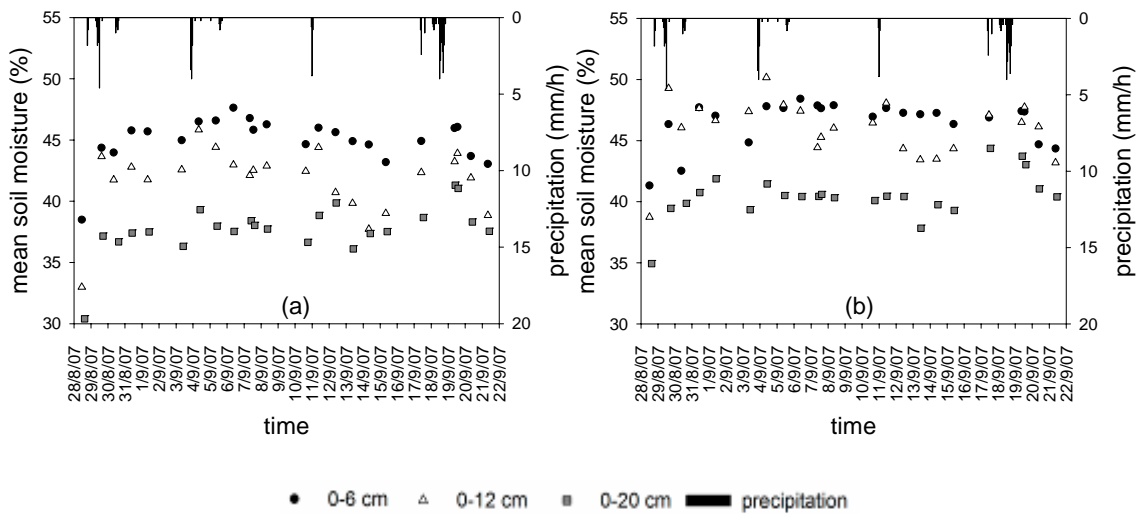


Figure 22: time series of hillslope-averaged soil moisture over different depths for 2007 for: a) Piramide; b) Emme

The comparison between soil moisture patterns at different depths was evaluated by examining: (i) summary statistical properties of the data set; (ii) distributional properties; (iii) evaluation of relationships between instantaneous hillslope average values and corresponding standard deviation and coefficient of variation; (iv) evaluation of correlation coefficients between soil moisture contents collected over different soil depths; (v) visual comparison of soil moisture maps.

3.1 Summary statistical analysis

Table 9, Table 10 and Table 11 show summary statistics for those periods when soil moisture data were available over the three depths for the three years, respectively. The hillslope-averaged soil content is highly dependent on sampling depth, as well as standard deviation. The soil moisture content over the 0-6 cm soil layer is typically higher than over deeper layers. Furthermore, the shallow soil layer has less variability than deeper layers. It is noteworthy in all tables that 0-6 cm soil moisture values are wetter and less variable than 0-12 cm and 0-20 cm values. This is contrary to what was reported by some researchers (Choi and Jacobs, 2007), who observed less variability for deeper layers than for shallower layers. Typically, several environmental factors (i.e., evaporation and rainfall) may cause higher variability at the surface than the subsurface. However, inspection of soil moisture data time series shows that hillslope-averaged data over different depths are relatively close to each other after rainfall events, and their difference increases with time during the dry-down. While influence of instrumental differences may not be excluded (even though the two soil moisture measurement devices were calibrated for local conditions), this calls for processes which are active during the dry periods and influence only the dynamics of the shallow layer. The partition of soil moisture in the first 6 cm with respect to deeper depths is consistent with the expected effects of observed dew formed through condensation, which reduces soil moisture depletion in the upper soil layers. The effect of condensation on soil moisture during the morning after clear-sky nights has been observed in the field and pretty high values of condensation (up to 1.8 mm per day) have been measured in the experimental site. These values are consistent with values reported by de Jong (2005). Similar effects were observed by Engstrom et al. (2005) in a site located in the Arctic coastal plain. Also, it is noteworthy that the formation of dew is essentially a nocturnal occurrence. The rate and duration of this process depends on the humidity, temperature and movement of the surface air layers, the sorption characteristics of the exposed surface, its radiation cooling and its heat supply from warmer soil layers. Therefore, the timing of the soil moisture surveys, conducted in the morning, may have influenced the measurement of soil moisture in the surface layer by enhancing the effect of dew. In all cases, the standard deviation, the coefficient of variation and skewness are highly dependent on depth. In all cases but Piramide 2005,

standard deviation and coefficient of variation increase going from 0-6 cm depth to 0-12 cm and then decrease (or remain equal in 2007 coefficient of variation). In general, the distribution of moisture values over 0-6 cm is more negatively skewed than values measured over 0-12 and 0-20 cm depths. The coefficient of kurtosis is positive for data collected at 0-6 cm depth at each of the three sites, while the other depths show either slightly negative kurtosis or values closer to zero (except in Emme 2007). Analysis of results corresponding to common sampling times across hillslopes shows that statistics are generally comparable across the three sites, with Emme slightly wetter than Piramide and Vallecola. This is probably due its main westward aspect.

Table 9: summary of soil moisture statistics over the three experimental sites for the various depths for 2005 (only common sampling times are considered)

Summary statistics 2005	Piramide			Emme			Vallecola	
	0-6 cm	0-12 cm	0-20 cm	0-6 cm	0-12 cm	0-20 cm	0-6 cm	0-12 cm
n. of sampling points	26	26	26	26	26	26	16	16
n. of sampling times	8	8	8	16	16	16	24	24
total n. of measures	208	208	208	416	416	416	384	384
mean (%)	43.8	39.2	36.5	45.2	40.0	38.5	43.0	39.3
median (%)	43.8	39.1	35.9	45.5	40.4	38.8	43.5	39.4
standard deviation (%)	3.3	5.2	5.5	3.2	5.8	4.9	3.0	6.5
coefficient of variation	0.07	0.13	0.15	0.07	0.15	0.13	0.07	0.16
skewness	-0.8	0.0	0.3	-0.9	-0.3	-0.4	-0.8	0.0
kurtosis	3.6	0.5	-0.5	1.5	-0.2	-0.2	0.5	-0.1
inter-quart. range (%)	3.5	7.0	7.7	3.9	8.0	6.8	3.8	8.9
10 th percentile (%)	40.1	33.1	29.6	41.4	32.2	31.6	38.8	30.8
90 th percentile (%)	47.3	45.7	44.4	48.8	47.4	44.4	46.3	46.9

Table 10: summary of soil moisture statistics over the three experimental sites for the various depths for 2006

Summary statistics 2006	Piramide			Emme		
	0-6 cm	0-12 cm	0-20 cm	0-6 cm	0-12 cm	0-20 cm
n. of sampling points	26	26	26	26	26	26
n. of sampling times	23	23	23	23	23	23
total n. of measures	598	598	598	598	598	598
mean (%)	39.9	36.6	33.3	41.7	37.6	35.1
median (%)	43.4	40.1	35.4	45.2	42.0	37.9
standard deviation (%)	8.3	11.4	9.1	8.3	12.1	9.0
coefficient of variation	0.21	0.31	0.27	0.20	0.32	0.26
skewness	-1.3	-0.9	-0.8	-1.4	-1.0	-1.1
kurtosis	0.5	-0.3	-0.1	1.0	-0.2	0.3
inter-quart. range (%)	8.4	14.6	10.7	8.9	16.1	10.4
10th percentile (%)	25.0	17.0	17.9	28.0	16.9	20.1
90th percentile (%)	46.9	48.4	42.9	48.6	49.3	43.5

Table 11: summary of soil moisture statistics over the three experimental sites for the various depths for 2007

Summary statistics 2007	Piramide			Emme		
	0-6 cm	0-12 cm	0-20 cm	0-6 cm	0-12 cm	0-20 cm
n. of sampling points	26	26	26	26	26	26
n. of sampling times	24	24	24	24	24	24
total n. of measures	624	624	624	624	624	624
mean (%)	44.9	41.7	37.8	46.4	45.9	40.5
median (%)	45.1	41.7	37.5	47.1	46.3	41.2
standard deviation (%)	2.7	5.1	4.6	2.5	4.1	3.8
coefficient of variation	0.06	0.12	0.12	0.05	0.09	0.09
skewness	-1.0	-0.2	-0.2	-1.9	-1.2	-1.1
kurtosis	3.5	0.8	0.4	6.9	5.1	2.4
inter-quart. range (%)	3.0	6.9	6.4	3.0	4.8	4.3
10th percentile (%)	42.1	35.9	32.5	43.4	41.4	35.6
90th percentile (%)	47.8	48.1	44.0	48.9	50.6	44.7

3.2 Data distribution

From other field experiments, it is known that soil moisture tend to follow a normal distribution (Oldak et al., 2002, Cosh et al., 2004) as soil depth increases (Choi and Jacobs, 2007). Although there is no fundamental reason

why soil moisture should follow a Gaussian distribution, this has advantages (Teuling et al., 2006) because prevents from using more complex analysis approaches, i.e. non parametric statistical tests. The Gaussian distribution is a reasonable approximation of the soil moisture probability density function (PDF) but divergence from normality do occur and they are more likely under very wet or very dry conditions (Western et al., 2002). Appropriate probability distributions were identified for the various instantaneous soil moisture fields, differentiating by depth and by site. The normal distribution and log-normal distribution were analyzed as they are the most widely used PDFs for soil moisture analysis. Probability plot correlation coefficient (PPCC) tests (Vogel, 1986) were conducted to determine whether the data follow normal or log-normal distributions (Figure 23). Due to the relatively low number of sampling points at Vallecola site, the PPCC test was not performed for this hillslope. In the PPCC test, if the correlation coefficient (r) between the data and standardized quantile for the specified distribution is smaller than the critical r^* (derived by Looney and Gullledge, 1985), the null hypothesis H_0 (H_0 : the data are drawn from the considered distribution) is rejected. A large significance level (i.e. 0.01) was applied to increase the power to detect non-normality. As expected, the distribution at the 0-12 and 0-20 cm soil depths differed from the one at the surface. The range of skewness values decreases markedly from the shallow layer to deeper layers: skewness ranges between -1,3 to 1,3 at 0-6 cm and this range is reduced by 50% and 40% at 0-12 and 0-20 cm, respectively. In general, surface distributions have a larger percentage of negatively skewed cases than deeper layers. This is due to the combined effect of precipitation (negatively skewed distribution are found after rainfall events) and dew (negatively skewed distributions are found also during the dry-down). Normal patterns, with low skewness are found for mid-range soil moisture contents, while highly skewed distribution (generally with more log-normal shape) are found at dry and wet conditions. 65% of the distributions were well described by both the normal and log-normal distributions. Normal or log-normal distributions were appropriate for 12% and 2% of the datasets, respectively. Neither a normal, nor a log-normal distribution was appropriate for 21% of the datasets.

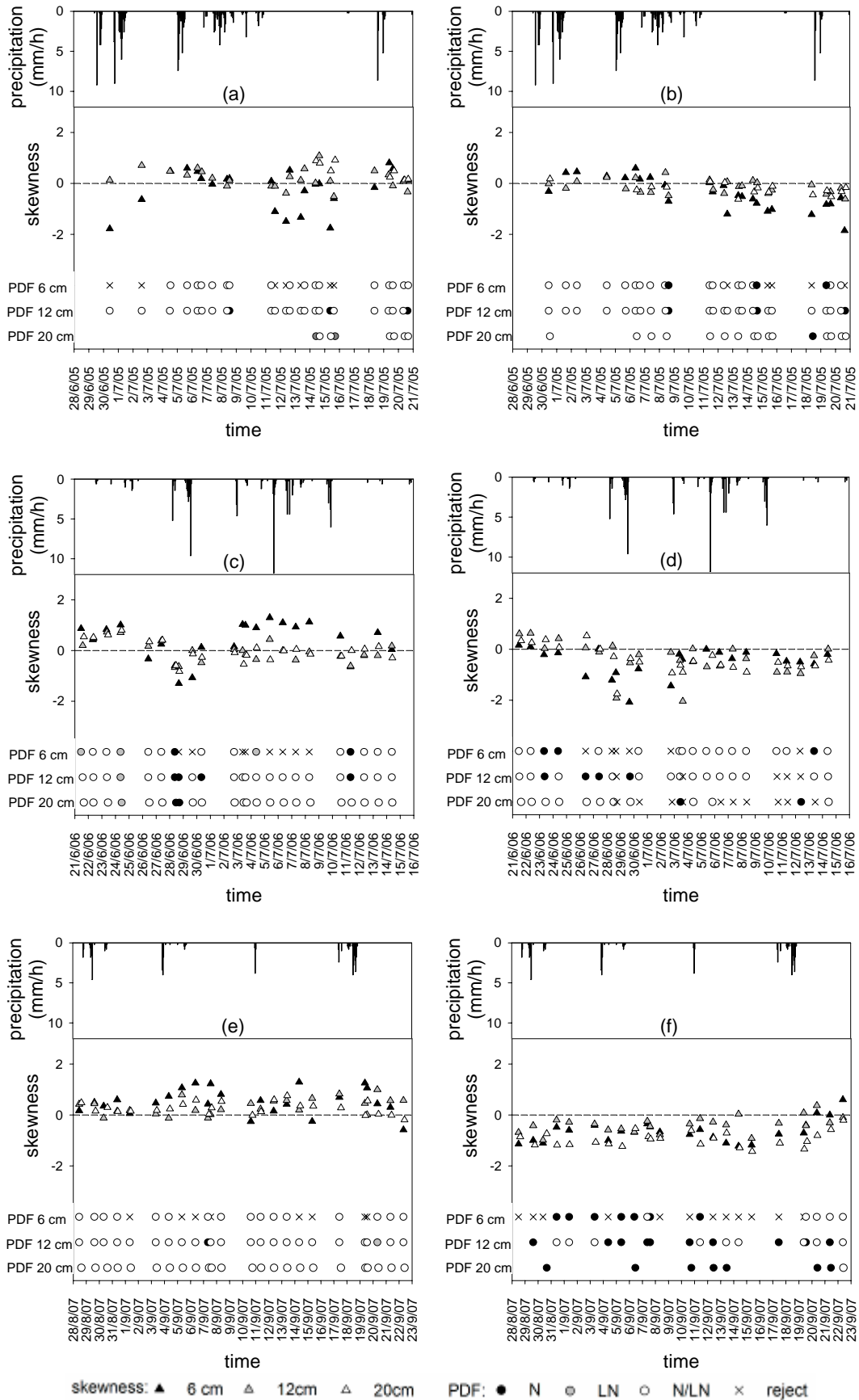


Figure 23: plots of probability density functions according to PPCC test. a) Piramide 2005; b) Emme 2005; c) Piramide 2006; d) Emme 2006 ; e) Piramide 2007; f) Emme 2007

3.3 Relationship between mean and standard deviation

Figure 24 (a-h) shows the relationship between the mean soil moisture and the standard deviation by soil depth and hillslope. While considerable scatter exists, negative relationships are evident for all soil depths and for Piramide and Emme. Overall, soil moisture variability shows the highest values at moderate moisture conditions (25–35%) and reduced values for wetter and drier conditions for all depths. When soil dried starting from saturation, a few sites remained wet resulting in an enhanced spatial variability. Examination of spatial patterns (Figure 27, Figure 28, Figure 29) shows that the spatial organization of these sites was markedly homogeneous for the three depths, suggesting similar processes at work for the three soil depths. Sites remaining wet as soil dried were generally characterised by high clay content and/or high degree of compaction. With further increasing drying, the spatial variability starts to decrease. A positive relationship between mean values and standard deviation can be identified for water content less than 25% over Piramide and Emme. These results are consistent with those reported by Ryu and Famiglietti (2005), Famiglietti et al. (1999) and Choi and Jacobs (2007). Standard deviation ranges between 3 and 8 over Piramide and Emme for 0-12 and 0-20 soil depth, while it ranges between 1 and 6,5 for 0-6 cm soil depth. The range of values is much less over Vallecola, for which only 2005 data are available; due to this reason, any relationship between statistical moment is hardly identifiable over this hillslope.

3.4 Relationship between mean and coefficient of variation

The relationships between the coefficient of variation and the mean water content for the different depths and hillslopes are shown in Figure 25 (a-h). The coefficient of variation exponentially decreases as the mean soil moisture increases for all depths over the three hillslopes, with the exception of Vallecola, for which the limited range of mean soil moisture inhibits verification of the exponential model. This is consistent with the previous studies of Famiglietti et al. (1999) and Choi and Jacobs (2007) for surface soil moisture. Jacobs et al. (2004) characterized the negative relationship between the surface mean soil moisture content and the coefficient of variation using an exponential fit for

four fields of the SMEX02. Here, the profile results are well characterized by the exponential fit

$$CV = C \exp(B\mu) \quad (9)$$

where CV is the coefficient of variation and μ is the mean value. The fitting parameters C and B describe the relative variability range and the variability change as related to mean soil moisture contents, respectively. Parameters C and B are varying consistently with depth over Piramide and Vallecola, with C and B both exhibiting a minimum for 0-12 cm soil depth and the strength of the exponential relationship increasing with depth. It is interesting to note that the fitted exponential relationships identified over Piramide and Emme for 0-12 and 0-20 cm soil depth are indistinguishable from a statistical point of view (with significance of 0.05). This shows that topographic structure has a negligible effect on the relationship between coefficient of variation and average values.

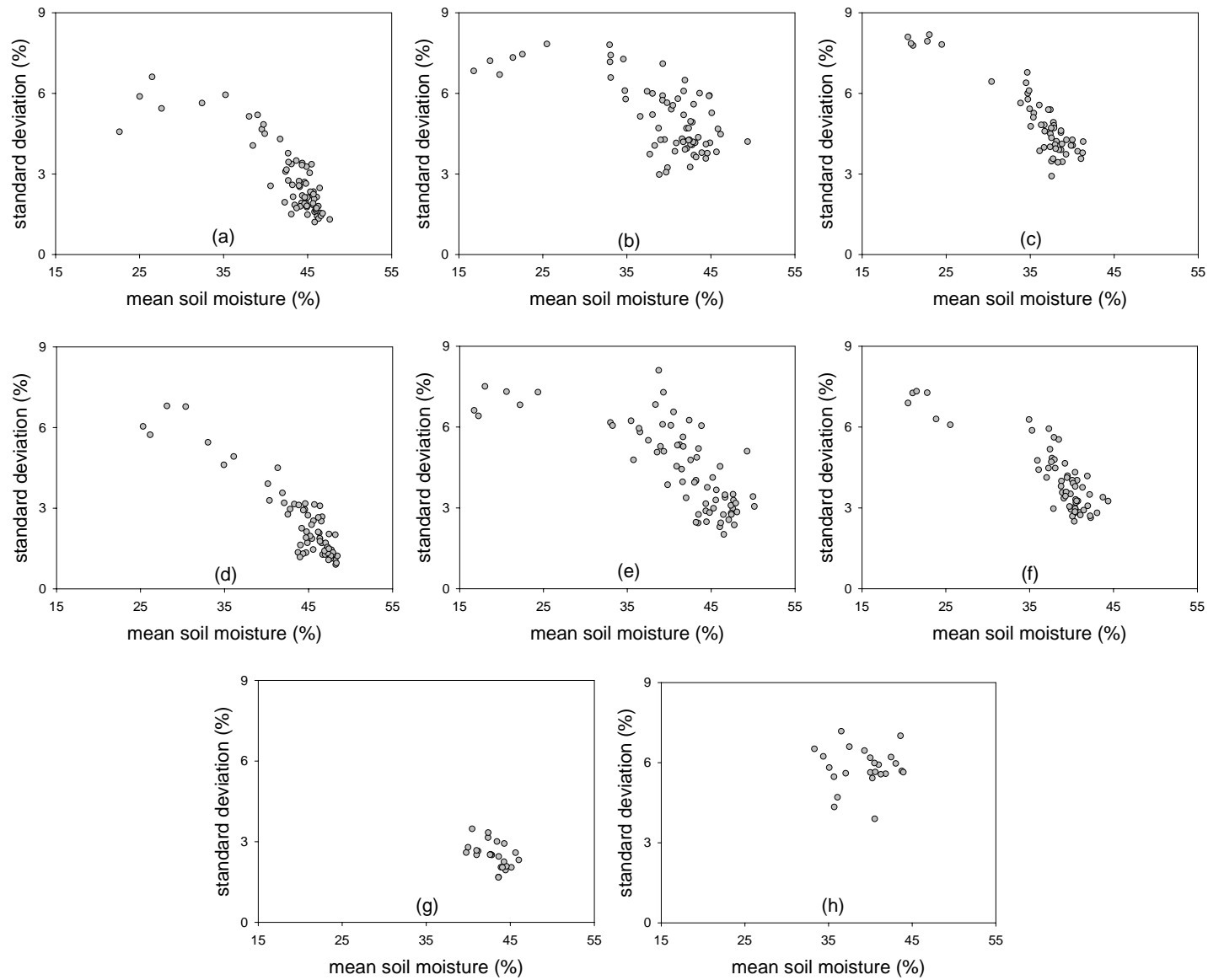


Figure 24: relationship between mean and standard deviation for 2005, 2006 and 2007 data as a whole. Piramide: a) 0-6 cm; b) 0-12 cm; c) 0-20 cm. Emme: d) 0-6 cm; e) 0-12 cm; f) 0-20 cm. Vallecola: g) 0-6 cm; h) 0-12 cm

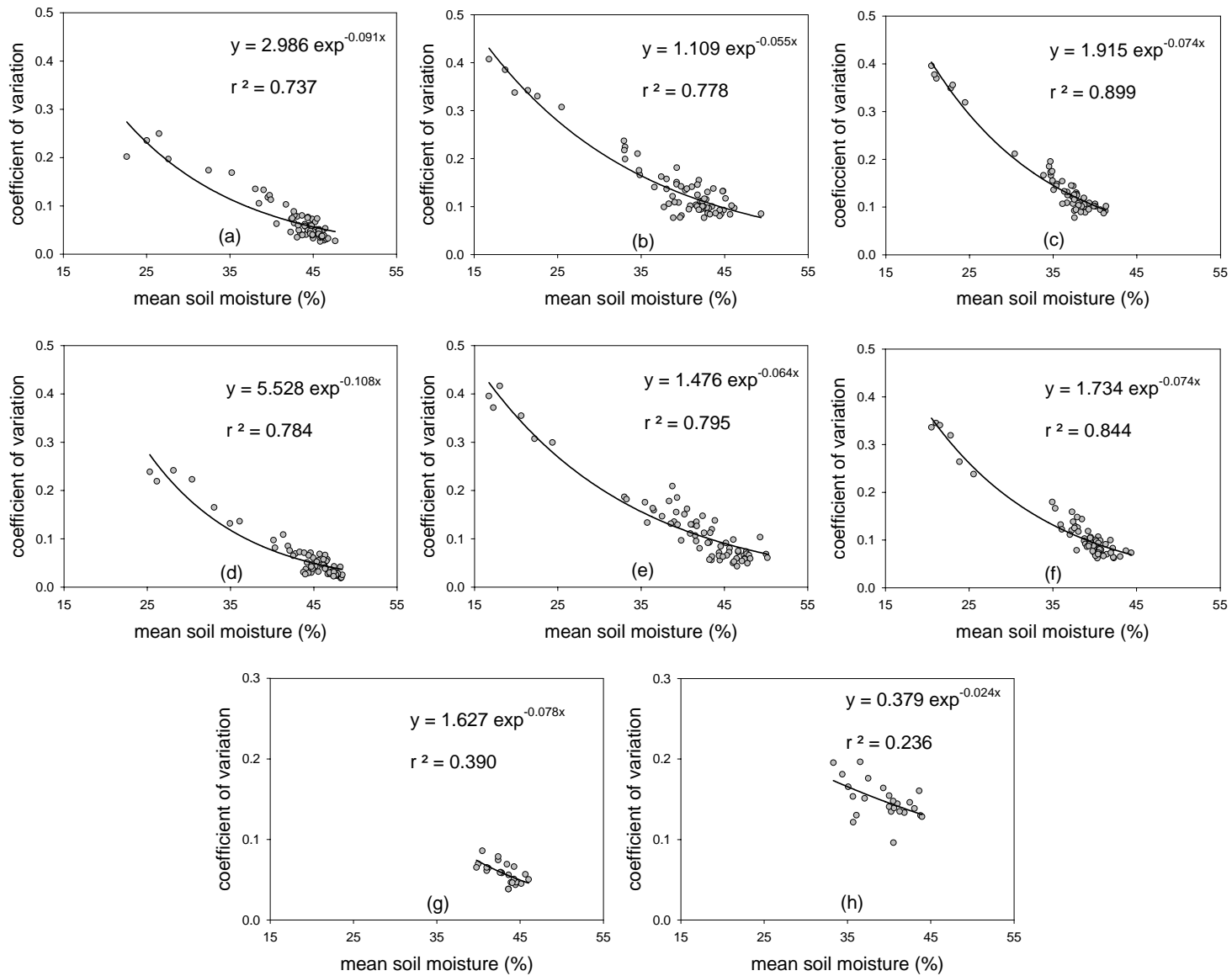
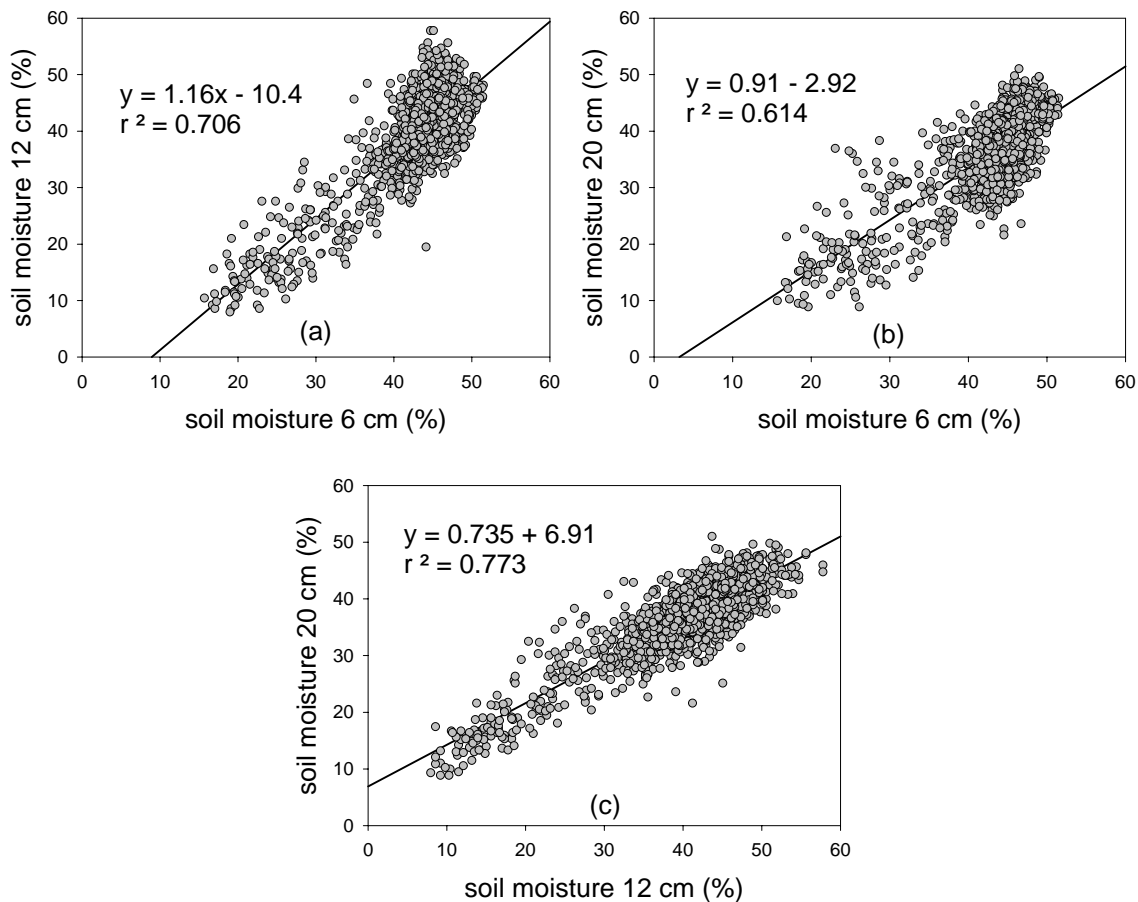


Figure 25: relationship between mean and coefficient of variation for 2005, 2006 and 2007 data as a whole. Piramide: a) 0-6 cm; b) 0-12 cm; c) 0-20 cm. Emme: d) 0-6 cm; e) 0-12 cm; f) 0-20 cm. Vallecola: g) 0-6 cm; h) 0-12 cm

3.5 Correlation between point measurements at different depths

Correlation between point measurements at different depths are shown as scatter plots in Figure 26 (a-g) for the three hillslopes (in Vallecola only 0-6 cm depth and 0-12 cm depth soil moisture data for 2005 could be compared). Scatter plots suggest that a positive correlation existed between moisture contents over the three depths for the three sites, and that the relationships were generally relatively good, particularly over Piramide and Emme, with R^2 ranging from 0.61 to 0.80. Over Vallecola, where only 2005 data were collected, R^2 between 0-6 and 0-12 cm depth soil moisture pairs is lower and amounts to 0.41. Relatively large correlations are reported for relationships between 0-6 and 0-12 cm depth, and for 0-12 and 0-20 cm depth (with R^2 ranging from 0.77 to 0.80), probably due to the proximity of the sampled depths. The relationships between 0-6 cm depth and 0-20 cm depth are generally characterized by lower correlations, with R^2 equal to 0.61 and 0.69 for Piramide and Emme respectively. All these linear relationships are significant with alpha equal to 0.01.



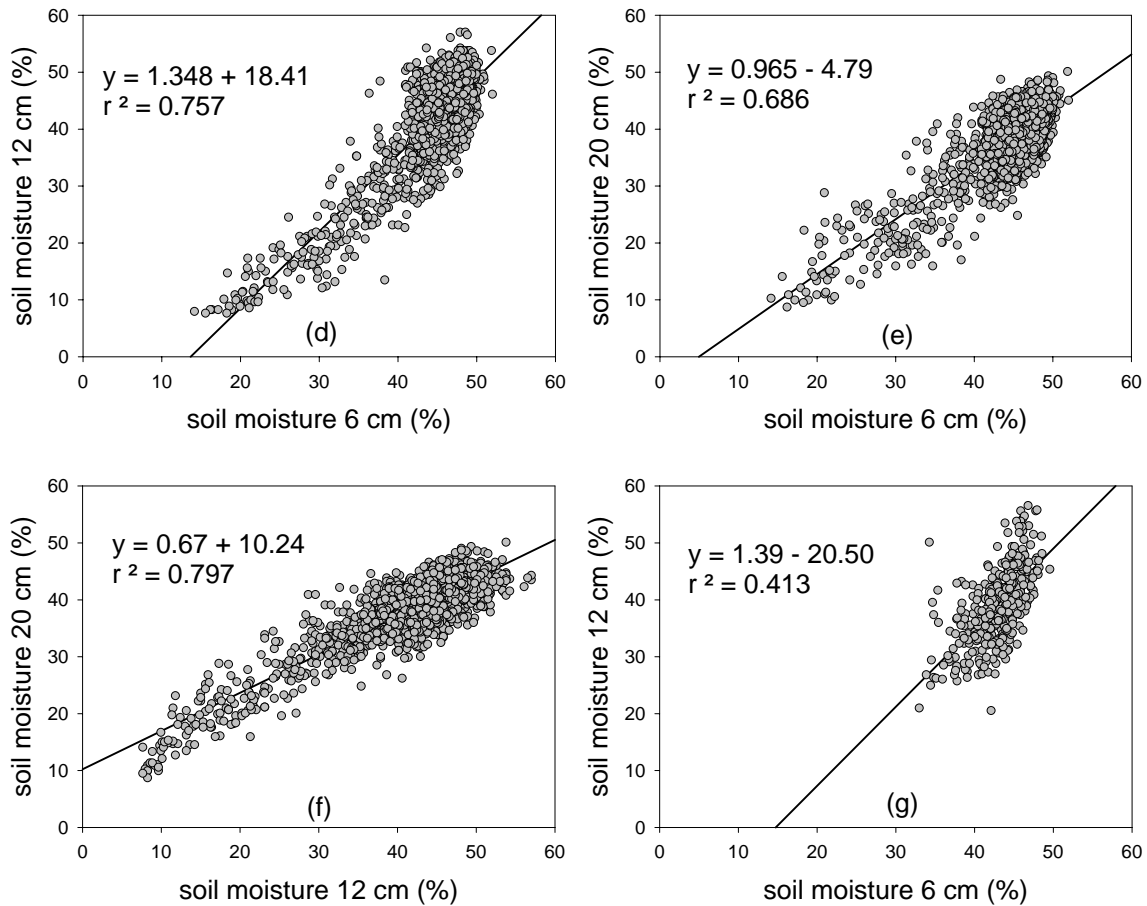


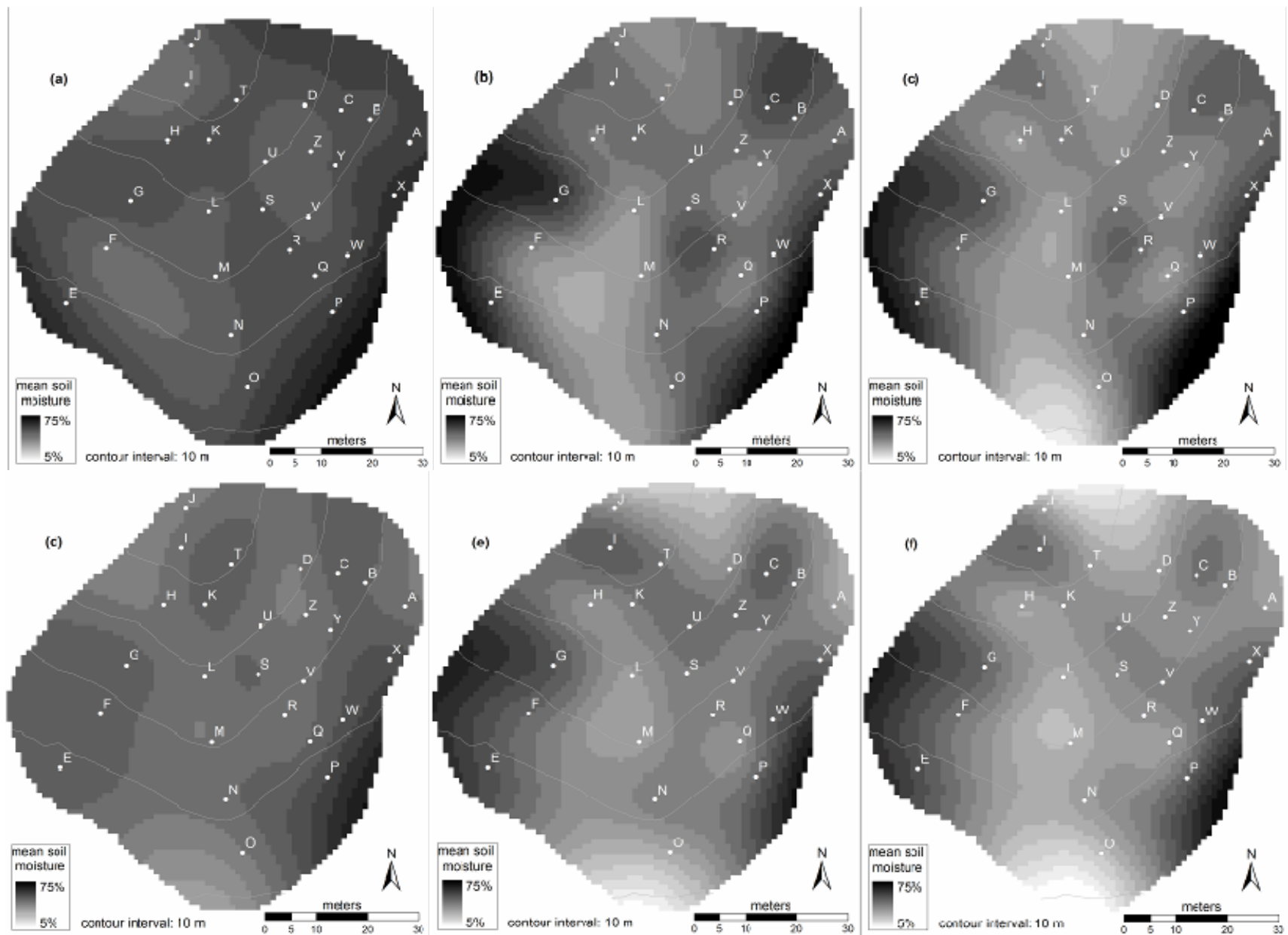
Figure 26: scatter plots for 2005, 2006 and 2007 soil moisture data in total at different depths. Piramide: a) 0-6 cm vs. 0-12 cm; b) 0-12 cm vs. 0-20 cm, c) 0-6 cm vs. 0-20 cm. Emme: d) 0-6 cm vs. 0-12 cm; e) 0-12 cm vs. 0-20 cm; f) 0-6 cm vs. 0-20 cm. Vallecola: g) 0-6 cm vs. 0-12 cm

Spearman rank correlation coefficients (ρ) for overall water content data were also computed and reported in Table 12. ρ values are all significant at 0.01 and confirm the good correlation previously observed; again, the best correlation is shown between 0-12 and 0-20 cm layers. Moreover, because of the ranking nature of this non parametric coefficient, high correlation values suggest a similar organization of soil moisture data in every layer and a good persistence of spatial patterns with depth.

Table 12: Spearman rank correlation coefficient for the complete soil moisture dataset 2005, 2006 and 2007

Piramide	0-6 cm	0-12 cm	0-20 cm
0-6 cm	1		
0-12 cm	0.636	1	
0-20 cm	0.620	0.795	1
Emme	0-6 cm	0-12 cm	0-20 cm
0-6 cm	1		
0-12 cm	0.645	1	
0-20 cm	0.598	0.766	1
Vallecola	0-6 cm	0-12 cm	
0-6 cm	1		-
0-12 cm	0.676	1	-

Visual comparison indicates a good consistency between patterns: generally, wettest and driest points are the same at the three depths (for the wettest locations, see points E, P, X on Piramide site, and A, C, V on Emme site; for the driest locations, see points V, Q and the central area in Piramide, L, K, J forming the middle part in Emme site, G, O, K, J in Vallecola site). It is interesting to note that these spatial patterns are in general non consistent with topography (gullies are not wetter than hillslopes), with the notable exception of Piramide. For this site, drier points are located over the main ridge, reflecting higher exposure to winds and more active transpiration processes. Overall, spatial organization and spatial consistency is controlled by soil effects, reflecting high organization in the distribution of soils. This is consistent with the pedological characteristics of these soils, which exhibit a relatively homogeneous vertical structure. It has been noted that soil moisture spatial variability is partially controlled by borrows due to borrowing mammals.



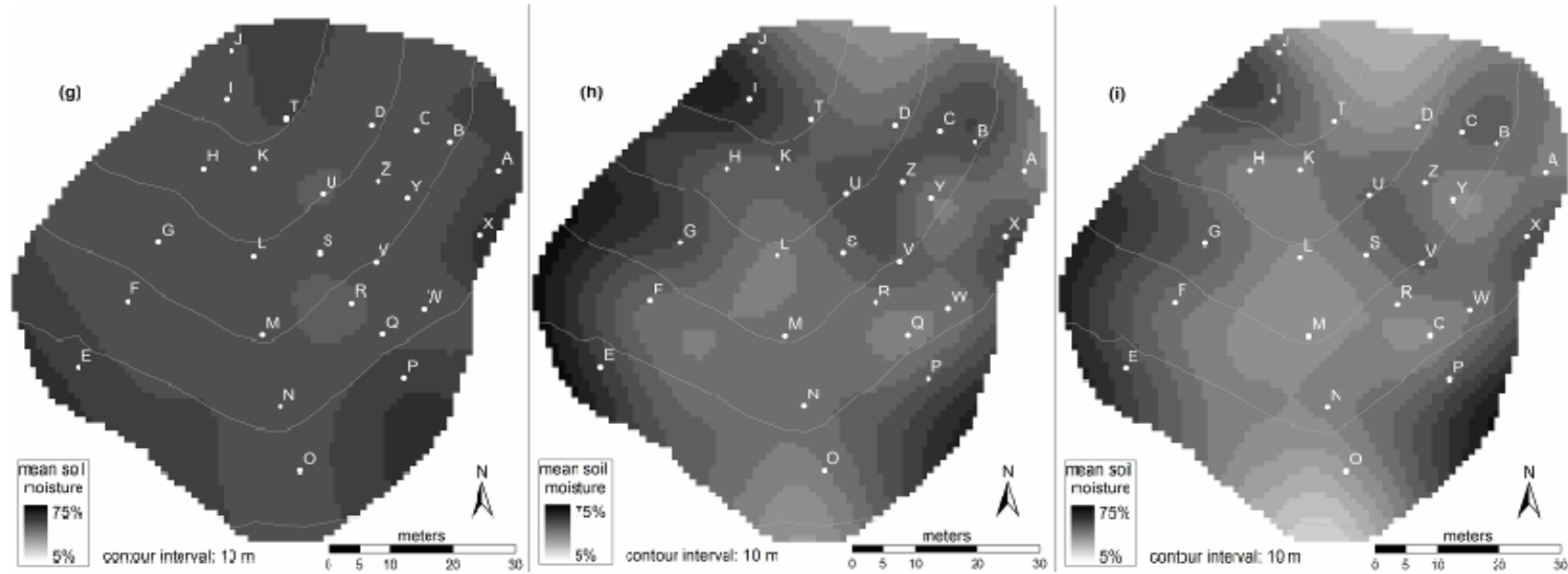
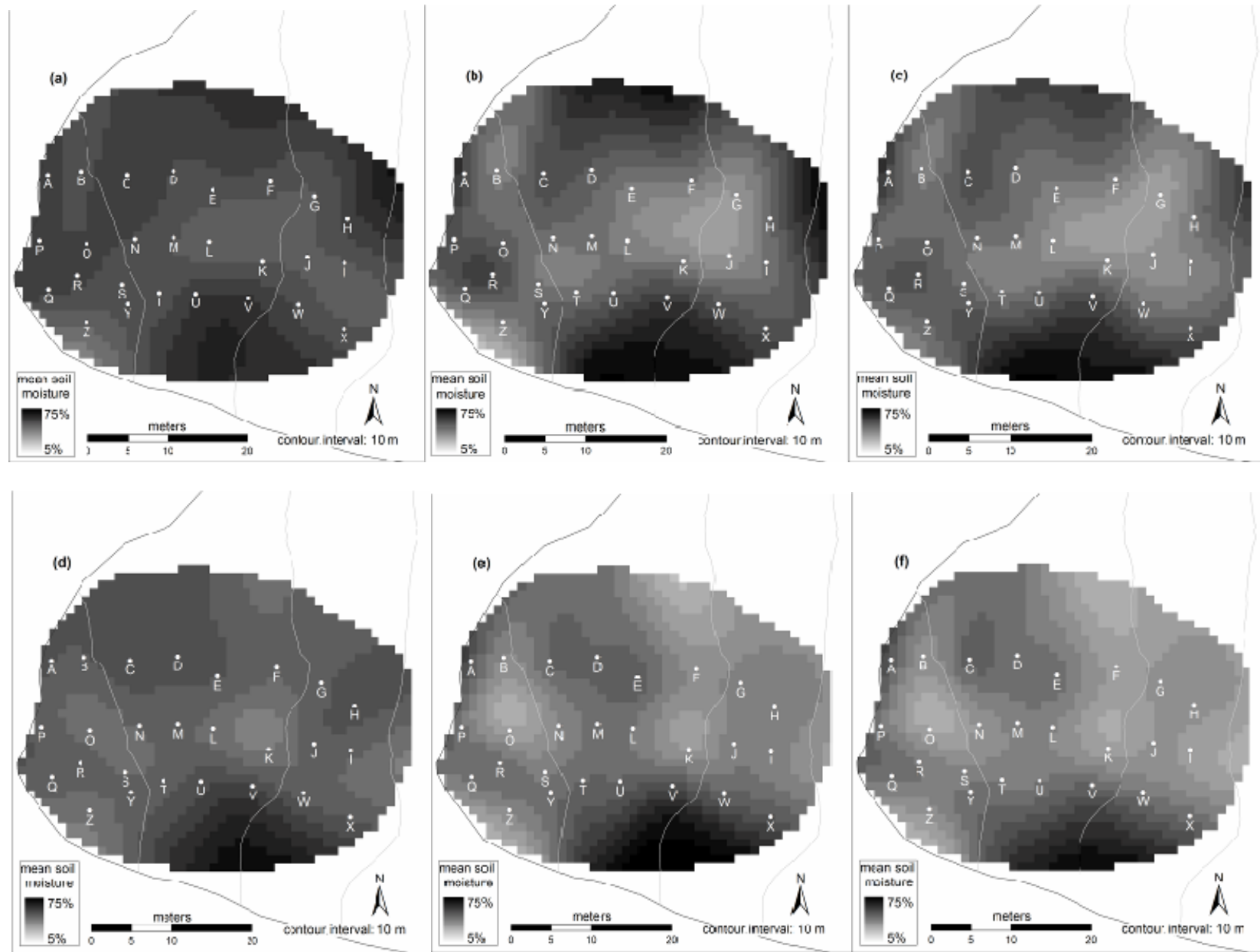


Figure 27: maps of mean soil moisture at Piramide site at different depths over three years. 2005: a) 0-6 cm; b) 0-12 cm; c) 0-20 cm (only common sampling times are considered); 2006: d) 0-6 cm; e) 0-12 cm; f) 0-20 cm; 2007: g) 0-6 cm; h) 0-12 cm; i) 0-20 cm



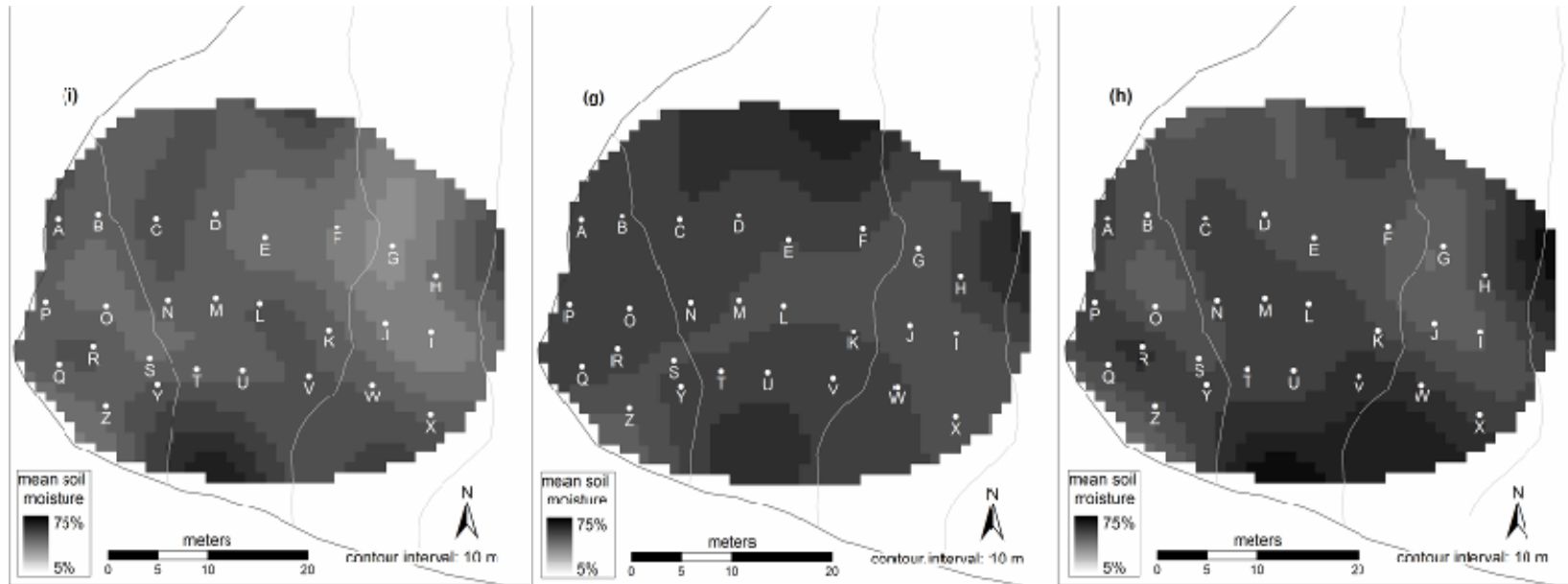


Figure 28: maps of mean soil moisture at Emme site at different depths over three years. 2005: a) 0-6 cm; b) 0-12 cm; c) 0-20 cm (only common sampling times are considered); 2006: d) 0-6 cm; e) 0-12 cm; f) 0-20 cm; 2007: g) 0-6 cm; h) 0-12 cm; i) 0-20 cm

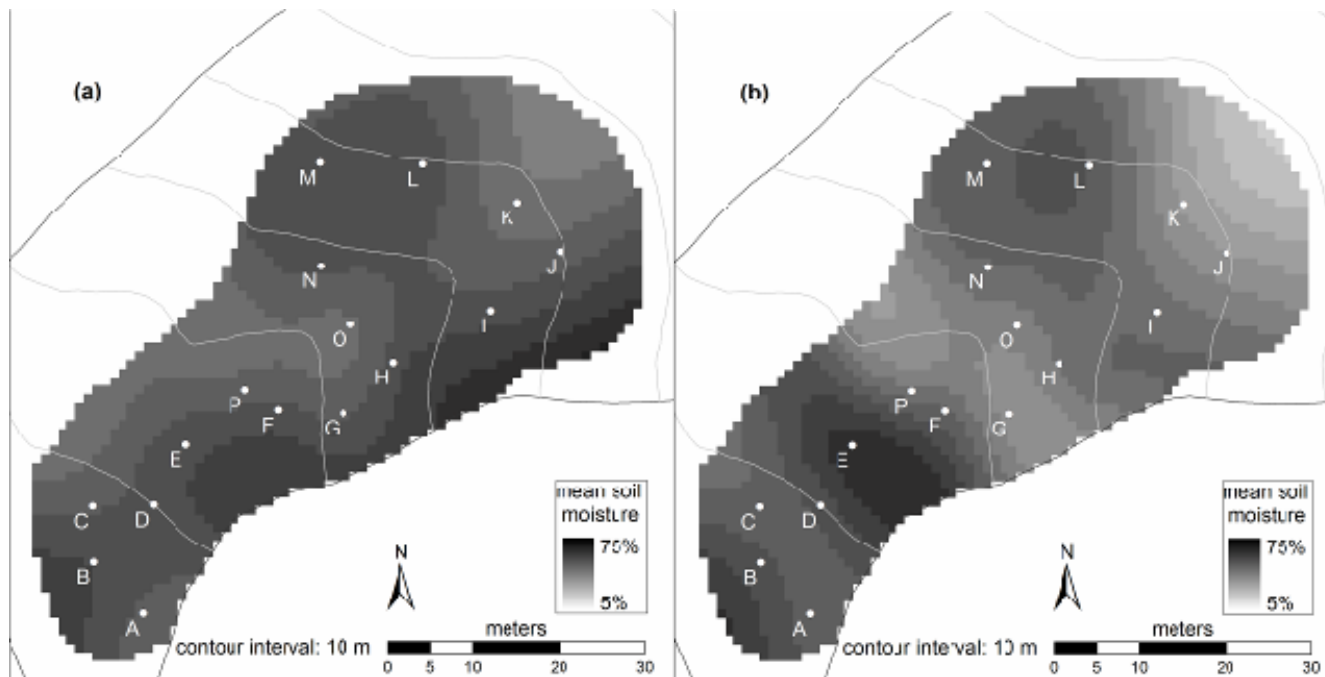


Figure 29: maps of mean soil moisture at Vallecola site at different depths for 2005: a) 0-6 cm; b) 0-12 cm (only common sampling times are considered)

Teuling e Troch (2005) argued that vegetation, soil and topography controls interact to either create or destroy spatial variability. In our experimental hillslopes, soil structure seems to be the factor which exerts the major control on soil moisture variance in relation to its mean value. Vegetation is mainly composed by low grass alpine species which are fairly homogeneously distributed over the studied hillslopes. According to some field surveys, the influence of roots appears to be constant in space: though a certain degree of small variations can not be excluded, these diversities did not appear to influence significantly the near-surface soil properties and water fluxes.

The role of topography is of primary importance (Svetlitchnyi et al., 2003) and has been already underlined: the hillslopes main morphology controls the storage of water in concave zones and at the foot of hillslopes and determinates the lower values on the ridges; i.e., topography is indirectly related to soil moisture variability through the water content of different parts of the site. In future studies, it might be interesting to map standard deviation values and comparing them to soil moisture maps in order to verify that the wettest areas show low variability and vice versa.

Unlike other works with automatic measurements, the manual sampling of soil moisture at the three considered depths did not allow long monitoring periods; thus, in this study, seasonal changes were not included. Besides precipitation, the main climate-related features which can exert a certain control on water content variability are diel temperature range, air humidity, cloud cover, radiation, winds, dew etc.; among them, dew can be very important in keeping high soil moisture values during dry-down, as discussed in section 3.1.

Thus, changes in soil properties with depth are thought of as one of the most important factor influencing vertical water content variability, as also observed by Grant et al, (2004). Heterogeneity of soil properties increases with depth: the organic matter content decreases, the amount of fine particle size increases, compression is higher, porosity is lower and hydraulic conductivity decreases, creating assumptions for differences between surface and deeper layers.

Distribution of soil moisture over different depths: concluding remarks

Analysis of soil moisture data at 0-6, 0-12 and 0-20 cm depth is presented for three experimental hillslopes with steep relief and shallow soil depth in the Dolomites (central-eastern Italian Alps). The data have been collected during three summer seasons (2005, 2006 and 2007) with different precipitation distribution. The hillslopes have mainly convex, planar and concave topographic structure and have been described by using the two hillslope similarity parameters approach. Analysis of soil moisture data showed that different physical processes control the distribution of soil moisture at the three soil depths, with a marked effect of dew on the 0-6 cm soil depth layer. Due to this effect, the surface layer was usually wetter and had lower variability than deeper soil layers, particularly during dry-down. As expected, the distribution at the 0-12 and 0-20 cm soil depths differed from the one at the surface. The range of skewness values decreased markedly from the shallow layer to deeper layers. In general, surface distributions have a larger percentage of negatively skewed cases than deeper layers. This is due to the combined effect of precipitation (negatively skewed distribution were found after rainfall events) and dew (negatively skewed distributions were found also during the dry-down). Normal patterns, with low skewness were found for mid-range soil moisture contents, while highly skewed distribution (generally with more log-normal shape) were found at dry and wet conditions.

A general negative relationship has been indentified between the instantaneous hillslope averaged soil moisture and the corresponding standard deviation for all soil depths and hillslope. Vertical water content variability was mainly attributed to the increase of soil properties heterogeneity with depth. Overall, soil moisture variability showed the highest values at moderate moisture conditions (25–35%) and reduced values for wetter and drier conditions for all depths. For all the cases here examined, the spatial variability patterns were well represented by negative exponential functions between the mean and the coefficient of variation of soil moisture. The fitted exponential relationships identified over Piramide and Emme for 0-12 and 0-20 cm soil depth were indistinguishable from a statistical point of view (with significance of 0.05). This shows that topographic structure has a negligible effect on the relationship between coefficient of variation and average values. Scatter plots drawn for the whole data set and the analysis of the correlation coefficients

suggested a good persistence of patterns along the soil profile: the highest degree of correlation was observed between data collected at 0-12 and 0-20 cm. Interpolated mean soil moisture maps for each hillslope and depth were drawn and visually compared in order to assess the spatial distribution of water content: observation confirmed the higher wetness of surface layers, the distribution of dry points over ridges and wet area at the hillslope foot and the persistence of patterns at the three sampled soil depths.

CHAPTER 4: TIME STABILITY OF SOIL MOISTURE

Introduction

An approach to characterize the mean soil moisture content at the hillslope or catchment scale by using minimal measurements for the spatio-temporal variability of soil moisture is the time stability concept (Vachaud et al., 1985). Temporal stability was defined by these authors as the time-invariant association between spatial location and classical statistical parameters of a given soil property; the concept was reviewed by Kachanoski and de Jong (1988) who described time stability of soil moisture as the temporal persistence of a spatial pattern. Because the measurement of soil moisture requires sophisticated techniques, is time consuming, and is hence costly, the aim of these studies was to develop a method that would reduce the number of measuring points required for characterising the behaviour of the soils of a given area. When a field or a small watershed is repeatedly surveyed for soil water content, sites often can be spotted where soil is consistently wetter or consistently dryer than average across the study area. Existence of such sites is important for selection of sites to infer the area-average soil water content to use at coarser scale characterization and simulation, that is, to compare with remote sensing data or establishing field- or catchment-wide antecedent moisture conditions for runoff simulations (Grayson and Western, 1998). Grayson and Western (1998), Mohanty and Skaggs (2001), Jacobs et al. (2004), Cosh et al. (2004), Martinez-Fernandez and Ceballos (2005) and Starks et al. (2006), among others, demonstrated that a few time stable sites well represent the mean soil moisture within small watersheds. Particularly, Grayson and Western (1998) use the concept of time stability to investigate the existence of certain parts of the landscape which consistently exhibit mean behaviour of soil moisture irrespective of the overall wetness of the whole study area: they called this parts CASMM (Catchment Average Soil Moisture Monitoring) sites. More recently, Martinez-Fernandez e Ceballos (2005) reviewed this concept introducing the equivalent idea of RMSM (Representative Mean Soil Moisture) stations, defined as those measurement points representative of the mean soil moisture of the

entire catchment. There has been considerable debate as to whether temporal stability is greater in dry periods or in wet ones. Certain authors feel that there is greater stability during dry periods (Robinson and Dean, 1993; Famiglietti et al., 1998, Martinez-Fernandez and Ceballs, 2003, Grant et al., 2004), while others consider that instability is greater when the soil contains less water (Van Wesenbeeck and Kachanoski, 1988, Gómez-Plaza et al., 2000, Qiu et al., 2001, Hupet and Vanclooster, 2002); moreover, others found mixed situations (Lin, 2006). These studies generally examined time stability for gentle topographies. Few studies have investigated the validity of this approach for mountainous settings. In general, the spatial variability of soil moisture in mountainous regions is expected to be higher relatively to other landscapes due to heterogeneous conditions of surface and bedrock topography, soil characteristics, wind patterns, interaction between evaporation, condensation and precipitation. However, only few field studies have examined the characteristics of soil moisture patterns in steep terrain and high altitude (above tree line) conditions (Grant et al., 2004).

This section of the thesis aims at evaluating the temporal stability of water content patterns at three soil depths at the hillslope scale.

Results and discussion

Temporal stability of soil moisture patterns at three depths over the experimental hillslopes was assessed by a multiple approach: i) ranking stability analysis; ii) slope-intercept analysis of linear regression; iii) autocorrelation analysis; (iv) evolution of correlation against mean soil moisture over time and relationship with piezometric increase.

4.1 Ranking stability analysis

The primary method for determining the temporal stability of a soil moisture field is the mean relative difference plot. This plot represents the ability of a particular soil moisture location to estimate the average over the ensemble of soil moisture measurements. Building on Vachaud et al. (1985) and Grayson and Western (1998), this type of analysis was applied to the data collected over the three experimental hillslopes. The relative difference is defined as:

$$\delta_{i,j} = \frac{S_{i,j} - \bar{S}_j}{\bar{S}_j} \quad (10)$$

where $S_{i,j}$ is the soil moisture value collected at site i and time j , and

$$\bar{S}_j = \frac{1}{n} \sum_{i=1}^n S_{i,j} \quad (11)$$

represents the mean value of soil moisture at time j , while n is the number of sites. The mean relative difference (MRD) for site i is defined as

$$MRD_i = \frac{1}{m} \sum_{j=1}^m \delta_{i,j} \quad (12)$$

where m represents the number of sampling times. Similarly, the standard deviation of the relative difference at site i is defined as:

$$\sigma_i = \sqrt{\frac{\sum (\delta_{i,j} - DRM_i)^2}{m}} \quad (13)$$

The mean relative difference gives a direct measure of how a particular site compares to the average of the hillslope, whether it is consistently greater or less than the mean and how variable is such relationship. The mean relative difference of each site is then plotted by rank with error bounds of one standard deviation of the relative differences to determine which site best estimates the mean of the watershed. There are two criteria for selecting the ideal site for average soil moisture estimation. Proximity of a site's mean relative difference to zero indicates that it can accurately estimate the hillslope average and small standard deviations (narrow error bars) indicate low variance of that estimate. If a site has both of these characteristics, it can be concluded that it accurately and precisely predicts the hillslope averaged soil moisture.

Plots reported in Figure 30, Figure 31 and Figure 32 show the time stability results by depth and by year for Piramide, Emme and Vallecola, respectively. Negative or positive mean relative differences indicate that corresponding sites are drier or wetter compared to the field mean soil moisture. Several features are noteworthy in these figures. First, the figures show a relatively strong temporal stability in the ranks of the monitoring sites and with depth; in fact, all values of MRD are fairly low, suggesting a good overall time stability of moisture patterns. However, MRD values closest to 0 and with the lowest standard deviation (small error bars) are observed for 2005 and 2007 whereas MRD is consistently greater in 2006 at each sampling depth. We relate this difference to the diverse distributions of rainfalls during the three sampling periods: 2005 and 2007, independently of the total amount of precipitation occurred, showed a similar repartition of rainfalls, presenting an alternation between rain events and some successive sunny days; on the contrary, in the 2006 field campaign, a series of rainfalls occurred at short distance not allowing a clear division between wet and dry periods (hyetographs can be seen in Figure 20, Figure 21 and Figure 22).

At 0-6 soil depth, the MRD ranges between -0.11 and 0.12 for 2005 across the three hillslopes and increases slightly for 2006, while the lowest values, ranging between -0.7 and 0.9, are observed in 2007. In general, absolute values of MRD increase at 0-12 cm depth and then remain stable at 0-20 cm depth, hence reflecting a common pattern arising from the statistical analysis of data.

Standard deviation of relative difference increases generally from 0-6 cm depth (with mean values ranging around 0.03 for 2005, around 0.083 for 2006 and 0.025 for 2007) to 0-12 cm depth (where the mean values ranges from 0.049 to 0.062 for 2005, around 0.13 for 2006 and 0.049 for 2007), and then it slightly decreases from 0-12 cm depth to 0-20 cm depth (where the mean values range around 0.04 for 2005, around 0.11 for 2006 and around 0.041 for 2007), reaching the lowest values in 2007 dataset.

For Piramide, the sampling point “s” is always included, for the three soil depths and for the three years, among the sampling sites representing hillslope average soil moisture within 3% volumetric soil moisture. Another representative sampling site is point “k”, which represents hillslope average soil moisture within 3% volumetric water content for all situations, with the exception of 0-20 soil depth for 2006. Temporal standard deviation ranges between 3% and 18% and between 3% and 16% for “s” and for “k”, respectively. Site “k” is located on the upper part of the ridge of the convex hillslope, whereas site “s” is located at a central position on the lateral hillside. For Emme, site “m” represents hillslope average soil moisture within 3% volumetric soil moisture for all situations, with the exception of 0-6 cm soil depth for 2005 and 0-12 cm for 2007. Temporal standard deviation ranges between 3% and 19% for this site. Site “m” is located mid slope of the Emme planar hillslope. On Vallecola, for which only 2005 data are available, sites “n”, “f” and “i” represent hillslope average soil moisture within 3% volumetric soil moisture for both 0-6 and 0-12 soil depth. Temporal standard deviation ranges between 3% and 13% for these sites, which are also located in a rather central position of this hollow.

A comparison of the mean relative difference rankings between soil depths and sampling years was conducted using the Spearman rank correlation coefficient:

$$\rho = 1 - 6 \sum \frac{d^2}{N(N^2 - 1)} \quad (14)$$

where d is the difference in rank of the corresponding variables. The closer is ρ to 1, the more stable the process involved. All possible combinations of depths were examined by comparing all depths and both sampling years, for a total of 73 non-trivial intercomparisons. Results are reported in Table 13. In general,

correlation coefficient is relatively high, showing that time stability patterns identified using surface measurements are preserved also for 0-12 and 0-20 soil depths and across years. In thirteen cases out of those considered here, significance was higher than 0.05. These cases always included inter-annual comparison involving 0-6 cm soil depth: this shows that the climatic differences between 2005, 2006 2007 and have a major influence on time stability when comparing surface data with deeper values. Martinez-Fernandez and Ceballos (2005) found that for comparable absolute values of the mean relative differences, dry sites had lower standard deviations than wetter sites at several soil depths (i.e., 0–100 cm). Jacobs et al. (2004) and Mohanty and Skaggs (2001) confirmed this finding for surface soil moisture measurements. In our study, drier sites and wetter sites have comparable standard deviations at the three soil depths and at the three hillslopes, probably because of the wetter situations analysed here. Based on this finding, recommended time stable sampling sites may include either slightly drier or wetter sites.

Table 13: Spearman rank coefficients reported for MRD, for the three different depths and the three years (two layers and one year for Vallecolla): a) Piramide; b) Emme; c) Vallecolla
a)

Piramide	6cm 2005	12cm 2005	20 cm 2005	6 cm 2006	12cm 2006	20 cm 2006	6cm 2007	12cm 2007	20cm 2007
6 cm 2005	1								
12 cm 2005	0.682	1							
20 cm 2005	0.571	0.862	1						
6 cm 2006	0.536	0.439*	0.579	1					
12 cm 2006	0.286**	0.597	0.682	0.781	1				
20 cm 2006	0.410*	0.692	0.850	0.726	0.888	1			
6 cm 2007	0.388**	0.249**	0.394*	0.284**	0.167**	0.305	1		
12 cm 2007	-0.032**	0.511	0.519	0.187**	0.587	0.545	0.443*	1	
20 cm 2007	0.160**	0.616	0.761	0.412*	0.717	0.839	0.490*	0.839	1

b)

Emme	6cm 2005	12cm 2005	20 cm 2005	6 cm 2006	12cm 2006	20 cm 2006	6cm 2007	12cm 2007	20cm 2007
6 cm 2005	1								
12 cm 2005	0.783	1							
20 cm 2005	0.651	0.845	1						
6 cm 2006	0.628	0.522	0.315**	1					
12 cm 2006	0.478*	0.693	0.519	0.782	1				
20 cm 2006	0.530	0.701	0.627	0.675	0.914	1			
6 cm 2007	0.917	0.685	0.603	0.502	0.414*	0.512	1		
12 cm 2007	0.322**	0.683	0.547	0.203**	0.564	0.619	0.315**	1	
20 cm 2007	0.411*	0.662	0.651	0.185**	0.511	0.630	0.499	0.877	1

c)

Vallecola	6 cm 2005	12 cm 2005
6 cm 2005	1	
12 cm 2005	0.747	1

*: not significant at 0.01, significant at 0.05; ** : not significant at 0.05

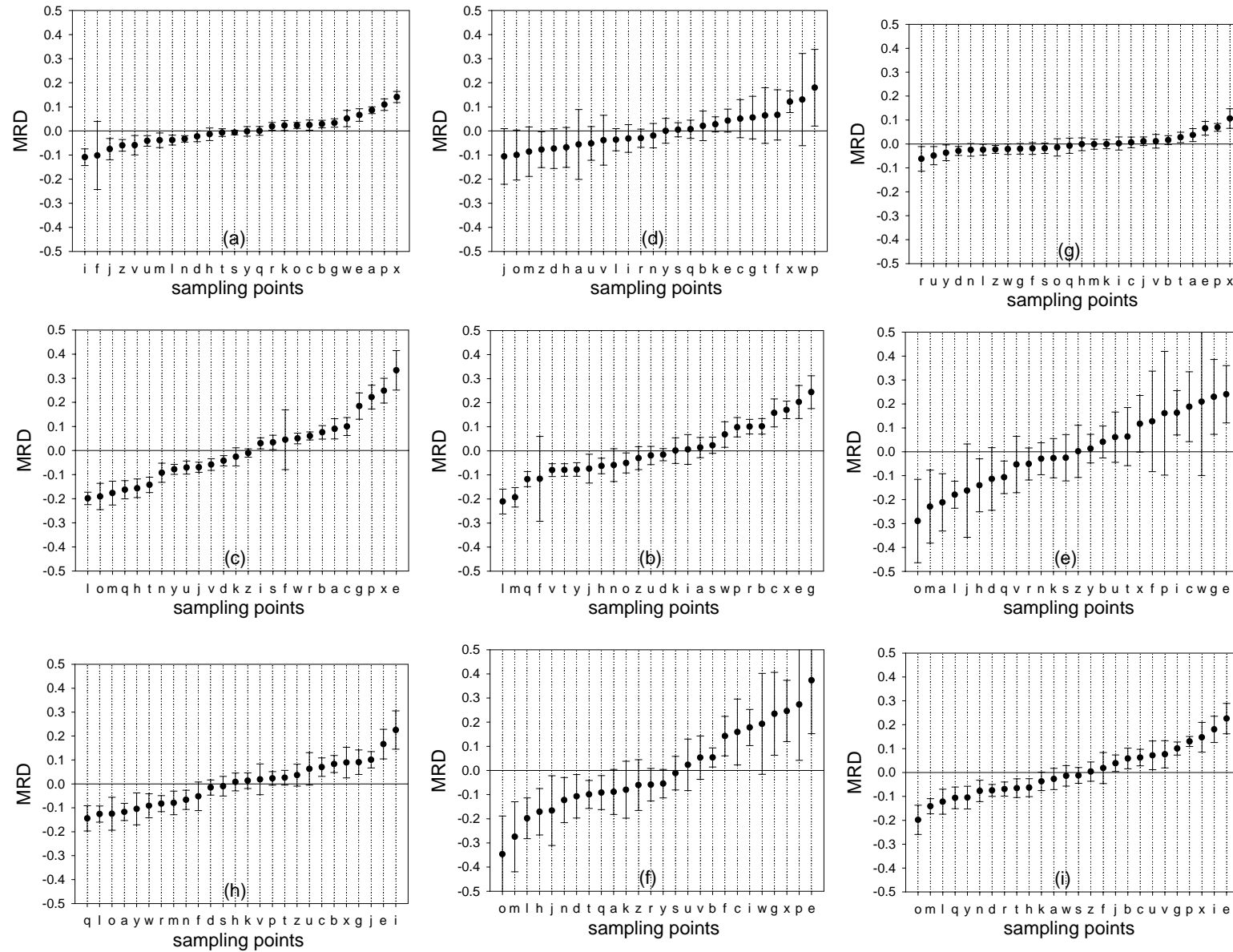


Figure 30: ranked ordered mean relative difference with standard deviation error bars for Piramide: a) 0-6 cm 2005; b) 0-12 cm 2005; c) 0-20 cm 2005; d) 0-6 cm 2006; e) 0-12 cm 2006; f) 0-20 cm 2006; g) 0-6 cm 2007; h) 0-12 cm 2007; i) 0-20 cm 2007

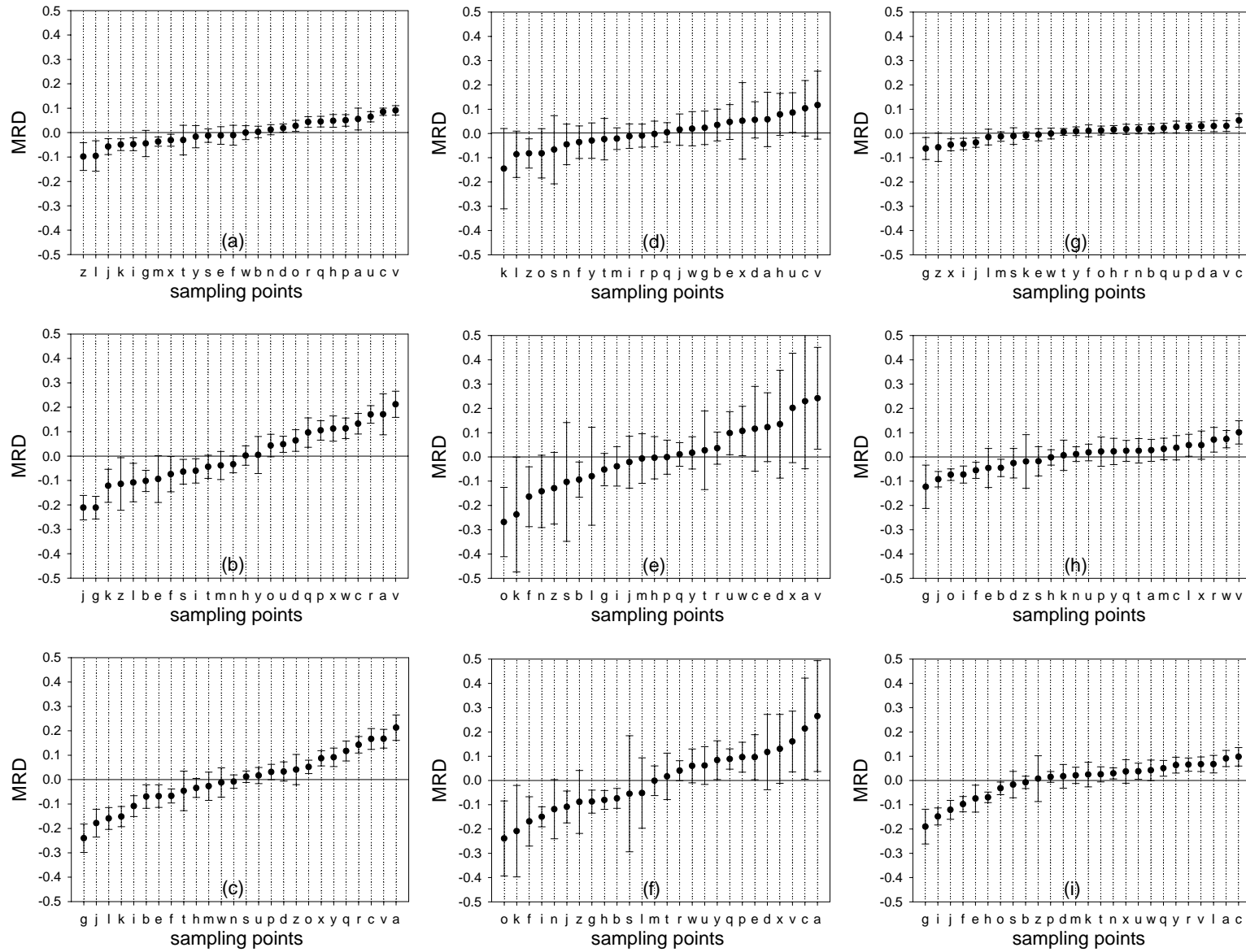


Figure 31: ranked ordered mean relative difference with standard deviation error bars for Emme: a) 0-6 cm 2005; b) 0-12 cm 2005; c) 0-20 cm 2005; d) 0-6 cm 2006; e) 0-12 cm 2006; f) 0-20 cm 2006; g) 0-6 cm 2007; h) 0-12 cm 2007; i) 0-20 cm 2007

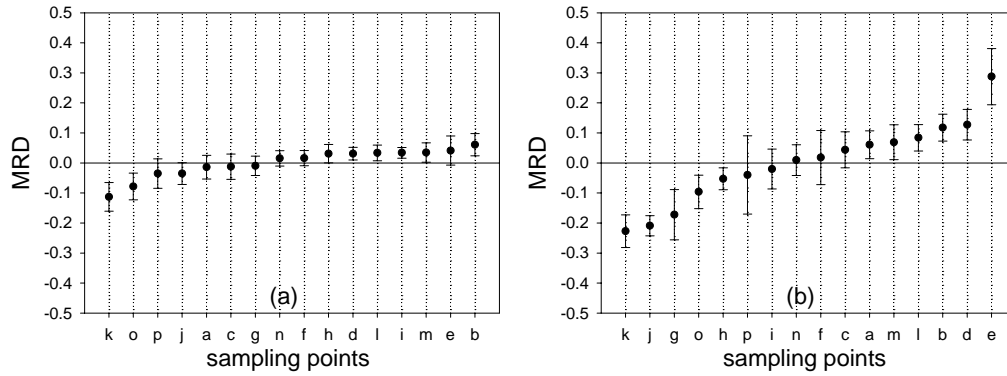


Figure 32: ranked ordered mean relative difference with standard deviation error bars for Vallecola: a) 0-6 cm 2005; b) 0-12 cm 2005

4.2 Slope-intercept analysis of linear regression

In addition to the ranking stability analysis, temporal stability of soil moisture patterns can be evaluated by the slope-intercept analysis of linear regression, suggested by Kachanoski and de Jong (1988) and followed by other authors (Grant et al., 2004, Lin, 2006). Given the linear relationship between soil water content at successive times across all spatial locations (Vachaud et al, 1985), a linear regression and simple correlation between consecutive time intervals can be thought as good indicators of time stability. Regression between water storage θ at a site i at two consecutive times (t_1 and t_2) can be expressed as:

$$\theta_{t_2}(i) = a_{t_2-t_1}\theta_{t_1}(i) + b_{t_2-t_1} + \varepsilon_{t_2-t_1} \quad (15)$$

where $a_{t_2-t_1}$, $b_{t_2-t_1}$ and $\varepsilon_{t_2-t_1}$ are the regression slope, intercept and error, respectively. Spearman rank correlation coefficient (equation 14) was preferred to Pearson's due to the non normal distribution of data. A two-tail t test with a high level of significance ($\alpha=0.01$) was performed for soil moisture data at three depths to test whether the intercept (b) in equation 15 is significantly different from 0 and an F test was used to test whether slope (a) is significantly different from 1. Thus, four temporal stability conditions can be described using all the possible combinations of a and b (Grant et al., 2004, Lin, 2006):

Condition "a": it occurs if a and b are not significantly different from 1 and 0, respectively. Water contents at different times are nearly identical; it may be

due to relatively little input and/or output, or output at each site equals input, or to an extended period that buffers catchment response.

Condition “**b**”: it is characterized by b significantly different from 0 while a is not significantly different from 1. This implies a nearly uniform change in soil water pattern over catchment; it may be caused by uniform input (rain) and/or output (plant water uptake, shallow evaporation and/or drainage).

Condition “**c**”: it is characterized by b near to 0 and a significantly different from 1. This suggests non-uniform change with time; may be due to a lack of uniform input/output while some locations are drying or wetting more than others or redistribution occurs.

Condition “**d**”: it occurs when a is significantly different from 1 and b is significantly different from 0. This condition indicates a complex and non-uniform change; caused by non-uniform input (rain-on-snow or snowmelt) or output (transpiration) or a combination of uniform input/output and redistribution.

Table 14: four time stability conditions according to the slope-intercept analysis of linear regression (from Grant et al., 2004, modified)

<i>Temporal stability condition</i>	<i>Slope (a) significantly different from 1</i>	<i>Intercept (b) significantly different from 0</i>
<i>Condition ‘a’ (no variation)</i>	No	No
<i>Condition ‘b’ (uniform variation)</i>	No	Yes
<i>Condition ‘c’ (non-uniform variation)</i>	Yes	No
<i>Condition ‘d’ (non uniform and complex variation)</i>	Yes	Yes

4.3 Autocorrelation analysis

Autocorrelation matrices of soil moisture values at 0-6, 0-12 and 0-20 cm depth for hillslopes Piramide and Emme in 2005, 2006 and 2007 are depicted in Figure 33, Figure 34 and Figure 35 (due to the few sampling occasions on Piramide in 2005 at 0-20 cm depth, autocorrelation matrices were not computed; besides, a smaller number of cases are available for Emme in 2005 at 0-20 cm). Spearman ρ values are shown in the lower part of each matrix whereas the four temporal stability conditions according to the slope-intercept analysis of linear

regression are presented in the upper part. Comparisons not statistically significant, both as correlation values and as letters representing the stability conditions, are marked; owing to the high level of significance ($\alpha=0.01$) chosen, poorly correlated comparison can be frequently observed. Generally, highest correlations are found for pairs of patterns near in time, while not statistically significant comparisons are usually noticed between patterns at the beginning and at the end of the monitoring period. Moreover, cases below the level of statistical significance very often correspond to those conditions which show a lack of stability according to the slope-intercept analysis of linear regression (conditions 'd'). Sometimes, a few comparisons between soil moisture patterns collected in wet and dry conditions, although marked as 'd', showed a positive correlation according to the ρ values: Spearman coefficient proves to be less sensitive and restrictive compared to Pearson's, even though correlation values are only slightly above the significance level. Generally, observation of autocorrelation matrices computed for the two hillslopes shows that the higher the water content the higher the degree of temporal stability; furthermore, for each year analyzed, correlation strongly increases with sampling depth and in a few cases all correlations are positive, according to both indicators (Piramide at 0-12 cm in 2005 and 2007, Piramide at 0-20 cm in 2006 and 2007, Emme in 2005 at 0-12 and 0-20 cm depth). However, the difference among the three years is sharp: in 2005 and 2007, high degrees of correlation are common over both sites whereas in 2006 poor correlations are more frequent: this behaviour reflects the higher values of MRD computed over the two hillslopes in 2006, confirming what has been already underlined by the ranking stability analysis. This difference is mainly imputable to the different distribution of rainfalls over time rather than to the diverse amount of total precipitation recorded during the three monitoring periods: thus, the 2006 field campaign can be quite clearly divided into wet and dry days and comparison between them tends to give moderate and low degrees of correlation. These findings suggest that when the mean water content increases across the hillslope, its spatial distribution and pattern organization tend to reflect the influence of different hydrological processes (Western et al., 2002): at small scales, in dry conditions, soil moisture appears to respond mainly to variations in vegetation and soil properties (texture, porosity...); on the contrary, during wet periods hillslope-scale processes dominate, driven by topographical factors (slope, aspect, overall

convex-concave hillslope morphology...) which also play an important role in generation and distribution of subsurface lateral flow.

(a)	30/6	2/7	4/7	5/7	6/7	6/7	7/7	8/7	8/7	11/7	11/7	12/7	12/7	13/7	13/7	14/7	14/7	15/7	15/7	18/7	19/7	19/7	20/7	20/7
30/6	1	a	a	d	b	d	b	d	d	b	d	d	d	d	d	d	d	d	d	d	d	d	d	d
2/7	0.88	1	a	b	b	b	b	b	b	b	d	d	b	d	d	b	d	d	d	b	b	b	b	b
4/7	0.76	0.89	1	b	b	b	b	b	b	b	d	d	b	d	d	b	b	c	d	b	b	b	b	b
5/7	0.62	0.70	0.77	1	a	a	a	b	b	b	b	c	b	a	a	b	a	c	a	a	b	b	b	b
6/7	0.65	0.84	0.92	0.79	1	a	a	b	b	b	d	c	b	c	a	a	a	c	c	a	b	b	b	a
6/7	0.62	0.83	0.89	0.78	0.95	1	a	b	b	b	d	d	b	d	b	b	b	c	c	a	b	b	b	b
7/7	0.81	0.90	0.87	0.85	0.88	0.87	1	b	b	b	d	d	b	d	d	b	d	c	d	a	b	b	b	b
8/7	0.57	0.78	0.84	0.80	0.88	0.85	0.84	1	a	a	c	c	a	c	c	a	a	c	c	a	a	a	a	a
8/7	0.68	0.84	0.89	0.75	0.89	0.89	0.85	0.89	1	a	c	a	a	a	a	a	a	a	a	a	a	a	a	a
11/7	0.76	0.88	0.83	0.74	0.82	0.79	0.89	0.81	0.86	1	d	c	a	a	a	a	a	c	a	a	b	b	a	a
11/7	0.25	0.37	0.55	0.67	0.58	0.53	0.47	0.62	0.57	0.49	1	a	a	a	a	a	a	a	a	c	b	b	d	a
12/7	0.31	0.48	0.61	0.61	0.59	0.60	0.49	0.61	0.66	0.57	0.86	1	b	a	a	b	a	a	a	c	b	b	b	b
12/7	0.47	0.58	0.65	0.57	0.65	0.64	0.54	0.58	0.71	0.68	0.71	0.86	1	a	a	a	a	a	a	a	b	b	a	a
13/7	0.44	0.61	0.65	0.71	0.63	0.66	0.60	0.66	0.66	0.74	0.79	0.88	0.84	1	a	b	a	a	a	c	b	b	d	b
13/7	0.47	0.58	0.66	0.60	0.64	0.62	0.59	0.59	0.66	0.74	0.73	0.85	0.91	0.87	1	b	a	a	a	a	b	b	b	b
14/7	0.55	0.68	0.73	0.52	0.71	0.68	0.66	0.64	0.75	0.77	0.70	0.82	0.82	0.78	0.89	1	a	a	a	a	b	b	a	a
14/7	0.36	0.53	0.63	0.55	0.66	0.67	0.50	0.56	0.65	0.66	0.70	0.87	0.93	0.87	0.91	0.81	1	a	a	a	b	b	b	b
15/7	0.44	0.61	0.69	0.55	0.68	0.67	0.56	0.62	0.74	0.72	0.68	0.85	0.96	0.83	0.91	0.86	0.90	1	b	d	b	b	d	b
15/7	0.33	0.52	0.58	0.52	0.62	0.63	0.50	0.64	0.69	0.62	0.76	0.91	0.91	0.85	0.88	0.85	0.90	0.91	1	a	b	b	b	b
18/7	0.62	0.72	0.74	0.59	0.72	0.74	0.65	0.64	0.74	0.66	0.48	0.67	0.75	0.65	0.72	0.73	0.73	0.72	0.74	1	b	b	b	b
19/7	0.36	0.54	0.62	0.72	0.66	0.66	0.58	0.68	0.72	0.67	0.73	0.87	0.78	0.84	0.74	0.69	0.81	0.75	0.79	0.72	1	a	a	a
19/7	0.53	0.70	0.80	0.70	0.84	0.81	0.69	0.81	0.85	0.75	0.69	0.82	0.83	0.77	0.81	0.81	0.84	0.82	0.83	0.87	0.83	1	a	a
20/7	0.49	0.63	0.74	0.66	0.72	0.77	0.65	0.69	0.76	0.60	0.60	0.81	0.70	0.68	0.71	0.74	0.74	0.70	0.76	0.89	0.78	0.90	1	a
20/7	0.50	0.66	0.72	0.59	0.72	0.72	0.59	0.62	0.69	0.63	0.66	0.84	0.84	0.78	0.81	0.79	0.88	0.80	0.81	0.86	0.79	0.90	0.85	1

(b)	30/6	2/7	4/7	5/7	6/7	6/7	7/7	8/7	8/7	11/7	11/7	12/7	12/7	13/7	13/7	14/7	14/7	15/7	15/7	18/7	19/7	19/7	20/7	20/7
30/6	1	a	a	b	b	b	b	b	b	b	b	b	b	b	b	b	b	b	b	b	b	b	b	b
2/7	0.91	1	a	b	b	b	b	b	b	b	b	b	b	b	b	b	b	b	d	b	b	b	b	b
4/7	0.80	0.87	1	b	b	b	a	b	b	b	b	b	b	b	b	b	b	b	b	b	b	b	b	b
5/7	0.92	0.93	0.87	1	a	a	a	b	b	b	b	b	b	a	a	a	a	b	a	b	b	b	b	b
6/7	0.89	0.89	0.91	0.93	1	a	a	b	b	b	b	b	b	a	b	b	a	b	a	a	b	b	b	b
6/7	0.93	0.92	0.91	0.91	0.97	1	a	b	a	b	b	b	b	a	a	a	a	a	a	a	b	b	b	b
7/7	0.90	0.94	0.86	0.93	0.89	0.91	1	b	b	b	b	b	b	b	b	b	b	b	b	a	b	b	b	b
8/7	0.92	0.91	0.88	0.93	0.92	0.92	0.94	1	a	a	a	a	a	a	a	a	a	a	a	a	a	b	a	a
8/7	0.89	0.91	0.89	0.91	0.92	0.93	0.93	0.96	1	a	a	a	a	a	a	a	a	a	a	a	b	b	b	b
11/7	0.74	0.73	0.70	0.74	0.77	0.80	0.75	0.80	0.79	1	a	a	a	a	a	a	a	a	a	a	b	b	b	b
11/7	0.68	0.69	0.62	0.68	0.67	0.69	0.69	0.72	0.70	0.93	1	a	a	a	a	a	a	a	a	c	b	b	b	b
12/7	0.71	0.71	0.64	0.74	0.73	0.74	0.72	0.75	0.74	0.94	0.93	1	a	a	a	a	a	a	a	c	b	b	b	b
12/7	0.63	0.74	0.64	0.70	0.67	0.70	0.68	0.68	0.71	0.88	0.92	0.88	1	a	a	a	a	a	a	c	b	b	b	b
13/7	0.70	0.72	0.70	0.67	0.74	0.77	0.70	0.71	0.71	0.92	0.88	0.92	0.83	1	a	a	a	a	a	c	b	b	b	b
13/7	0.72	0.75	0.70	0.77	0.74	0.77	0.70	0.76	0.73	0.92	0.91	0.92	0.91	0.89	1	a	a	a	a	a	b	b	b	b
14/7	0.71	0.74	0.80	0.74	0.81	0.80	0.75	0.77	0.73	0.92	0.88	0.89	0.82	0.93	0.91	1	a	a	a	a	b	b	b	b
14/7	0.74	0.75	0.73	0.71	0.71	0.77	0.76	0.74	0.72	0.81	0.85	0.82	0.80	0.83	0.87	0.87	1	a	a	a	b	b	b	b
15/7	0.54	0.66	0.71	0.61	0.65	0.64	0.68	0.63	0.63	0.82	0.83	0.83	0.79	0.86	0.81	0.90	0.81	1	a	a	b	b	b	b
15/7	0.68	0.73	0.72	0.73	0.75	0.76	0.72	0.71	0.71	0.93	0.91	0.94	0.87	0.92	0.92	0.93	0.84	0.91	1	d	b	b	b	b
18/7	0.72	0.82	0.88	0.78	0.79	0.78	0.79	0.74	0.74	0.55	0.56	0.57	0.53	0.62	0.62	0.73	0.74	0.73	0.68	1	b	b	b	b
19/7	0.77	0.86	0.79	0.78	0.78	0.79	0.87	0.86	0.86	0.75	0.74	0.70	0.73	0.71	0.71	0.74	0.79	0.72	0.73	0.73	1	a	a	a
19/7	0.79	0.84	0.81	0.81	0.84	0.85	0.78	0.82	0.83	0.82	0.84	0.85	0.84	0.81	0.84	0.84	0.86	0.78	0.86	0.77	0.81	1	a	a
20/7	0.60	0.66	0.72	0.60	0.70	0.71	0.66	0.67	0.67	0.87	0.86	0.83	0.80	0.87	0.83	0.92	0.88	0.89	0.91	0.67	0.76	0.86	1	a
20/7	0.72	0.69	0.78	0.70	0.75	0.73	0.72	0.73	0.69	0.62	0.55	0.65	0.51	0.65	0.63	0.76	0.71	0.72	0.69	0.75	0.68	0.75	0.70	1

(c)	30/6	2/7	4/7	5/7	6/7	7/7	8/7	8/7	11/7	11/7	12/7	12/7	13/7	13/7	14/7	14/7	15/7	15/7	18/7	19/7	19/7	20/7	20/7	
30/6	1	b	a	b	b	b	b	b	b	b	b	b	b	b	b	b	b	b	d	d	b	b	d	
2/7	0.80	1	a	a	b	b	b	b	b	b	b	b	b	b	b	b	b	b	b	b	b	b	d	
4/7	0.56	0.55	1	b	b	b	b	d	d	d	b	d	b	d	b	d	d	d	d	d	d	d	b	
5/7	0.71	0.81	0.53	1	a	a	b	b	b	b	b	a	b	b	b	a	b	a	b	a	b	b	b	
6/7	0.79	0.79	0.53	0.73	1	a	b	b	b	b	b	a	a	b	b	b	a	b	a	b	b	b	b	
6/7	0.78	0.87	0.67	0.73	0.76	1	b	b	b	b	b	a	a	b	b	b	a	b	a	b	b	b	b	
7/7	0.64	0.80	0.60	0.82	0.73	0.83	1	b	a	b	b	a	a	b	a	a	a	a	a	b	b	a	a	
8/7	0.67	0.86	0.55	0.88	0.68	0.88	0.89	1	a	a	a	a	a	a	a	a	a	a	a	a	a	a	c	
8/7	0.72	0.67	0.55	0.83	0.66	0.77	0.82	0.85	1	b	b	a	a	a	b	a	a	a	a	a	b	b	a	
11/7	0.74	0.79	0.49	0.89	0.79	0.73	0.80	0.84	0.89	1	a	a	a	a	a	a	a	a	a	a	a	a	a	
11/7	0.79	0.77	0.40	0.81	0.82	0.84	0.79	0.85	0.79	0.83	1	a	b	b	a	a	a	a	a	a	a	a	a	
12/7	0.73	0.71	0.40	0.64	0.75	0.79	0.65	0.73	0.68	0.75	0.87	1	a	b	b	a	a	a	a	a	b	b	a	
12/7	0.76	0.71	0.47	0.74	0.85	0.81	0.76	0.78	0.75	0.80	0.94	0.91	1	b	b	b	a	a	a	a	b	b	a	
13/7	0.71	0.73	0.52	0.74	0.81	0.88	0.76	0.83	0.77	0.80	0.91	0.91	0.94	1	b	b	a	a	a	a	b	b	a	
13/7	0.60	0.65	0.31	0.79	0.61	0.69	0.67	0.80	0.77	0.81	0.86	0.80	0.81	0.84	1	a	a	b	a	b	a	a	a	
14/7	0.60	0.61	0.52	0.78	0.67	0.71	0.69	0.74	0.77	0.83	0.79	0.79	0.83	0.87	0.84	1	a	a	a	a	b	b	a	
14/7	0.70	0.77	0.42	0.85	0.74	0.75	0.73	0.81	0.78	0.88	0.88	0.85	0.85	0.86	0.89	0.86	1	a	a	a	b	b	a	
15/7	0.62	0.64	0.46	0.80	0.66	0.72	0.73	0.81	0.80	0.80	0.85	0.79	0.80	0.85	0.91	0.87	0.87	1	a	a	b	b	b	
15/7	0.52	0.61	0.41	0.66	0.66	0.61	0.60	0.60	0.54	0.66	0.72	0.73	0.71	0.75	0.70	0.75	0.79	0.81	1	a	b	b	a	
18/7	0.59	0.66	0.45	0.75	0.65	0.78	0.69	0.77	0.74	0.74	0.82	0.82	0.81	0.90	0.89	0.87	0.87	0.91	0.86	1	b	b	b	
19/7	0.59	0.67	0.41	0.80	0.63	0.65	0.68	0.73	0.68	0.75	0.82	0.74	0.76	0.77	0.79	0.82	0.86	0.85	0.89	0.85	1	a	a	
19/7	0.68	0.72	0.41	0.81	0.64	0.79	0.71	0.83	0.77	0.77	0.89	0.83	0.84	0.86	0.90	0.81	0.90	0.86	0.78	0.92	0.84	1	a	
20/7	0.70	0.72	0.35	0.75	0.63	0.73	0.63	0.74	0.65	0.68	0.86	0.73	0.76	0.74	0.78	0.68	0.82	0.79	0.82	0.83	0.88	0.88	1	
20/7	0.68	0.69	0.51	0.80	0.68	0.76	0.74	0.79	0.75	0.70	0.85	0.69	0.80	0.79	0.80	0.73	0.82	0.86	0.83	0.86	0.83	0.91	0.90	1

(d)	30/6	2/7	4/7	5/7	6/7	7/7	8/7	8/7	11/7	11/7	12/7	12/7	13/7	13/7	14/7	14/7	15/7	15/7	18/7	19/7	19/7	20/7	20/7		
30/6	1.00	a	a	b	b	b	b	b	b	b	b	b	b	b	b	b	b	b	b	b	b	b	b	b	
2/7	0.86	1.00	a	b	b	a	b	b	b	b	b	b	b	b	a	b	b	a	b	b	b	b	b	b	
4/7	0.91	0.88	1.00	b	b	b	b	b	b	b	b	b	b	a	b	b	a	b	b	b	b	b	b	b	
5/7	0.89	0.88	0.86	1.00	a	a	a	a	a	a	a	a	a	a	a	a	a	a	a	a	b	b	b	b	
6/7	0.83	0.84	0.84	0.85	1.00	a	a	a	a	a	a	a	a	a	a	a	a	b	a	b	b	b	b	b	
6/7	0.84	0.79	0.86	0.79	0.83	1.00	a	b	b	b	a	b	a	b	b	b	a	b	b	b	b	b	b	b	
7/7	0.96	0.89	0.92	0.95	0.89	0.88	1.00	b	a	b	a	b	a	a	a	b	a	b	b	b	b	b	b	b	
8/7	0.82	0.79	0.83	0.74	0.83	0.84	0.83	1.00	a	b	a	a	a	a	a	b	b	b	b	b	b	b	b	b	
8/7	0.77	0.85	0.82	0.75	0.74	0.81	0.81	0.87	1.00	b	a	a	a	a	a	b	a	a	a	b	b	b	b	b	
11/7	0.79	0.74	0.80	0.72	0.74	0.79	0.80	0.90	0.87	1.00	a	a	a	a	a	b	a	a	a	a	a	b	b	b	
11/7	0.83	0.79	0.86	0.77	0.78	0.83	0.85	0.92	0.90	0.89	1.00	b	a	a	a	a	a	a	a	a	b	b	b	b	
12/7	0.82	0.85	0.85	0.79	0.78	0.86	0.85	0.94	0.96	0.90	0.94	1.00	a	a	a	a	b	a	a	a	b	b	b	b	
12/7	0.75	0.85	0.85	0.79	0.75	0.86	0.82	0.82	0.90	0.79	0.84	0.90	1.00	a	a	a	b	a	a	a	b	b	b	b	
13/7	0.78	0.83	0.84	0.72	0.76	0.80	0.80	0.86	0.94	0.86	0.95	0.93	0.87	1.00	a	a	b	a	a	a	b	b	b	b	
13/7	0.74	0.73	0.84	0.72	0.74	0.80	0.78	0.85	0.89	0.82	0.93	0.90	0.87	0.91	1.00	b	b	a	b	b	b	b	b	b	
14/7	0.77	0.77	0.84	0.75	0.82	0.83	0.82	0.90	0.90	0.87	0.92	0.90	0.91	0.92	0.92	1.00	b	a	a	a	b	b	b	b	
14/7	0.75	0.84	0.79	0.74	0.76	0.82	0.79	0.86	0.92	0.88	0.88	0.93	0.88	0.92	0.82	0.88	1.00	a	a	a	a	b	b	a	a
15/7	0.72	0.78	0.82	0.71	0.77	0.80	0.77	0.82	0.88	0.77	0.89	0.90	0.87	0.92	0.90	0.88	0.87	1.00	b	b	b	b	b	b	
15/7	0.74	0.79	0.80	0.69	0.73	0.79	0.77	0.83	0.88	0.85	0.90	0.88	0.84	0.93	0.85	0.90	0.94	0.84	1.00	a	b	b	b	b	
18/7	0.71	0.67	0.77	0.63	0.78	0.76	0.73	0.84	0.75	0.77	0.89	0.82	0.74	0.83	0.81	0.87	0.82	0.83	0.88	1.00	b	b	b	b	
19/7	0.75	0.75	0.81	0.71	0.83	0.81	0.78	0.89	0.85	0.83	0.90	0.87	0.82	0.88	0.83	0.92	0.89	0.84	0.91	0.93	1.00	b	b	a	
19/7	0.77	0.71	0.84	0.71	0.78	0.85	0.81	0.85	0.86	0.84	0.91	0.88	0.79	0.89	0.86	0.88	0.89	0.87	0.89	0.87	0.92	1.00	a	a	
20/7	0.65	0.64	0.68	0.65	0.74	0.74	0.66	0.68	0.65	0.68	0.73	0.71	0.66	0.73	0.66	0.73	0.80	0.74	0.83	0.84	0.85	0.82	1.00	a	
20/7	0.61	0.65	0.70	0.57	0.69	0.76	0.63	0.76	0.78	0.77	0.80	0.80	0.76	0.83	0.73	0.81	0.87	0.82	0.85	0.86	0.87	0.86	0.88	1.00	

(e)	30/6	6/7	7/7	8/7	11/7	12/7	13/7	14/7	14/7	15/7	15/7	18/7	19/7	19/7	20/7	20/7
30/6	1.00	b	a	b	b	b	b	b	b	b	b	b	b	b	b	b
6/7	0.87	1.00	a	b	b	b	a	b	a	a	a	a	a	b	b	b
7/7	0.92	0.93	1.00	b	b	b	b	b	b	b	a	a	b	b	b	b
8/7	0.83	0.90	0.94	1.00	a	a	a	a	a	a	a	a	b	b	a	a
11/7	0.82	0.85	0.89	0.92	1.00	a	a	a	a	a	a	a	b	b	b	b
12/7	0.82	0.90	0.93	0.95	0.92	1.00	a	a	a	a	a	a	b	b	b	b
13/7	0.82	0.92	0.93	0.92	0.86	0.95	1.00	a	a	a	a	a	b	b	b	b
14/7	0.69	0.82	0.84	0.91	0.88	0.92	0.90	1.00	a	a	a	a	b	b	b	b
14/7	0.75	0.81	0.87	0.89	0.92	0.92	0.89	0.90	1.00	a	a	a	b	b	b	b
15/7	0.84	0.86	0.93	0.94	0.87	0.92	0.94	0.88	0.89	1.00	a	a	b	b	b	b
15/7	0.80	0.94	0.88	0.89	0.87	0.93	0.94	0.91	0.88	0.88	1.00	a	b	b	b	b
18/7	0.75	0.82	0.82	0.82	0.80	0.90	0.91	0.88	0.85	0.87	0.89	1.00	b	b	b	b
19/7	0.85	0.90	0.92	0.93	0.90	0.91	0.92	0.85	0.85	0.93	0.90	0.86	1.00	a	a	a
19/7	0.80	0.91	0.90	0.95	0.89	0.90	0.90	0.89	0.87	0.91	0.93	0.82	0.96	1.00	a	a
20/7	0.91	0.90	0.93	0.89	0.87	0.92	0.91	0.84	0.84	0.94	0.89	0.90	0.92	0.87	1.00	a
20/7	0.79	0.86	0.87	0.87	0.82	0.92	0.92	0.90	0.91	0.89	0.93	0.91	0.81	0.83	0.89	1.00

Figure 33: autocorrelation matrices for 2005 soil moisture data. Non significant correlations ($\alpha:0.01$) and corresponding stability conditions are marked in light grey, days with rainstorms recorded 12 hours prior to soil moisture survey are marked in dark grey. a) Piramide 0-6 cm; b) Piramide 0-12 cm; c) Emme 0-6 cm; d) Emme 0-12 cm; e) Emme 0-20 cm

(a)	21/6	22/6	23/6	24/6	26/6	27/6	28/6	28/6	29/6	30/6	2/7	3/7	3/7	4/7	5/7	6/7	7/7	8/7	10/7	11/7	12/7	13/7	14/7
21/6	1	a	a	a	b	a	b	b	b	b	b	b	b	b	d	d	b	b	d	d	d	d	d
22/6	0.86	1	a	a	b	b	b	b	d	b	b	b	b	b	d	d	d	d	d	d	d	d	b
23/6	0.91	0.87	1	a	b	b	b	b	b	b	b	b	b	d	d	d	b	b	d	d	d	d	d
24/6	0.91	0.89	0.92	1	b	b	b	b	b	b	b	b	b	d	d	d	b	b	d	d	d	d	d
26/6	0.86	0.84	0.85	0.88	1	a	b	b	b	b	b	b	b	d	d	d	b	d	d	d	d	d	d
27/6	0.75	0.68	0.71	0.76	0.81	1	b	b	b	b	b	b	b	d	d	d	b	d	d	d	d	d	d
28/6	0.63	0.61	0.61	0.70	0.74	0.85	1	a	b	b	d	b	d	d	d	d	b	d	d	d	d	d	d
28/6	0.62	0.66	0.64	0.68	0.75	0.67	0.82	1	b	b	d	b	b	d	d	d	a	d	d	d	d	d	d
29/6	0.54	0.54	0.51	0.58	0.68	0.66	0.87	0.68	1	b	c	d	d	d	d	d	b	d	d	c	d	d	d
30/6	0.63	0.58	0.62	0.62	0.73	0.62	0.65	0.74	0.57	1	a	a	a	a	a	b	b	b	d	a	b	a	a
2/7	0.67	0.74	0.67	0.69	0.67	0.49	0.45	0.51	0.47	0.65	1	b	b	b	b	b	b	b	d	c	b	b	b
3/7	0.50	0.57	0.50	0.57	0.67	0.43	0.59	0.71	0.61	0.75	0.79	1	a	a	a	b	b	b	b	a	b	a	a
3/7	0.71	0.65	0.65	0.69	0.69	0.49	0.56	0.57	0.58	0.77	0.83	0.78	1	a	a	b	b	b	b	a	a	a	a
4/7	0.61	0.55	0.54	0.58	0.58	0.50	0.47	0.48	0.48	0.76	0.78	0.71	0.83	1	a	b	b	b	b	a	a	a	a
5/7	0.43	0.26	0.32	0.36	0.50	0.34	0.36	0.36	0.44	0.76	0.64	0.67	0.74	0.75	1	b	b	b	b	a	a	a	a
6/7	0.35	0.25	0.34	0.44	0.37	0.38	0.43	0.27	0.40	0.50	0.56	0.55	0.65	0.65	0.60	1	a	a	b	c	a	a	a
7/7	0.49	0.35	0.39	0.51	0.53	0.45	0.57	0.46	0.60	0.58	0.50	0.72	0.73	0.68	0.57	0.73	1	a	b	c	a	c	a
8/7	0.50	0.42	0.44	0.50	0.52	0.33	0.49	0.52	0.53	0.72	0.63	0.79	0.83	0.82	0.72	0.68	0.78	1	a	a	a	a	a
10/7	0.31	0.25	0.34	0.38	0.30	0.05	0.14	0.19	0.12	0.37	0.42	0.49	0.53	0.57	0.46	0.65	0.61	0.72	1	c	a	c	a
11/7	0.45	0.43	0.34	0.49	0.52	0.40	0.53	0.59	0.47	0.75	0.54	0.66	0.71	0.62	0.67	0.46	0.51	0.70	0.32	1	d	b	b
12/7	0.43	0.45	0.30	0.39	0.39	0.18	0.24	0.33	0.25	0.48	0.59	0.60	0.63	0.71	0.44	0.50	0.58	0.73	0.54	0.49	1	a	a
13/7	0.35	0.49	0.36	0.40	0.51	0.34	0.27	0.35	0.31	0.59	0.63	0.59	0.59	0.63	0.58	0.42	0.29	0.59	0.34	0.67	0.55	1	a
14/7	0.38	0.54	0.37	0.41	0.53	0.31	0.30	0.37	0.34	0.67	0.80	0.74	0.70	0.74	0.69	0.52	0.44	0.58	0.44	0.59	0.65	0.74	1

(b)	21/6	22/6	23/6	24/6	26/6	27/6	28/6	28/6	29/6	30/6	2/7	3/7	3/7	4/7	5/7	6/7	7/7	8/7	10/7	11/7	12/7	13/7	14/7	
21/6	1	a	a	a	a	a	b	b	b	b	b	b	b	b	b	b	b	b	b	b	b	b	b	b
22/6	0.97	1	a	a	a	a	b	b	b	b	b	b	b	b	b	b	b	b	b	b	b	b	b	d
23/6	0.93	0.90	1	a	b	a	b	b	b	b	b	b	b	b	b	d	b	d	d	d	d	d	d	d
24/6	0.92	0.88	0.88	1	b	b	b	b	b	b	b	b	b	b	b	b	b	b	b	d	d	b	b	d
26/6	0.84	0.82	0.78	0.78	1	a	b	b	b	b	b	b	b	b	b	b	b	b	b	d	b	b	b	d
27/6	0.90	0.91	0.88	0.87	0.91	1	b	b	b	b	b	b	b	b	b	b	b	b	b	d	b	b	b	d
28/6	0.86	0.85	0.83	0.81	0.84	0.87	1	b	b	b	b	b	b	b	b	b	b	b	b	b	b	b	b	b
28/6	0.87	0.87	0.80	0.87	0.80	0.87	0.94	1	b	b	b	b	b	b	b	b	b	b	b	b	b	b	b	b
29/6	0.82	0.81	0.77	0.75	0.74	0.78	0.94	0.93	1	a	a	a	a	a	a	a	b	a	b	a	b	a	a	
30/6	0.69	0.70	0.64	0.68	0.67	0.67	0.86	0.87	0.91	1	a	a	a	a	a	a	b	a	b	a	b	a	a	
2/7	0.79	0.80	0.70	0.78	0.69	0.76	0.79	0.86	0.84	0.82	1	b	b	b	a	b	b	b	b	b	b	b	b	b
3/7	0.68	0.67	0.57	0.57	0.60	0.58	0.78	0.80	0.88	0.88	0.83	1	a	a	a	a	b	a	b	a	b	a	a	
3/7	0.74	0.73	0.65	0.67	0.65	0.66	0.77	0.83	0.84	0.87	0.90	0.91	1	a	a	a	b	a	b	a	b	a	a	
4/7	0.79	0.79	0.75	0.77	0.65	0.70	0.84	0.90	0.91	0.92	0.89	0.87	0.92	1	a	a	b	a	b	a	b	a	a	
5/7	0.69	0.73	0.59	0.69	0.64	0.68	0.73	0.81	0.82	0.85	0.91	0.84	0.86	0.88	1	b	b	a	b	b	b	a	b	
6/7	0.73	0.75	0.62	0.67	0.65	0.66	0.83	0.86	0.84	0.90	0.81	0.85	0.86	0.91	0.84	1	a	a	a	a	a	a	a	
7/7	0.66	0.66	0.53	0.57	0.50	0.54	0.69	0.75	0.80	0.85	0.85	0.92	0.88	0.84	0.86	0.82	1	a	a	a	a	a	a	
8/7	0.64	0.62	0.53	0.64	0.49	0.51	0.74	0.78	0.85	0.88	0.80	0.87	0.82	0.86	0.87	0.85	0.87	1	a	a	a	a	a	
10/7	0.41	0.44	0.31	0.34	0.27	0.31	0.55	0.61	0.72	0.73	0.66	0.81	0.76	0.72	0.71	0.74	0.75	0.82	1	a	a	a	a	
11/7	0.54	0.56	0.45	0.48	0.41	0.46	0.64	0.72	0.74	0.79	0.77	0.85	0.87	0.84	0.80	0.84	0.78	0.83	0.87	1	a	a	a	
12/7	0.59	0.66	0.50	0.59	0.52	0.58	0.67	0.77	0.75	0.78	0.79	0.69	0.77	0.84	0.80	0.82	0.73	0.73	0.73	0.79	1	a	a	
13/7	0.69	0.72	0.61	0.62	0.60	0.61	0.77	0.82	0.82	0.87	0.79	0.86	0.90	0.93	0.86	0.94	0.79	0.84	0.77	0.90	0.83	1	a	
14/7	0.49	0.51	0.42	0.47	0.34	0.44	0.65	0.69	0.71	0.78	0.71	0.75	0.67	0.76	0.78	0.77	0.75	0.81	0.75	0.83	0.70	0.75	1	

(c)	21/6	22/6	23/6	24/6	26/6	27/6	28/6	28/6	29/6	30/6	2/7	3/7	3/7	4/7	5/7	6/7	7/7	8/7	10/7	11/7	12/7	13/7	14/7	
21/6	1	a	a	a	a	a	b	b	b	b	b	b	b	b	b	b	b	b	b	b	b	b	b	b
22/6	0.95	1	a	a	a	a	b	b	b	b	b	b	b	b	b	b	b	b	b	b	b	b	b	b
23/6	0.94	0.91	1	a	b	a	b	b	b	b	b	b	b	b	b	b	b	b	b	b	b	b	b	b
24/6	0.89	0.90	0.91	1	b	a	b	b	b	b	b	b	b	b	b	b	b	b	b	b	b	b	b	b
26/6	0.87	0.81	0.85	0.82	1	b	b	b	b	b	b	b	b	b	b	b	b	b	b	b	b	b	b	b
27/6	0.91	0.87	0.90	0.86	0.96	1	b	b	b	b	b	b	b	b	b	b	b	b	b	b	b	b	b	b
28/6	0.86	0.88	0.88	0.87	0.90	0.92	1	a	b	b	b	b	b	b	b	b	b	b	b	b	b	b	b	a
28/6	0.90	0.90	0.90	0.87	0.87	0.89	0.97	1	b	b	b	b	b	b	b	b	b	b	b	b	b	b	b	b
29/6	0.87	0.91	0.87	0.88	0.86	0.90	0.97	0.96	1	b	b	a	a	a	a	a	a	a	b	b	a	a	a	a
30/6	0.85	0.90	0.86	0.90	0.82	0.88	0.96	0.95	0.98	1	a	a	a	a	a	b	b	b	b	b	a	a	a	a
2/7	0.85	0.90	0.85	0.87	0.82	0.87	0.92	0.95	0.95	0.94	1	b	b	b	b	b	b	b	b	b	b	a	a	a
3/7	0.84	0.85	0.83	0.84	0.82	0.85	0.93	0.96	0.96	0.96	0.96	1	a	a	a	b	b	b	b	b	a	a	a	a
3/7	0.85	0.88	0.87	0.89	0.82	0.88	0.94	0.95	0.97	0.95	0.97	0.97	1	a	a	b	b	b	b	b	a	a	a	a
4/7	0.83	0.87	0.86	0.88	0.82	0.87	0.91	0.91	0.95	0.92	0.94	0.92	0.98	1	a	b	b	b	b	b	a	a	a	a
5/7	0.80	0.85	0.83	0.84	0.79	0.86	0.89	0.87	0.93	0.89	0.93	0.91	0.94	0.94	1	b	b	b	b	b	a	a	a	a
6/7	0.83	0.87	0.83	0.87	0.80	0.83	0.90	0.92	0.96	0.95	0.94	0.96	0.96	0.93	0.92	1	a	a	a	a	a	a	a	a
7/7	0.84	0.88	0.83	0.86	0.77	0.82	0.91	0.93	0.95	0.95	0.94	0.96	0.95	0.92	0.91	0.97	1	a	a	b	a	b	a	a
8/7	0.83	0.88	0.82	0.85	0.82	0.86	0.93	0.93	0.97	0.97	0.96	0.96	0.96	0.94	0.91	0.95	0.96	1	a	a	a	a	a	a
10/7	0.78	0.85	0.79	0.79	0.72	0.77	0.89	0.90	0.93	0.94	0.92	0.95	0.93	0.91	0.90	0.94	0.97	0.96	1	a	a	b	a	a
11/7	0.85	0.87	0.87	0.87	0.80	0.86	0.92	0.93	0.94	0.94	0.94	0.96	0.95	0.91	0.91	0.94	0.94	0.93	0.93	1	a	a	a	a
12/7	0.72	0.80	0.70																					

(d)	21/6	22/6	23/6	24/6	26/6	27/6	28/6	28/6	29/6	30/6	2/7	3/7	3/7	4/7	5/7	6/7	7/7	8/7	10/7	11/7	12/7	13/7	14/7
21/6	1	a	a	a	b	b	b	b	d	d	d	d	d	d	d	d	d	d	d	d	d	d	d
22/6	0.92	1	a	a	b	b	b	b	d	d	d	d	d	d	d	d	d	d	d	d	d	d	d
23/6	0.91	0.88	1	a	b	b	b	b	b	d	d	d	d	b	d	d	d	d	d	d	d	d	d
24/6	0.90	0.87	0.90	1	b	b	b	b	b	d	d	d	d	d	d	d	d	d	d	d	d	d	d
26/6	0.90	0.86	0.95	0.94	1	a	b	b	b	b	d	d	d	d	d	d	d	d	d	d	d	d	d
27/6	0.86	0.77	0.91	0.88	0.87	1	b	b	b	d	d	d	d	b	d	d	d	d	d	d	d	d	d
28/6	0.81	0.84	0.86	0.89	0.89	0.82	1	b	b	b	d	d	d	b	d	d	d	d	d	d	d	d	b
28/6	0.64	0.50	0.69	0.70	0.67	0.73	0.64	1	b	b	a	b	b	b	d	b	b	d	d	d	d	b	b
29/6	0.47	0.32	0.45	0.57	0.53	0.57	0.47	0.66	1	b	c	d	b	b	d	b	b	b	b	b	b	b	b
30/6	0.39	0.32	0.41	0.39	0.41	0.30	0.42	0.64	0.63	1	a	b	a	b	d	b	b	b	b	b	b	b	a
2/7	0.45	0.32	0.51	0.48	0.44	0.55	0.43	0.80	0.60	0.75	1	b	b	b	b	b	b	b	b	b	b	b	b
3/7	0.29	0.23	0.35	0.36	0.32	0.43	0.34	0.65	0.53	0.65	0.79	1	a	a	a	a	b	b	b	b	a	b	a
3/7	0.30	0.21	0.31	0.33	0.31	0.31	0.35	0.65	0.48	0.78	0.82	0.74	1	b	b	b	b	b	b	b	b	b	b
4/7	0.43	0.34	0.47	0.53	0.49	0.51	0.52	0.70	0.62	0.73	0.83	0.82	0.77	1	a	a	a	a	b	b	a	a	a
5/7	0.13	0.06	0.11	0.09	0.11	0.14	0.06	0.36	0.19	0.46	0.56	0.78	0.64	0.58	1	b	b	b	b	b	a	b	d
6/7	0.38	0.26	0.42	0.46	0.43	0.49	0.43	0.73	0.71	0.72	0.83	0.81	0.80	0.91	0.62	1	a	b	b	b	a	a	a
7/7	0.28	0.21	0.35	0.38	0.37	0.35	0.42	0.63	0.64	0.84	0.75	0.79	0.84	0.88	0.63	0.92	1	a	b	b	a	a	a
8/7	0.30	0.20	0.26	0.30	0.27	0.38	0.35	0.52	0.65	0.69	0.69	0.78	0.79	0.78	0.64	0.84	0.86	1	b	a	a	a	a
10/7	0.12	0.03	0.14	0.17	0.11	0.26	0.19	0.54	0.68	0.69	0.73	0.76	0.74	0.77	0.58	0.86	0.85	0.88	1	a	b	a	a
11/7	0.25	0.17	0.24	0.30	0.28	0.25	0.32	0.53	0.65	0.83	0.75	0.78	0.76	0.84	0.62	0.81	0.87	0.87	0.86	1	b	a	a
12/7	0.25	0.12	0.25	0.28	0.24	0.32	0.26	0.62	0.73	0.81	0.80	0.81	0.74	0.77	0.61	0.84	0.84	0.83	0.89	0.91	1	b	a
13/7	0.22	0.10	0.19	0.20	0.15	0.27	0.21	0.60	0.66	0.75	0.77	0.77	0.67	0.79	0.56	0.80	0.78	0.81	0.90	0.86	0.93	1	a
14/7	0.40	0.37	0.41	0.46	0.40	0.38	0.48	0.63	0.69	0.87	0.75	0.78	0.78	0.82	0.50	0.85	0.89	0.82	0.81	0.86	0.88	0.85	1

(e)	21/6	22/6	23/6	24/6	26/6	27/6	28/6	28/6	29/6	30/6	2/7	3/7	3/7	4/7	5/7	6/7	7/7	8/7	10/7	11/7	12/7	13/7	14/7
21/6	1	a	a	a	b	b	b	b	d	b	b	b	d	d	d	d	d	d	d	d	d	d	d
22/6	0.96	1	a	a	b	b	b	b	b	b	b	b	b	d	d	d	d	d	d	d	d	d	d
23/6	0.90	0.91	1	a	b	a	b	b	b	b	b	d	b	d	d	d	d	d	d	d	d	d	d
24/6	0.88	0.91	0.95	1	b	b	b	b	b	b	b	d	b	d	d	d	d	d	d	d	d	d	d
26/6	0.86	0.90	0.91	0.94	1	a	b	b	b	b	b	d	b	d	d	d	d	d	d	d	d	d	d
27/6	0.84	0.86	0.90	0.95	0.91	1	b	b	b	b	b	b	b	d	d	d	d	d	d	d	d	d	d
28/6	0.73	0.80	0.78	0.75	0.76	0.70	1	a	b	b	b	b	b	b	b	b	b	b	b	b	b	b	b
28/6	0.57	0.65	0.64	0.64	0.68	0.61	0.87	1	b	b	d	b	b	b	b	b	b	d	d	d	b	b	d
29/6	0.43	0.54	0.57	0.50	0.53	0.49	0.79	0.84	1	a	a	a	a	a	a	b	b	b	b	b	b	b	a
30/6	0.43	0.51	0.51	0.46	0.50	0.45	0.82	0.88	0.90	1	a	a	a	b	a	b	b	b	b	b	b	b	a
2/7	0.45	0.53	0.47	0.47	0.46	0.46	0.67	0.59	0.59	0.60	1	a	c	b	a	b	b	b	b	b	d	b	a
3/7	0.47	0.57	0.47	0.49	0.49	0.53	0.68	0.71	0.77	0.78	0.65	1	a	b	a	a	b	b	b	b	b	b	a
3/7	0.46	0.57	0.51	0.53	0.59	0.57	0.73	0.83	0.76	0.85	0.58	0.71	1	b	b	b	b	b	b	b	b	b	b
4/7	0.37	0.43	0.49	0.41	0.40	0.41	0.69	0.79	0.85	0.86	0.57	0.65	0.75	1	a	a	a	b	b	a	b	a	a
5/7	0.24	0.33	0.37	0.33	0.41	0.40	0.63	0.74	0.76	0.85	0.67	0.64	0.76	0.81	1	a	b	b	b	b	b	b	a
6/7	0.33	0.45	0.39	0.40	0.44	0.43	0.77	0.82	0.82	0.91	0.73	0.77	0.86	0.78	0.88	1	a	b	b	a	b	a	a
7/7	0.27	0.38	0.38	0.35	0.34	0.36	0.65	0.67	0.73	0.74	0.68	0.65	0.61	0.79	0.85	0.81	1	b	a	a	a	a	a
8/7	0.19	0.25	0.28	0.22	0.21	0.26	0.57	0.48	0.66	0.70	0.62	0.59	0.65	0.71	0.77	0.81	0.75	1	a	a	a	a	a
10/7	0.26	0.30	0.33	0.32	0.41	0.39	0.59	0.56	0.59	0.68	0.54	0.60	0.70	0.52	0.72	0.76	0.54	0.77	1	a	a	a	a
11/7	0.25	0.33	0.40	0.35	0.39	0.39	0.62	0.76	0.83	0.80	0.59	0.69	0.67	0.86	0.86	0.80	0.81	0.71	0.62	1	a	a	a
12/7	0.10	0.21	0.19	0.20	0.22	0.26	0.49	0.60	0.71	0.71	0.39	0.67	0.61	0.64	0.72	0.80	0.74	0.72	0.70	0.74	1	a	a
13/7	0.21	0.33	0.28	0.24	0.27	0.32	0.58	0.59	0.72	0.75	0.61	0.75	0.69	0.73	0.85	0.84	0.87	0.85	0.71	0.79	0.84	1	a
14/7	0.24	0.26	0.38	0.33	0.36	0.43	0.56	0.52	0.68	0.66	0.52	0.52	0.50	0.68	0.79	0.67	0.65	0.67	0.64	0.68	0.62	0.67	1

(f)	21/6	22/6	23/6	24/6	26/6	27/6	28/6	28/6	29/6	30/6	2/7	3/7	3/7	4/7	5/7	6/7	7/7	8/7	10/7	11/7	12/7	13/7	14/7
21/6	1	a	a	a	b	b	b	b	d	b	b	b	b	b	b	b	b	b	b	b	b	b	b
22/6	0.93	1	a	a	b	b	b	b	b	b	b	b	b	b	b	b	b	b	b	b	b	b	b
23/6	0.92	0.92	1	a	b	b	b	b	d	b	b	b	b	b	b	b	d	d	b	b	b	b	b
24/6	0.94	0.93	0.97	1	b	b	b	b	d	b	b	b	b	b	b	b	d	d	b	b	b	b	b
26/6	0.89	0.86	0.88	0.90	1	a	b	b	b	b	b	b	b	b	b	b	b	b	b	b	b	b	b
27/6	0.88	0.81	0.88	0.90	0.94	1	b	b	d	b	b	b	b	b	b	b	b	b	b	b	b	b	b
28/6	0.75	0.70	0.77	0.79	0.81	0.86	1	a	b	a	b	b	b	a	b	b	b	b	b	b	b	b	b
28/6	0.73	0.76	0.73	0.78	0.82	0.85	0.88	1	d	b	b	b	b	b	b	b	b	b	b	b	b	b	b
29/6	0.49	0.54	0.46	0.50	0.54	0.54	0.66	0.75	1	a	a	a	a	a	a	a	a	b	b	b	a	b	b
30/6	0.73	0.72	0.67	0.70	0.75	0.73	0.85	0.84	0.74	1	a	a	a	a	a	a	a	b	b	b	a	b	b
2/7	0.63	0.69	0.61	0.63	0.70	0.69	0.79	0.89	0.68	0.85	1	b	a	b	a	b	b	b	b	b	b	b	b
3/7	0.56	0.58	0.51	0.56	0.67	0.67	0.74	0.86	0.73	0.90	0.85	1	a	a	a	a	a	b	b	b	a	b	b
3/7	0.73	0.75	0.71	0.72	0.81	0.78	0.83	0.84	0.66	0.93	0.87	0.83	1	b	a	b	a	b	b	b	b	b	b
4/7	0.60	0.70	0.60	0.66	0.69	0.67	0.73	0.88	0.75	0.84	0.88	0.90	0.80	1	a	a	a	b	b	b	a	b	b
5/7	0.60	0.68	0.63	0.65	0.70	0.68	0.75	0.83	0.65	0.82	0.84	0.82	0.84	0.89	1	b	b	b	b	b	b	b	b
6/7	0.56	0.63	0.53	0.60	0.66	0.68	0.73	0.87	0.73	0.86	0.85	0.96	0.80	0.94	0.88	1	a	b	b	b	a	b	b
7/7	0.56	0.55	0.46	0.48	0.56	0.53	0.73	0.75	0.74	0.88	0.77	0.85	0.79	0.73	0.68	0.77	1	b	b	b	a	b	b
8/7	0.55	0.57	0.48	0.53	0.58	0.61	0.66	0.75	0.75	0.84	0.78	0.85	0.76	0.86	0.79	0.87	0.77	1	a	a	a	a	a
10/7	0.51	0.59	0.49	0.50	0.59	0.55	0.63	0.77	0.69	0.84	0.89	0.90	0.82	0.88	0.84	0.87	0.84	0.88	1	a	a	a	a
11/7	0.53	0.65	0.53	0.57	0.61	0.61	0.66	0.83	0.70	0.80	0.90	0.88	0.82	0.95	0.91	0.92	0.73	0.87	0.94	1	a	a	a
12/7	0.52	0.59	0.49	0.52	0.61	0.55	0.63	0.74	0.65	0.80	0.81	0.81	0.81	0.80	0.77	0.79	0.83	0.83	0.90</				

(a)	28/8	29/8	30/8	31/8	1/9	3/9	4/9	5/9	6/9	7/9	7/9	8/9	10/9	11/9	12/9	13/9	14/9	15/9	17/9	19/9	19/9	20/9	21/9	22/9
28/8	1	b	b	b	a	b	b	b	d	d	b	b	b	b	b	b	b	b	b	b	b	b	d	b
29/8	0.70	1	a	a	a	a	b	b	b	b	b	b	a	b	b	b	b	a	b	b	b	b	d	b
30/8	0.73	0.78	1	b	b	b	b	b	b	b	b	b	b	b	b	b	b	a	b	b	b	b	d	b
31/8	0.61	0.73	0.65	1	a	a	b	b	b	b	b	b	a	b	a	b	a	a	b	b	b	b	b	a
1/9	0.69	0.75	0.76	0.71	1	a	a	b	b	b	b	b	a	b	b	b	a	a	b	b	b	b	d	b
3/9	0.69	0.72	0.61	0.77	0.67	1	b	b	b	b	b	b	a	b	b	b	a	a	b	b	b	b	b	a
4/9	0.77	0.76	0.72	0.81	0.80	0.80	1	a	b	a	a	a	a	a	a	a	a	a	a	a	a	a	a	a
5/9	0.52	0.53	0.56	0.77	0.65	0.61	0.77	1	a	a	a	a	b	a	a	a	a	a	a	a	a	a	a	a
6/9	0.35	0.43	0.49	0.68	0.63	0.67	0.73	0.72	1	a	a	a	a	a	a	a	a	a	a	a	a	a	a	a
7/9	0.39	0.46	0.46	0.70	0.60	0.72	0.79	0.73	0.90	1	a	a	a	a	a	a	a	a	a	a	a	a	a	a
7/9	0.66	0.62	0.66	0.67	0.75	0.71	0.80	0.67	0.57	0.65	1	a	a	a	a	a	a	a	a	a	a	a	a	a
8/9	0.49	0.67	0.60	0.59	0.58	0.75	0.71	0.69	0.71	0.75	0.73	1	a	a	a	a	a	a	a	a	a	a	a	a
10/9	0.57	0.54	0.57	0.74	0.55	0.75	0.77	0.85	0.68	0.70	0.72	0.75	1	b	a	b	a	a	b	b	b	b	b	a
11/9	0.54	0.46	0.53	0.71	0.63	0.67	0.78	0.85	0.73	0.81	0.70	0.74	0.73	1	a	a	a	a	a	a	a	a	a	a
12/9	0.43	0.45	0.47	0.53	0.41	0.58	0.60	0.75	0.67	0.65	0.65	0.80	0.81	0.61	1	a	a	a	a	a	a	a	a	b
13/9	0.69	0.58	0.59	0.57	0.67	0.74	0.81	0.64	0.68	0.72	0.77	0.67	0.64	0.66	0.67	1	a	a	a	a	a	a	d	a
14/9	0.45	0.68	0.59	0.57	0.64	0.55	0.69	0.66	0.67	0.68	0.62	0.76	0.58	0.55	0.75	0.73	1	a	b	a	a	b	a	a
15/9	0.56	0.55	0.44	0.51	0.48	0.70	0.74	0.52	0.63	0.70	0.58	0.67	0.57	0.61	0.58	0.84	0.73	1	b	b	b	b	b	
17/9	0.58	0.68	0.62	0.53	0.42	0.70	0.69	0.54	0.54	0.56	0.56	0.75	0.65	0.59	0.69	0.68	0.73	0.77	1	a	a	a	b	a
19/9	0.67	0.58	0.59	0.66	0.66	0.80	0.80	0.79	0.65	0.69	0.76	0.78	0.80	0.82	0.66	0.71	0.60	0.72	0.66	1	a	a	b	a
19/9	0.41	0.52	0.47	0.47	0.51	0.53	0.58	0.67	0.56	0.59	0.69	0.76	0.63	0.60	0.80	0.65	0.81	0.61	0.75	0.68	1	a	b	a
20/9	0.35	0.51	0.46	0.45	0.52	0.54	0.66	0.59	0.62	0.67	0.63	0.68	0.55	0.58	0.70	0.61	0.77	0.68	0.73	0.60	0.82	1	b	a
21/9	0.35	0.52	0.43	0.61	0.31	0.54	0.64	0.69	0.53	0.59	0.51	0.70	0.83	0.59	0.76	0.47	0.61	0.54	0.67	0.60	0.53	0.56	1	a
22/9	0.34	0.49	0.45	0.47	0.37	0.63	0.57	0.58	0.55	0.60	0.39	0.67	0.63	0.66	0.52	0.55	0.57	0.65	0.67	0.69	0.53	0.55	0.62	1

(b)	28/8	29/8	30/8	31/8	1/9	3/9	4/9	5/9	6/9	7/9	7/9	8/9	10/9	11/9	12/9	13/9	14/9	15/9	17/9	19/9	19/9	20/9	21/9	22/9
28/8	1	b	b	b	b	b	b	b	b	b	b	b	b	b	b	b	b	b	b	b	b	b	b	b
29/8	0.87	1	a	b	a	b	b	b	b	b	b	b	b	b	b	b	b	b	b	b	b	b	b	b
30/8	0.87	0.92	1	b	b	b	b	b	b	b	b	b	b	b	b	b	b	b	b	b	b	b	b	b
31/8	0.85	0.92	0.91	1	a	a	b	b	b	b	b	b	a	b	b	b	b	a	a	b	b	b	b	b
1/9	0.85	0.92	0.89	0.97	1	b	b	b	b	b	b	b	b	b	b	b	b	a	b	b	b	b	b	b
3/9	0.84	0.93	0.91	0.93	0.89	1	a	b	b	b	b	b	b	b	b	b	b	a	b	b	b	b	b	b
4/9	0.81	0.91	0.87	0.95	0.94	0.94	1	a	b	a	b	a	a	b	a	b	a	a	a	b	b	a	b	b
5/9	0.77	0.91	0.82	0.89	0.88	0.88	0.90	1	a	a	b	a	a	a	a	a	a	a	a	a	a	a	b	b
6/9	0.60	0.75	0.66	0.70	0.76	0.75	0.76	0.76	1	a	a	a	a	a	a	a	a	a	a	a	a	a	a	a
7/9	0.75	0.87	0.87	0.88	0.87	0.90	0.92	0.86	0.75	1	b	a	a	b	a	b	a	a	a	a	a	a	a	b
7/9	0.81	0.89	0.79	0.88	0.88	0.90	0.91	0.93	0.80	0.87	1	a	a	a	a	a	a	a	a	a	a	a	a	a
8/9	0.82	0.90	0.86	0.92	0.94	0.91	0.95	0.94	0.78	0.91	0.93	1	a	b	a	b	a	a	a	b	a	b	b	b
10/9	0.76	0.81	0.74	0.86	0.90	0.78	0.86	0.89	0.74	0.78	0.89	0.90	1	b	a	b	a	b	a	b	b	a	b	b
11/9	0.79	0.87	0.84	0.88	0.89	0.90	0.94	0.83	0.80	0.90	0.89	0.90	0.82	1	a	a	a	a	a	a	a	a	a	a
12/9	0.74	0.79	0.73	0.77	0.87	0.74	0.81	0.80	0.78	0.78	0.84	0.89	0.92	0.83	1	b	a	a	a	a	a	a	b	b
13/9	0.75	0.79	0.71	0.78	0.84	0.78	0.83	0.87	0.81	0.79	0.89	0.89	0.90	0.82	0.88	1	a	a	a	a	a	a	a	a
14/9	0.76	0.88	0.85	0.84	0.90	0.81	0.88	0.88	0.79	0.85	0.82	0.87	0.82	0.80	0.82	0.82	1	a	a	b	a	b	b	b
15/9	0.78	0.83	0.80	0.85	0.88	0.84	0.88	0.89	0.80	0.86	0.87	0.91	0.89	0.82	0.88	0.88	0.92	1	a	b	b	b	b	b
17/9	0.80	0.87	0.84	0.91	0.92	0.88	0.93	0.89	0.74	0.90	0.90	0.93	0.87	0.86	0.85	0.82	0.92	0.95	1	b	b	a	b	b
19/9	0.74	0.85	0.83	0.88	0.90	0.81	0.85	0.84	0.75	0.83	0.81	0.86	0.77	0.83	0.77	0.74	0.90	0.89	0.91	1	a	a	a	a
19/9	0.76	0.83	0.82	0.89	0.87	0.89	0.91	0.86	0.66	0.86	0.85	0.89	0.77	0.82	0.74	0.75	0.87	0.91	0.94	0.89	1	a	a	a
20/9	0.76	0.76	0.74	0.78	0.82	0.82	0.86	0.76	0.74	0.75	0.82	0.87	0.77	0.86	0.82	0.84	0.80	0.86	0.85	0.79	0.86	1	b	b
21/9	0.68	0.71	0.62	0.70	0.78	0.63	0.71	0.73	0.70	0.64	0.75	0.79	0.73	0.72	0.83	0.76	0.75	0.77	0.77	0.80	0.72	0.81	1	a
22/9	0.79	0.85	0.86	0.83	0.85	0.87	0.86	0.82	0.88	0.85	0.86	0.88	0.78	0.84	0.83	0.82	0.89	0.89	0.89	0.86	0.84	0.87	0.73	1

(c)	28/8	29/8	30/8	31/8	1/9	3/9	4/9	5/9	6/9	7/9	7/9	8/9	10/9	11/9	12/9	13/9	14/9	15/9	17/9	19/9	19/9	20/9	21/9	22/9
28/8	1	b	b	b	b	b	b	b	b	b	b	b	b	b	b	b	b	b	b	b	b	b	b	b
29/8	0.86	1	a	b	b	a	b	b	b	b	b	b	b	b	b	b	b	b	b	b	b	b	b	b
30/8	0.92	0.94	1	a	a	a	b	b	b	b	b	b	b	b	b	b	b	a	a	b	b	b	b	b
31/8	0.83	0.87	0.91	1	a	a	a	a	b	b	b	b	a	b	b	a	a	a	a	b	b	b	b	b
1/9	0.91	0.91	0.96	0.90	1	a	b	b	b	b	b	b	b	b	b	b	b	a	a	b	b	b	b	b
3/9	0.91	0.91	0.94	0.89	0.96	1	b	b	b	b	b	b	b	b	b	b	b	a	a	b	b	b	b	b
4/9	0.80	0.89	0.92	0.93	0.94	0.92	1	a	b	a	a	a	a	b	a	a	a	a	a	a	b	b	b	a
5/9	0.80	0.89	0.89	0.91	0.92	0.91	0.94	1	b	a	a	a	a	b	a	a	a	a	a	a	b	b	b	a
6/9	0.75	0.87	0.86	0.91	0.90	0.89	0.95	0.95	1	a	a	a	a											

(d)	28/8	29/8	30/8	31/8	1/9	3/9	4/9	5/9	6/9	7/9	7/9	8/9	10/9	11/9	12/9	13/9	14/9	15/9	17/9	19/9	19/9	20/9	21/9	22/9
28/8	1	b	b	b	b	b	b	b	b	b	b	b	b	b	b	b	b	b	b	b	b	d	d	d
29/8	0.76	1	a	b	a	a	b	b	b	b	b	b	b	b	b	b	b	a	b	b	b	a	d	d
30/8	0.47	0.50	1	b	b	b	b	b	b	b	b	b	b	b	b	b	d	d	b	d	b	d	d	d
31/8	0.64	0.82	0.65	1	a	a	b	a	b	a	b	a	b	a	b	a	a	a	a	b	a	a	b	b
1/9	0.69	0.81	0.65	0.87	1	a	b	b	b	b	b	b	b	b	b	b	a	a	b	b	a	a	b	b
3/9	0.52	0.78	0.57	0.76	0.81	1	b	b	b	b	b	b	b	b	b	b	b	a	b	b	b	a	d	b
4/9	0.57	0.77	0.53	0.89	0.81	0.82	1	a	a	a	a	a	a	a	a	a	a	a	a	a	a	a	a	d
5/9	0.63	0.87	0.58	0.91	0.82	0.72	0.85	1	a	a	a	b	a	a	a	a	a	a	a	a	a	b	a	d
6/9	0.63	0.86	0.64	0.95	0.86	0.81	0.92	0.93	1	a	a	a	a	a	a	a	a	a	a	a	a	a	a	a
7/9	0.63	0.74	0.69	0.85	0.87	0.81	0.85	0.82	0.84	1	a	a	a	a	a	a	a	a	a	a	a	b	a	a
7/9	0.66	0.85	0.65	0.92	0.89	0.84	0.90	0.89	0.93	0.89	1	a	a	a	a	a	a	a	a	a	a	a	a	a
8/9	0.60	0.81	0.60	0.83	0.79	0.82	0.90	0.85	0.88	0.84	0.86	1	a	a	a	a	a	a	a	a	a	b	a	d
10/9	0.62	0.69	0.47	0.65	0.78	0.60	0.74	0.72	0.68	0.73	0.68	0.79	1	a	a	a	a	a	a	a	a	b	c	d
11/9	0.67	0.88	0.59	0.83	0.78	0.67	0.83	0.93	0.88	0.82	0.87	0.85	0.76	1	a	a	a	a	a	a	a	a	c	c
12/9	0.64	0.79	0.54	0.67	0.73	0.72	0.79	0.73	0.78	0.80	0.77	0.81	0.80	0.87	1	a	a	a	a	a	a	b	a	b
13/9	0.66	0.81	0.61	0.83	0.85	0.71	0.87	0.83	0.86	0.86	0.83	0.88	0.89	0.90	0.87	1	a	a	a	a	b	a	b	d
14/9	0.68	0.90	0.61	0.90	0.82	0.78	0.90	0.93	0.95	0.84	0.93	0.90	0.72	0.95	0.84	0.89	1	a	a	a	b	a	b	d
15/9	0.67	0.81	0.49	0.71	0.72	0.65	0.77	0.77	0.78	0.77	0.77	0.75	0.78	0.89	0.85	0.92	0.84	1	b	b	b	a	d	d
17/9	0.68	0.79	0.67	0.82	0.81	0.69	0.80	0.84	0.80	0.83	0.84	0.77	0.72	0.89	0.81	0.86	0.89	0.81	1	a	b	a	b	b
19/9	0.65	0.84	0.51	0.82	0.75	0.78	0.86	0.89	0.87	0.82	0.85	0.87	0.71	0.90	0.85	0.81	0.90	0.77	0.78	1	b	a	b	d
19/9	0.73	0.76	0.55	0.72	0.78	0.71	0.80	0.76	0.78	0.88	0.75	0.84	0.85	0.81	0.87	0.88	0.79	0.84	0.78	0.82	1	a	a	a
20/9	0.30	0.56	0.38	0.71	0.61	0.49	0.64	0.61	0.68	0.64	0.66	0.55	0.40	0.58	0.50	0.58	0.57	0.50	0.49	0.58	0.56	1	b	b
21/9	0.27	0.36	0.34	0.55	0.51	0.27	0.51	0.50	0.52	0.59	0.48	0.43	0.44	0.46	0.47	0.54	0.44	0.39	0.41	0.46	0.58	0.78	1	b
22/9	0.41	0.38	0.38	0.48	0.56	0.46	0.43	0.39	0.47	0.52	0.44	0.50	0.44	0.37	0.41	0.49	0.43	0.32	0.46	0.40	0.58	0.47	0.51	1

(e)	28/8	29/8	30/8	31/8	1/9	3/9	4/9	5/9	6/9	7/9	7/9	8/9	10/9	11/9	12/9	13/9	14/9	15/9	17/9	19/9	19/9	20/9	21/9	22/9
28/8	1	b	b	b	b	b	d	b	d	b	d	d	d	d	d	d	d	d	b	d	b	d	d	d
29/8	0.83	1	a	b	b	b	b	b	b	b	b	b	b	b	b	b	b	b	b	d	b	d	d	d
30/8	0.82	0.84	1	b	b	b	b	b	b	b	d	b	d	d	b	b	b	d	b	d	b	d	b	d
31/8	0.71	0.75	0.89	1	a	b	b	a	b	b	b	b	b	d	a	b	a	b	b	d	b	b	b	d
1/9	0.66	0.72	0.70	0.75	1	b	b	b	b	b	b	b	d	d	a	b	b	b	b	d	b	b	d	d
3/9	0.53	0.78	0.69	0.76	0.74	1	a	a	a	a	a	b	a	a	a	a	a	a	a	b	b	b	a	a
4/9	0.46	0.58	0.60	0.70	0.72	0.78	1	a	a	b	a	b	a	a	a	a	a	a	a	b	b	b	a	a
5/9	0.51	0.70	0.75	0.78	0.70	0.78	0.81	1	b	b	a	b	b	b	a	b	a	a	b	b	b	b	b	d
6/9	0.34	0.54	0.60	0.59	0.57	0.75	0.59	0.69	1	b	c	b	d	a	a	a	a	a	b	b	b	a	a	a
7/9	0.56	0.69	0.70	0.72	0.68	0.62	0.64	0.80	0.49	1	a	b	c	c	a	a	a	c	a	d	b	a	a	d
7/9	0.41	0.56	0.39	0.56	0.70	0.73	0.79	0.62	0.40	0.56	1	b	b	c	a	b	a	a	b	b	b	b	b	d
8/9	0.27	0.45	0.47	0.60	0.51	0.73	0.61	0.64	0.48	0.42	0.59	1	a	c	a	c	a	a	a	b	a	c	c	c
10/9	0.25	0.53	0.40	0.52	0.38	0.57	0.56	0.56	0.38	0.53	0.67	0.59	1	a	a	b	a	a	a	b	b	d	a	d
11/9	0.15	0.53	0.36	0.34	0.40	0.60	0.69	0.55	0.47	0.43	0.54	0.39	0.66	1	a	a	a	a	a	b	d	d	a	d
12/9	0.40	0.63	0.62	0.70	0.64	0.79	0.81	0.85	0.77	0.65	0.65	0.61	0.66	0.67	1	b	b	a	b	b	b	b	b	d
13/9	0.40	0.61	0.52	0.45	0.52	0.68	0.64	0.61	0.57	0.74	0.53	0.32	0.52	0.61	0.67	1	a	a	a	b	b	a	a	d
14/9	0.33	0.53	0.57	0.70	0.60	0.76	0.80	0.65	0.44	0.65	0.72	0.59	0.63	0.65	0.65	0.57	1	a	b	b	b	b	a	a
15/9	0.38	0.57	0.42	0.46	0.49	0.72	0.70	0.57	0.45	0.41	0.77	0.52	0.74	0.75	0.70	0.56	0.70	1	b	b	b	b	b	d
17/9	0.64	0.74	0.63	0.61	0.69	0.69	0.75	0.69	0.51	0.52	0.73	0.51	0.62	0.70	0.69	0.51	0.57	0.80	1	b	a	a	a	c
19/9	0.29	0.34	0.31	0.36	0.35	0.53	0.68	0.51	0.46	0.34	0.70	0.51	0.61	0.54	0.56	0.45	0.55	0.77	0.69	1	a	a	a	a
19/9	0.49	0.50	0.60	0.69	0.67	0.67	0.77	0.80	0.58	0.67	0.66	0.66	0.49	0.38	0.78	0.52	0.67	0.57	0.65	0.63	1	a	a	a
20/9	0.39	0.42	0.45	0.54	0.55	0.65	0.70	0.62	0.65	0.65	0.62	0.40	0.40	0.41	0.65	0.63	0.65	0.54	0.52	0.54	0.71	1	a	a
21/9	0.34	0.55	0.57	0.53	0.39	0.66	0.67	0.72	0.56	0.51	0.53	0.46	0.56	0.65	0.67	0.54	0.71	0.70	0.66	0.54	0.64	0.65	1	a
22/9	0.33	0.32	0.39	0.44	0.31	0.51	0.50	0.40	0.53	0.25	0.42	0.33	0.30	0.32	0.40	0.29	0.53	0.53	0.47	0.57	0.54	0.72	0.62	1

(f)	28/8	29/8	30/8	31/8	1/9	3/9	4/9	5/9	6/9	7/9	7/9	8/9	10/9	11/9	12/9	13/9	14/9	15/9	17/9	19/9	19/9	20/9	21/9	22/9	
28/8	1	b	b	b	b	b	b	b	b	b	b	b	b	b	b	b	b	b	b	b	b	d	b	d	
29/8	0.85	1	b	b	a	a	b	b	b	a	b	b	b	b	b	b	b	b	b	b	b	b	d	b	b
30/8	0.87	0.88	1	a	a	a	b	a	a	b	a	b	b	b	b	a	b	a	b	a	b	b	b	b	b
31/8	0.85	0.79	0.89	1	a	a	b	a	a	a	a	b	b	a	a	a	a	a	a	a	a	b	b	b	a
1/9	0.64	0.65	0.75	0.90	1	a	b	b	b	a	b	b	b	b	b	b	b	a	b	b	b	b	b	b	b
3/9	0.80	0.89	0.93	0.87	0.79	1	b	b	b	a	b	b	b	b	b	b	b	a	b	b	b	b	b	b	b
4/9	0.82	0.85	0.82	0.90	0.85	0.89	1	a	a	a	a	a	a	a	a	a	a	a	a	a	a	a	a	a	a
5/9	0.75	0.90	0.89	0.81	0.78	0.94	0.83	1	a	a	a	b	b	a	a	a	a	a	a	a	a	b	a	a	a
6/9	0.63	0.83	0.81	0.79	0.76	0.91	0.81	0.92	1	a	a	a	a	a	a	a	a	a	a	a	a	a	a	a	a
7/9	0.61	0.75	0.77	0.75	0.61	0.83	0.71	0.78	0.82	1	b	b	b	b	b	b	b	a	b	b	b	b	b	b	b
7/9	0.75	0.74	0.87	0.80	0.72	0.89	0.78	0.86	0.78	0.72	1	b	b	a	a	a	a	a	a	a	a	b	b	a	a
8/9	0.78	0.87	0.83	0.84	0.76	0.90	0.91	0.86	0.85	0.73	0.78	1	a	a	a	a	a	a	a	a	a	a	a	a	a
10/9	0.77	0.86	0.85	0.85	0.80	0.89	0.86	0.88	0.87	0.69	0.77	0.83	1	a	a	a	a	a	a	a	a	a	a	a	a
11/9	0.70	0.85	0.82	0.78	0.69	0.90	0.80	0.88	0.91	0.77	0.84	0.82	0.83	1	a	a	a	a	a	a	a	a	a	a	a
12/9	0.66	0.81	0.77	0.83	0.80	0.89	0.88	0.84	0.89	0.84	0.77	0.87	0.81	0.91	1	a	a	a	a	a	a	a	a	a	a
13/9	0.50	0.76	0.68	0.61	0.59	0.80	0.74	0.83	0.90	0.71	0.68	0.76	0.79	0.84	0.82	1	a	a	a	a	b	b	a	a	
14/9	0.60	0.62	0.70	0.68	0.60	0.82	0.77	0.68	0.68	0.72	0.81	0.73													

Spearman correlation coefficients extracted from autocorrelation matrices were grouped according to the temporal lag between a single sampling time and all the following ones; ρ values were then averaged and correlograms depicted in Figure 36 were obtained (no data are available at 0-20 cm depth for Piramide in 2005). For each hillslope at any depth, correlation decreases when time lag between sampling occasions increases. The curves at the different soil depths have a similar pattern and display a strong correlation up to 15 days in 2005, 11 days in 2006 and 19 days in 2007. Beyond this time interval, autocorrelation values are less significant, because of the great temporal distance between samplings and of the small number of samples that fall in such intervals. Again, as previously observed in the ranking stability, autocorrelation matrices and linear regression analysis, a clear difference can be noted among the three monitoring periods: correlation values were higher in 2005 and 2007 and stayed longer above the level of statistical significance (correlation at 0-12 and 0-20 cm depth are even always positive for the whole season over Piramide in 2007); on the contrary, in the correlogram referred to the field work in 2006 the significance level is reached earlier, the curve slope is more marked reflecting the higher variability of rainfalls and the consequent different soil moisture cases occurring in comparing wet and dry periods.

4.4 Mean soil moisture, correlation between successive days and piezometric increase

In order to assess the trend of correlation between consecutive sampling times, Spearman rank correlation coefficient between values of a given day with respect to the values of the previous day was computed. Furthermore, ρ values were plotted with mean soil moisture time series at three depths and with the percentage of capacitance probes that recorded an increase in the level of water table compared to the level at the time corresponding to the previous soil moisture sampling (Figure 37). Especially in the 2006 and 2007 field campaigns, Spearman coefficients showed a clear decrease after rainfalls, followed by a slow increase; particularly, if the antecedent moisture conditions were fairly dry, the drop of correlation was more marked. Such behaviour is more patent in the surface layers, submitted to greater variations in ρ values: 0-6 cm moisture patterns are more likely to be influenced by precipitation inputs earlier in time

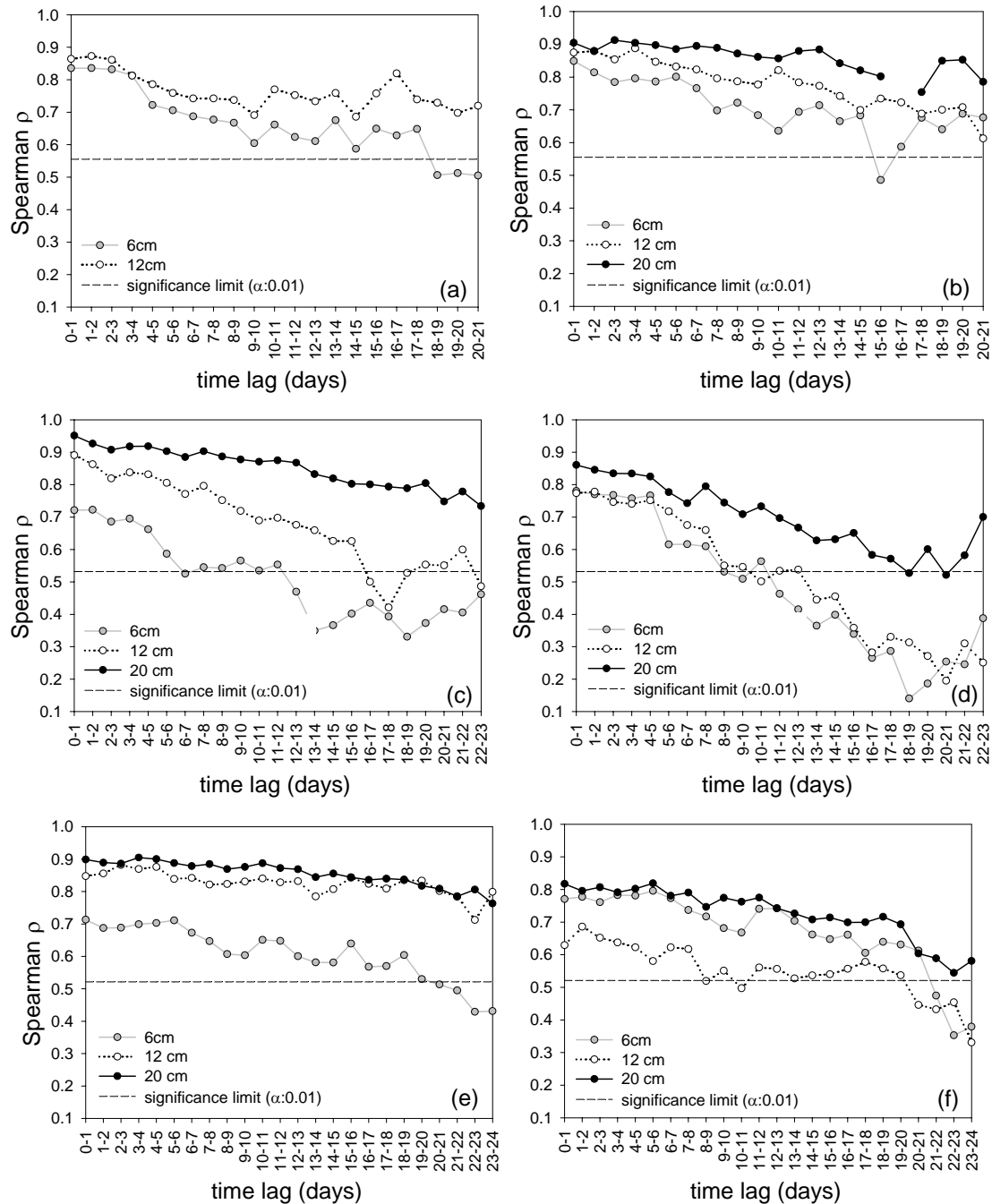
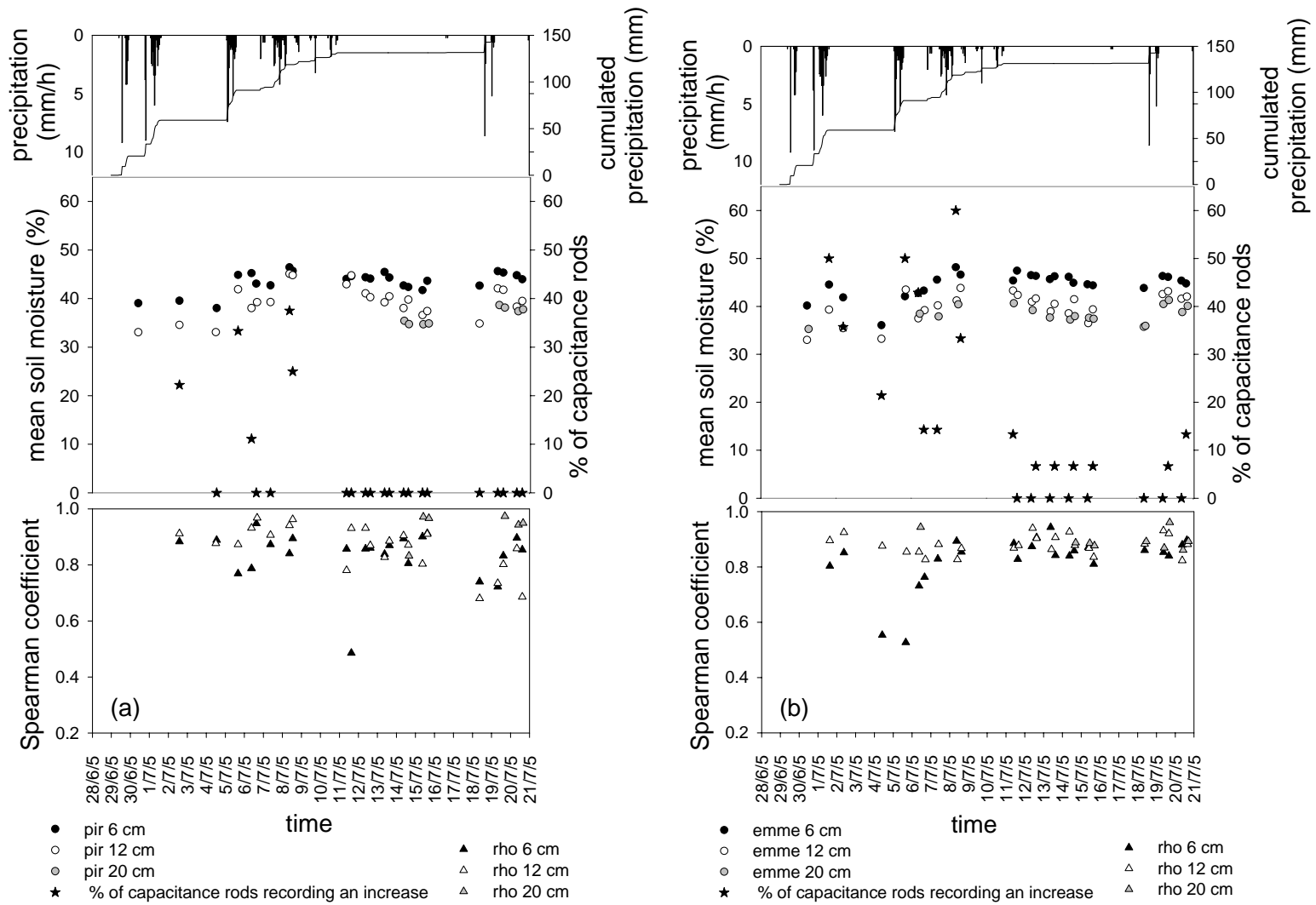


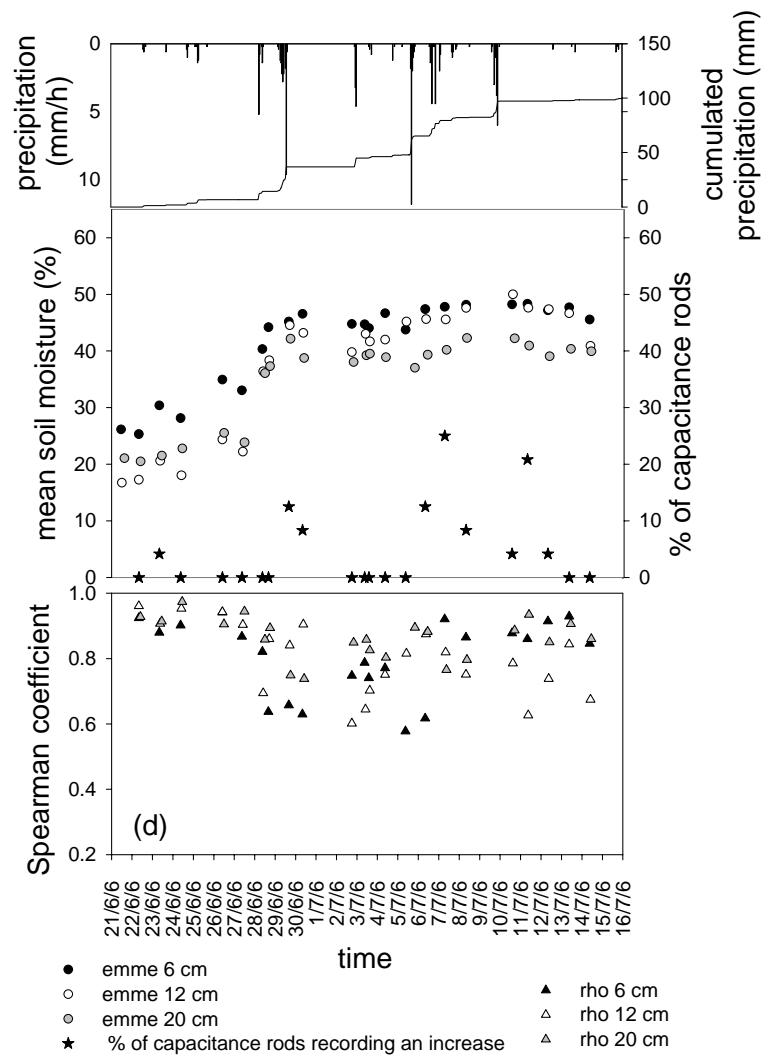
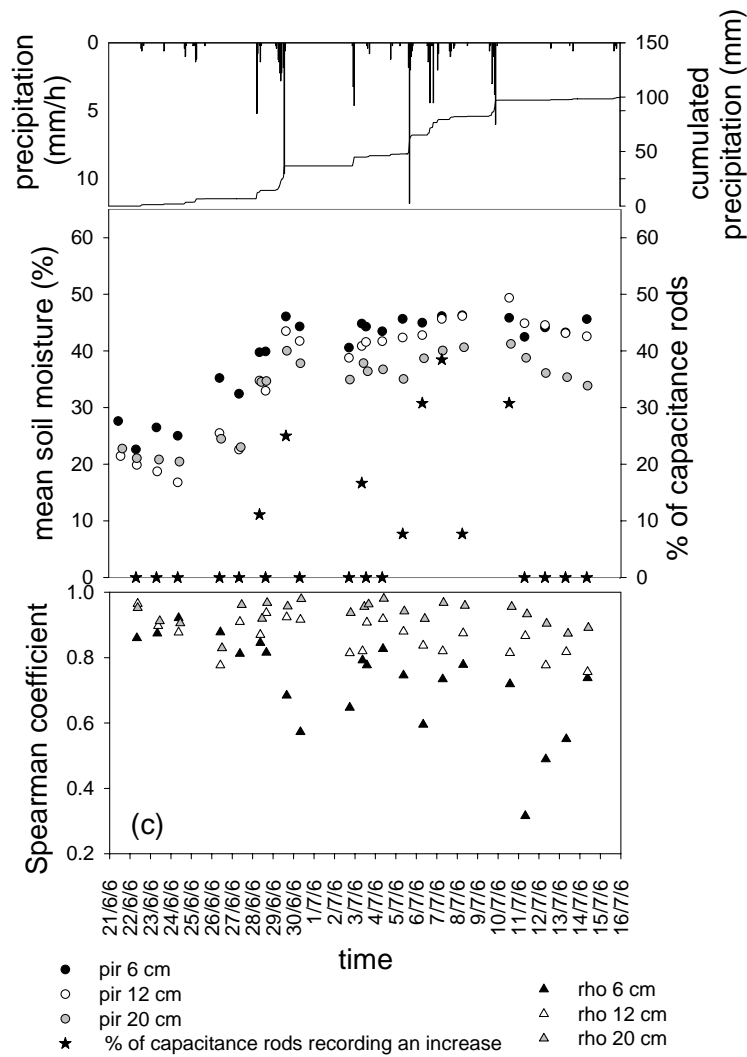
Figure 36: correlograms for soil moisture values at three soil depths: a) Piramide 2005; b) Emme 2005; c) Piramide 2006; d) Emme 2006; e) Piramide 2007; f) Emme 2007

and more clearly compared to the other depths. Thus, as found in other studies (Martinez-Fernandez and Ceballos, 2003), the decline of correlation occurs at times of transition from a dry to a wetter state, while during the drying phase the coefficients are higher. The end of the 2005 monitoring period constitutes an exception from this behaviour: after several days without precipitation, the rain event occurred on July 18-19 did not produce any significantly decrease in

correlation (and any increase in the water level either, as pointed out later): this is imputable to the relatively high intensity of the first shower (11 mm in 75 minutes), compared to the other rainfalls; this rainstorm was believed to generate overland flow rather than allowing water to percolate in depth, thus neither influencing the variation of piezometric level nor the correlation between soil moisture patterns.

Water table variations, similar over the three years on the two target hillslopes, generally displayed an opposite trend compared to that of Spearman correlation coefficients: the hillslope area characterized by water table rise respect to the previous soil moisture sampling increased after rainfalls, as correlation between soil moisture patterns decreased; the piezometric level then decreased during dry-down. An odd behaviour was observed at Emme site in 2005 (Figure 37, b): an alternation between increase/no increase occurred various times during the dry period from July 11 to July 18; although an instrumental error cannot be excluded, this trend is probably due to the site topography, formed by a flat area with shallow soil at the hillslope foot and a steep relief with greater soil depth at the higher elevations. This morphology can influence the time lag between the start of precipitation and the begin of the piezometric response: capacitance rods at the hillslopes foot responded more quickly compared to those at the top and such delay is reflected in different times of overall water table arise. Generally, the piezometric response appeared to be mainly related to the precipitation cumulated in many days rather than to a high-intensity single rain event, as observed by other authors (Scanlon et al., 2000); this is confirmed by the short and relatively intense rainfall described above, which generated no water table increase on Piramide and only a late piezometric response on Emme. In the 2007 field campaign, though, groundwater rise was triggered even by short and moderate rainstorms due to the overall high moisture condition of the whole catchment during the monitoring period.





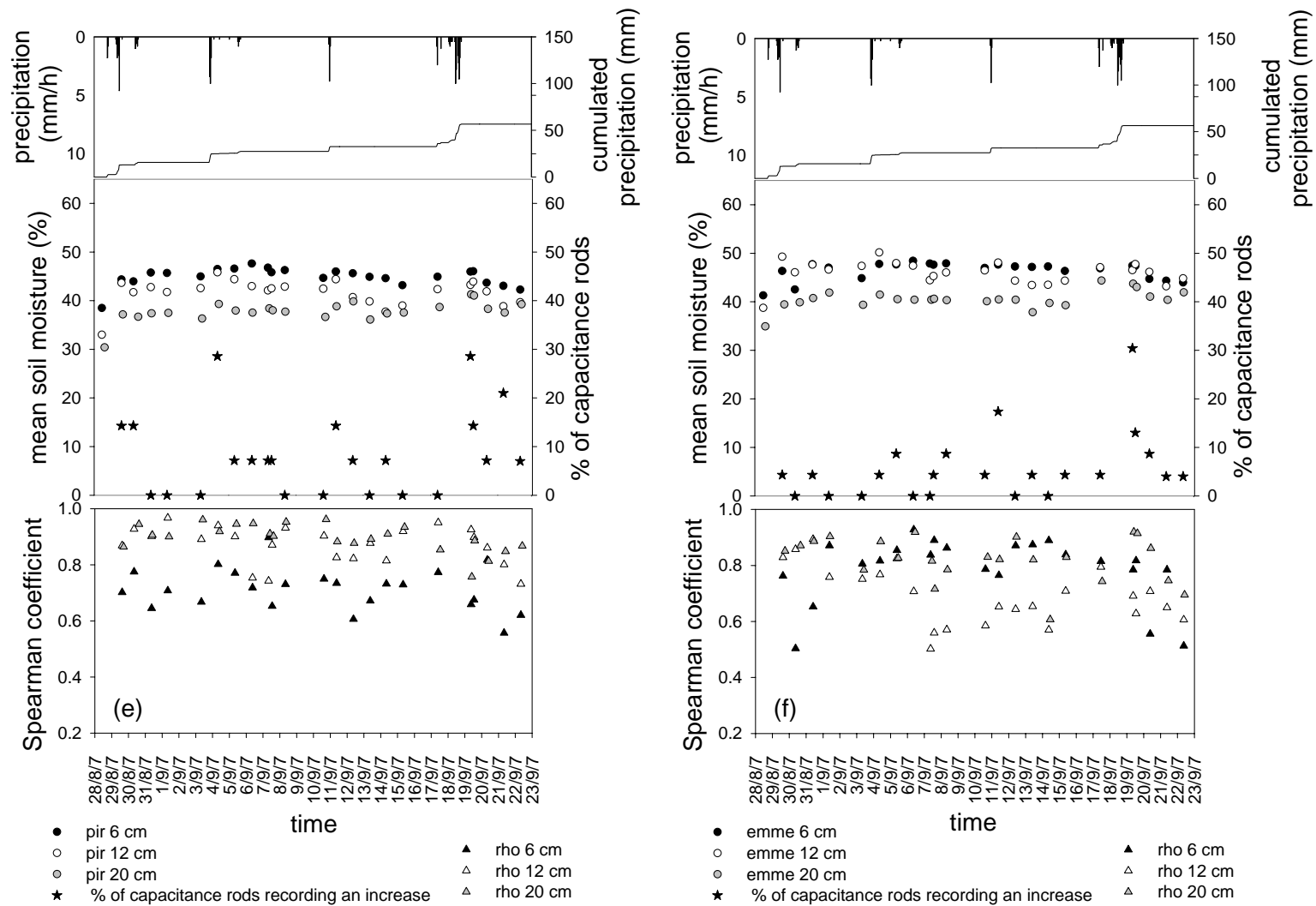


Figure 37: time series over different depths of hillslope-averaged soil moisture and Spearman rank correlation coefficient computed between values of a given day with respect to the values of the previous day. The stars indicate the percentage of capacitance rods that record an increase in the water table compared to the time corresponding to the previous soil moisture sampling, 2005: a) Piramide; b) Emme. 2006: c) Piramide; d) Emme. 2007: e) Piramide; f) Emme

A common remark about the different behaviours of surface layers compared to the deeper ones can be drawn from the observation of the plots presented above (from Figure 33 to Figure 37): the highest number of non statistically significant comparisons and of “c” and “d” stability conditions in the autocorrelation matrices can be generally found for soil samples taken at 0-6 cm whereas often the deeper layers exhibit a greater degree of autocorrelation; similarly, all correlograms show that correlation is high for soil moisture pairs at 0-20 cm depth and then decreases with the sampling depth. This is consistent with the patterns highlighted by Spearman rank correlation coefficients computed between values of a given day with respect to the values of the previous day (Figure 37). On the other hand, statistical properties (sections 3.1, 3.3, 3.4) and ranking stability analysis (section 4.1) revealed that water content in the shallow layers displayed the lowest values of standard deviation, mean relative difference, standard deviation of relative difference and thus the best degree of temporal stability. This issue yields to a paradox: why are soil moisture patterns at the surface layers less variable, more temporally stable compared to the other depths and, at the same time, less correlated to each other? In our dataset, standard deviation of soil moisture decreases with the increase of water content and increases with the increase of soil depth: this is consistent with the fact that shallow layers are wetter than the deeper ones, which are dryer and characterized by a more marked variability. When the soil is totally wet, all values are more homogeneously high and less variations in water content are likely to occur; on the contrary, when the soil is dry altogether, zone with higher values are more probable to be found, both spatially and in depth. Thus, the contradiction can be probably explained considering processes which are active during the dry periods and influence only the dynamics of the shallow layer. Particularly, the low variability of data at 0-6 cm depth is strictly related to the high overall water content of the sampling points; surface layers, despite being more stable, are nevertheless more likely to be influenced by precipitation inputs earlier in time and more clearly compared to the other depths.

Time stability of soil moisture: concluding remarks

Temporal stability of soil moisture patterns has been investigated over three experimental hillslopes with steep relief and shallow soil depth in the Dolomites (central-eastern Italian Alps). A multiple approach was applied: i) ranking stability analysis; ii) slope-intercept analysis of linear regression; iii) autocorrelation analysis; (iv) evolution of correlation against mean soil moisture over time and relationship with piezometric increase.

Low values of mean relative difference and standard deviation of relative difference suggested a good overall time stability of moisture patterns at each depth over the studied hillslopes for data collected in 2005, 2006 and 2007. A difference in time stability can be observed between the three periods: MRD values were higher and correlation and autocorrelation values were lower in 2006, indicating slightly less stable sites. This diversity was attributed to the different distribution of rainfalls and was highlighted by all approaches followed in this study. Generally, time stability analysis shows that spatial patterns of sampling points are reasonably well preserved at the three soil depths. Even though different physical processes control variability of soil moisture at various depths, time stability of surface measurements is a good indicator of subsurface time stability. The representative points identified over the three hillslopes represent hillslope mean soil moisture content within $\pm 3\%$ volumetric soil moisture. These points are generally located in a topographically central position over the various hillslopes. This shows that, while topographic structure has a negligible impact on differences among soil moisture patterns across the three hillslopes, it may have an impact concerning the distribution of soil moisture at the individual hillslope scale.

Matrices summarizing the results of autocorrelation and slope-intercept analysis of linear regression revealed that the highest degree of temporal stability was associated to wet conditions; autocorrelation values clearly increased with sampling depth on each hillslopes for the three years and in a few cases all correlations are statistically significant ($\alpha:0.01$). Poorly correlated patterns were more commonly found in 2006 at all depths and this difference was again imputed to the different distributions of rainfalls during the field works: the campaign carried out in 2006 can be divided into wet and dry days whose comparison tends to give low correlations.

Correlograms for each hillslope at any depth displayed that correlation decreased when time lag between sampling occasions increased. Correlation was not significant anymore beyond a certain temporal threshold. The curve patterns were similar for the three depths but correlations were higher in 2005 and 2007, as also revealed by the previous analyses.

Trend of Spearman rank correlation coefficient computed between values of a given day with respect to the values of the previous day showed a clear decrease after rainfalls: the decline of correlation occurs at times of transition from a dry to a wetter state, as found by other studies. This behaviour is more evident for the surface layers, earlier and more quickly affected by precipitation inputs. The hillslope were interested by water table increases after rainfalls and, generally, the piezometric response appeared to be mainly related to the cumulated precipitation rather than to high-intensity rain events.

The various analyses performed revealed a contradiction: soil moisture patterns at the surface layers were less variable, more temporally stable compared to the other depths but, at the same time, less correlated to each other. We explained this paradox considering processes which influence only the dynamics of the shallow layers, more likely to be influenced by precipitation inputs earlier in time and more clearly, compared to the other depths.

CHAPTER 5: WATER TABLE VARIATIONS AND RUNOFF RESPONSE

Introduction

The surface water available as input for runoff generation comes from snowmelt and from the fraction of precipitation which is not intercepted and retained by the vegetation (throughfall). The portion of this water which does not accumulate in depression storage moves freely over the ground surface as overland flow; when overland flow concentrates in channels is called channel flow and combination of the two kinds of movements is generally defined as surface flow. Overland flow can be generated by two mechanisms. Infiltration excess (Horton mechanism) occurs when the soil is saturated from above: the amount of rain and water from upslope areas exceeds the soil's infiltration capacity. The saturation excess process (Dunne mechanism), on the contrary, occurs when the soil is saturated from below: the matrix pressure of the soil is positive due to pressure from soil water in situ or from upslope soil volumes. Excess saturation runoff is controlled by fluctuations of the groundwater surface, so runoff will occur in the catchment at any time or place where the water table is at the ground surface; the rise of water table is related to topographic convergence areas where the subsurface flow increases (Molénat et al., 2005). Overland flow can significantly contribute to the total stream discharge and plays an important role in determining the size and the shape of flood peaks (Troch et al., 1994); furthermore, overland flow is strictly connected to sediment (Lane et al., 1997) and agrochemical transports which reside on the soil surface (Jolánkai and Rast, 1999). Despite its intrinsic importance, overland flow has hardly ever been observed over areas larger than a few hectares through direct measurements, and also qualitative field observations of overland flow occurrence are scarce (Van Loon, 2001).

During inter-storm periods, stream water comes only from groundwater through lateral flow in the soil or return flow on the ground surface. During storm periods, groundwater flow and return flow remain active and can even contribute significantly to the stream discharge (Sklash and Farvolden, 1979, Weiler et al., 2005); talus groundwater can be also an important contributor to

streamflow, particularly during storm events (Clow et al., 2003). The occurrence of shallow groundwater flow in catchments is often due to the presence of a shallow impervious layer. In such pedogenic and lithological environments, percolating water flow is stopped or limited and a saturated zone is developed, which, in turn, produces lateral groundwater flow in response to the downslope hydraulic gradient. It is thus accepted that (i) lateral water movement is affected predominately by gravity forces, rather than hydrostatic or capillary forces and (ii) topography controls the water flux and flow-path geometry. As a consequence, saturated areas are located in zones of topographic convergence where subsurface flow is routed by gravity (Molénat et al., 2005). However, in analyses concerning runoff generation, any possible hydrological pathway should be considered until there is evidence to the contrary, rather than excluding potential pathways a priori because contrary to the current thinking (Elsenbeer and Lack, 1996). Hillslopes hydrology studies in the recent decades developed models with the purpose of representing the variations of water table, the quantification of runoff and the extent of soil saturation area in relation to the site topography. Topmodel (Beven and Kirkby, 1979) is an example of conceptual model: it considers gravity as the main force driving water within the soil and represents subsurface flow as a water sheet running locally parallel to the topographic surface. The flow is then expressed using Darcy's law and three main assumptions are made: (1) the local hydraulic gradient is constant in time and equal to the local topographic slope; (2) the discharge per unit area is steady in space; and (3) the transmissivity and the hydraulic conductivity decrease exponentially with depth. According to the Topmodel's assumptions, the dynamics of the simulated outflow from the groundwater zone always follow the simulated rise and fall in groundwater levels. These groundwater levels always go up and down in parallel. The simulated runoff from the groundwater zone follows the same dynamic. Thus it is assumed implicitly that the groundwater storage and runoff can be described as a succession of steady state flow conditions (Seibert et al., 2003).

Various studies focused on the observation and modelling of shallow water table fluctuations and subsurface flow at different catchment scales: Thompson and Moore (1996), Lamb et al. (1997), Seibert et al. (1997), Myrabø (1997), Scanlon et al. (2000); only few of them, though, have sought to test the validity of the concepts at the basis of Topmodel (Moore and Thompson, 1996, Blazkova et al., 2002, Seibert et al., 2003, Molénat et al., 2005); particularly,

Moore and Thompson (1996), followed by Seibert et al. (2003) and Molénat et al. (2005) examined whether ground water table variations were consistent with the steady state assumption. The latter noticed that in simulating the groundwater depth distribution along the entire hillslope, the steady-state assumption was quite constraining and led to unacceptable water-table depths in the midslope and summit areas. Moore and Thompson (1996) found that for a catchment in Canada the steady state assumption was satisfied; the upslope sites of their dataset, though, lacked representation because the piezometric wells were located mainly in convergent zones, close to the stream or in the lower third of the hillslope. Thus, they speculated that the far-stream zone of their experimental catchment might not follow the steady state assumption and suggested a revision of the Topmodel concept using a two-areas catchment model. Seibert et al. (2003) reviewed such extended concept and showed that the steady state assumption might be appropriate for the riparian zones in a Swedish till catchment but inappropriate for the upslope zone. Riparian zones and upslope zones show distinctly different groundwater level-runoff relationships: groundwater levels closest to the stream were in phase with runoff, whereas areas further away lagged behind the streamflow.

This work aims at assessing: i) the possible interconnections between the development of ephemeral river network and fluctuations of water table, soil moisture and stream discharge during rain storms; ii) the consistency of water table variations with the steady state assumption at the basis of the Topmodel concept.

Results and discussion

Rio Larici subcatchment (3.3 ha), localized in the south-western part of the Rio Vauz catchment (Figure 9) was selected and instrumented since 2006 in order to extend the experimental sites for hydro-meteorological data collection. As described in chapter 2.1, precipitation was recorded by a tipping bucket rain gauge, stage was measured at 15-minute interval by a pressure transducer installed by a V-notch sharp-crested weir on Rio Larici creek, soil moisture values at 0-30 cm depth were collected hourly by means of a water content reflectometer (positioned in 2005 and 2006 on Emme hillslope and then moved to Rio Larici subcatchment in 2007) and level of water table were monitored by 12 capacitance probes scattered across the site. In order to evaluate the dynamics of the ephemeral river network developed during or immediately after rainfalls, 25 Overland Flow Detectors (OFDs) were installed on concentrated flow lines in the subcatchment where overland flow was expected to occur. Volumetric soil moisture data collected manually during the 2007 field work at 0-6 and 0-20 cm depth on a 0.1 ha experimental grid are still being analyzed and were not reported in this thesis.

5.1 Runoff response and interaction of processes

The total amount of precipitation collected during the field works carried out during 2006 and 2007 was partitioned in single rainstorms in order to assess the behaviour of the various hydrological processes at the hillslope and rainfall scale. An arbitrary threshold of 9 mm of rain was chosen; 16 main events were identified from June 26 to October 16, 2006 and 23 events from May 15 to October 17, 2007. OFDs were checked on 10 and 7 occasions in 2006 and 2007, respectively.

Overland Flow Detectors give a dichotomous answer (yes/no) according to the presence or absence of water collected into the instrument's vertical chamber; a segment of the ephemeral stream network forming during rainfalls was assigned to each instrument so that the extension of the saturated area could be identified after rain events. Maps of OFD response were created: the ephemeral network was considered inactive if the OFD corresponding to a

certain segment did not record any presence of overland flow whereas the network was considered active if the instrument was filled with water. An example of such maps is depicted in Figure 38.

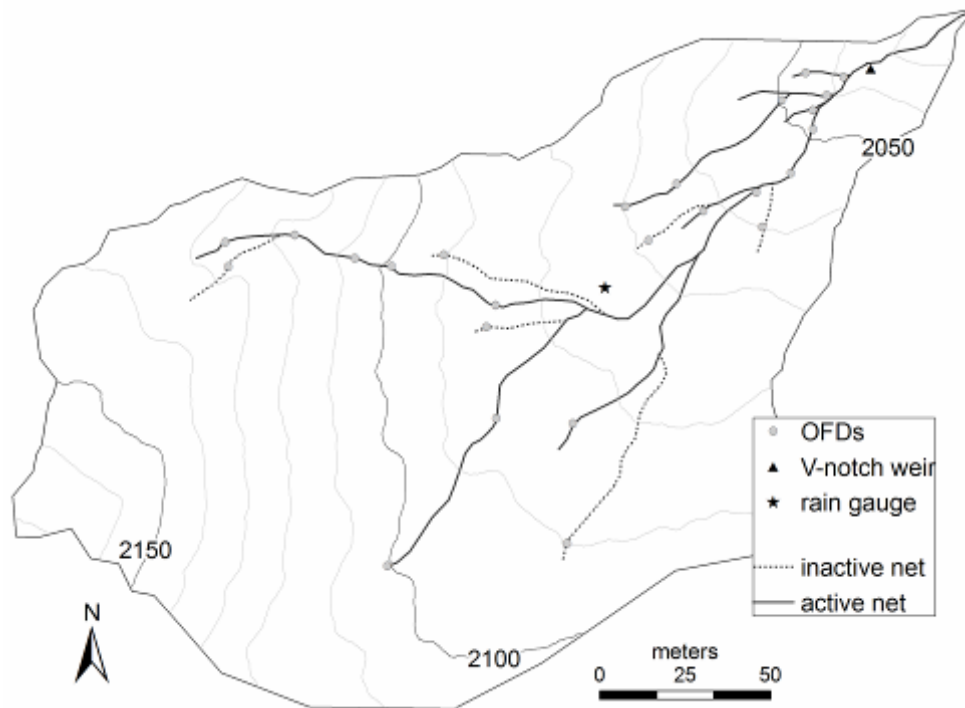


Figure 38: river network developed during rain storm number 22-07 and recorded by the OFD response

Overland flow generation was believed to be related to mechanisms of saturation from above, especially in the upper part of the subcatchment, where steep slopes are. The central and lower parts of the site, close to the creek, are often characterized by accumulation of water even during inter-storm periods due to topographic convergence; here, the water table is much nearer to the ground surface and overland flow is supposed to generate by return flow water which infiltrates in the higher parts of the hillslope, follows preferential flow paths and emerges downstream. The percentage of instruments reporting presence of water tends to increase with frequent rainfalls of high cumulated value rather than after short and intense storms.

The length of stream network developed during rainfalls was calculated as percentage over the total length; the 2006 and 2007 rain events were considered together and plotted against several variables measured or calculated at the rainfall scale. The saturated area of the hillslope appeared to be better related to peak discharge, to the highest level of water table, to the antecedent soil moisture conditions and to the maximum value of water content

measured at 0-30 cm depth during or immediately after the precipitation (Figure 39). The relationship between the length of active stream network, peak discharge and maximum rise of water table suggests a spatial and temporal consistency and a good interconnection between subsurface and surface runoff, which respond with similar dynamics to precipitation inputs at the rainstorm scale. The soil moisture value at 0-30 cm depth was obtained as the mean among the four probes installed across the hillslope. The relation between stream network expansion and maximum soil water content during rainfalls was stronger than the one with antecedent moisture condition because the increase of soil moisture during or after rain events represents a quick and direct effect of precipitation but, at the same time, an effect of the occurrence of overland flow itself. This confirms the relationship between soil moisture and saturated areas found by others (Van Loon 2001, Godsey et al. 2004).

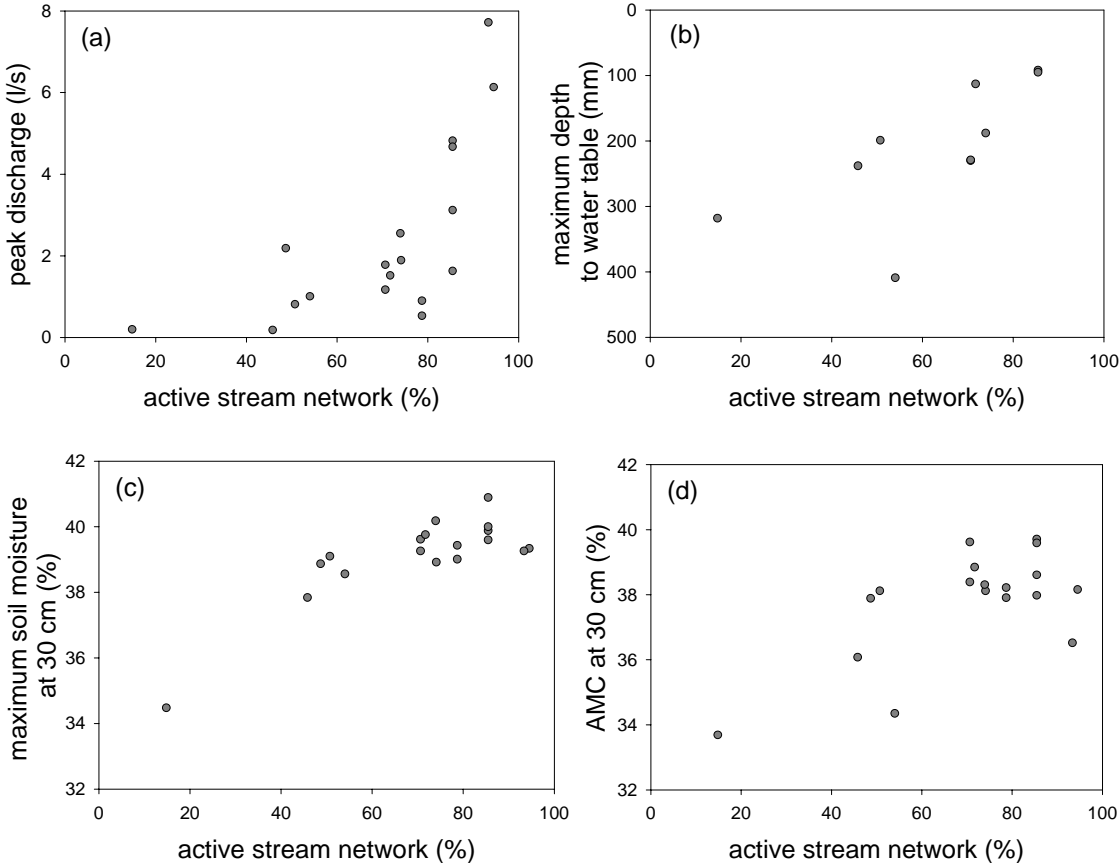


Figure 39: relationship between percentage of Rio Larici active network and peak discharge (a), maximum rise of water table (b), maximum water content (c) and antecedent moisture conditions (d)

Runoff coefficient was calculated for each rainstorm and regressed against other variables: the best relationships were found with maximum soil moisture, maximum rise of water table and active stream network (Figure 40): although the correlation was weaker between runoff coefficient and the length of network interested by surface flow, the three point clouds have a similar shape suggesting that an increase of runoff corresponds to analogous increase of water table, of saturated areas and of water content in the surface soil profile, underlining once again the connections between surface and subsurface movements of water.

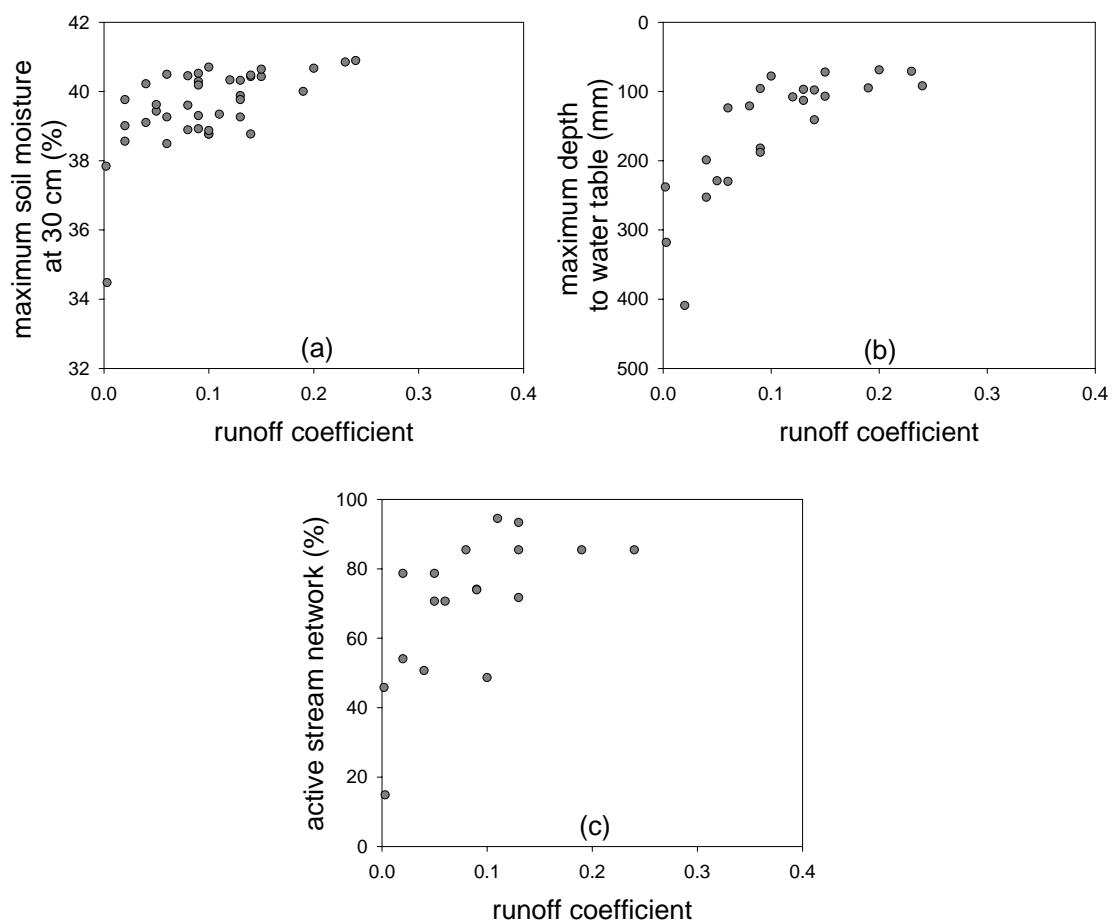


Figure 40: relationship between runoff coefficient and maximum water content (a), maximum rise of water table (b) and active stream network (c)

Moreover, the highest levels of groundwater recorded over all piezometric wells across the hillslope were found to be related to other hydrological variables. Point clouds determined by maximum rise of water table with peak and pre-event discharge (Figure 41 a, b) showed a shape similar to the ones observed in Figure 40: high values of peak discharge and pre-event discharge

correspond to increases of water table which tends to rise almost up to the ground surface. The highest level of water table occurred during rain events was also related to the moisture conditions of soil (Figure 41 c, d): although a certain degree of scatter exists, a clear similar tendency could be however noted, both with the maximum water content and with antecedent moisture conditions. Once more, it is evident the connection between water movements under and on the ground surface. Moreover, the positive correlations between pre-event discharge, AMC and maximum rise of water table induce to consider the value of discharge measured at Rio Larici weir before rain event as representative of the groundwater height and of overall soil moisture condition of the entire subcatchment.

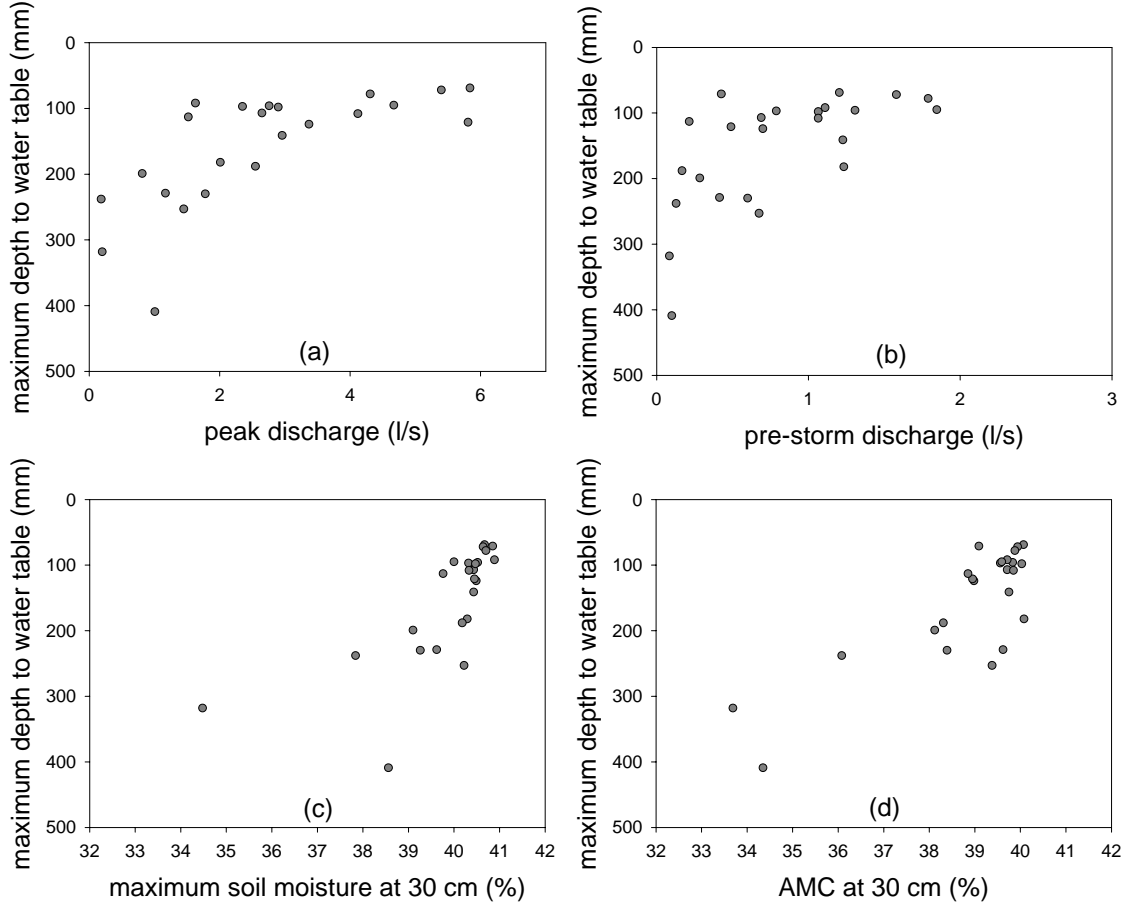


Figure 41: relationship between maximum rise of water table and peak discharge (a), pre-event discharge (b), maximum water content (c) and antecedent moisture conditions (d)

All these observations highlight the strict interaction, and sometimes the cause-effect dependences, of processes that play an important role in generating runoff both at small spatial scale (hillslope) and at short temporal scale (rainstorm). Furthermore, examination of data revealed synchronous time lags

between increase of discharge and attainment of peak discharge after or during rainfalls; equally, the same time interval occurs between the rise of water table and the achievement of the maximum groundwater level: this observations suggest similar response dynamics of the processes across the hillslope to the precipitation inputs at the rainfall scale.

In addition to analysis at the rain event scale, time series of measurements taken continuously during the field campaigns were compared in order to assess the connection of processes over storm and inter-storm periods. Figure 42 a, b display the regression between soil moisture collected hourly at 0-30 cm depth and Rio Larici discharge (measured at the same time interval) for 2006 and 2007, respectively. A clear and similar relationship can be observed in both plots confirmed by the high statistical significance ($p < 0.01$) of Spearman rank correlation coefficient which is equal to 0.84 for 2006 and 0.83 for 2007 dataset (see also Table 15 and Table 16). The point clouds in each plot can be fitted by a power interpolation; in 2007 the soil moisture range is wider than in 2006 and this disparity is reflected in the greater frequency of attainment of high values of discharge (even though the range of discharge values is the same for both years). This difference can be attributed to a real higher overall wetness of the sites between the two campaign though, obviously, the diverse location of the water content reflectometer (on Emme in 2006, on Rio Larici subcatchment in 2007) must be taken in account.

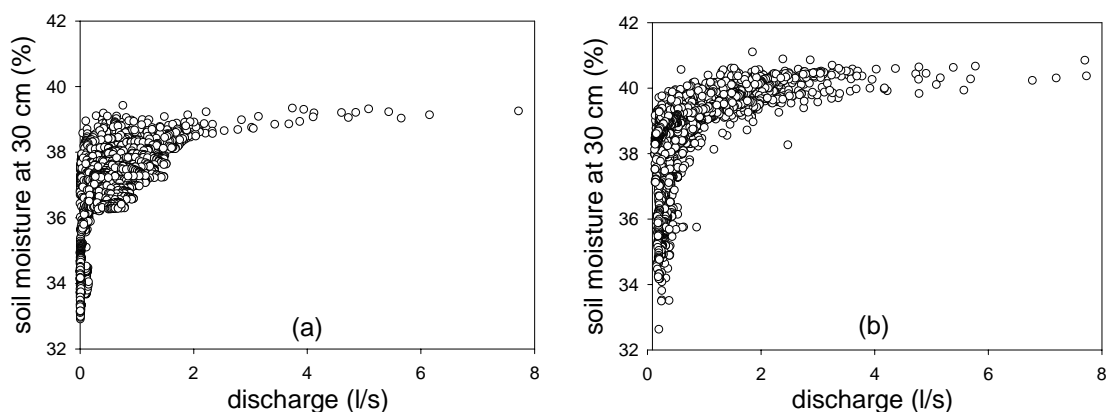


Figure 43: regression between Rio Larici stream discharge and soil moisture at 0-30 cm depth for the whole 2006 (hourly from June 26 to October 16) and 2007 (hourly from May 16 to October 15) datasets

Multiple correlations were performed among all water level measurements across the Rio Larici hillslope, soil moisture and discharge values for 2006 and 2007 field works (Table 15 and Table 16). Out of 12

capacitance probes installed over the subcatchment, in the 2006 campaign four piezometric wells did not record any change in water table level whereas in 2007 only instrument L9 did not respond at all. Furthermore, installation problems occurred in 2006: it was noted that sometimes the capacitance probes responded very quickly to precipitation inputs, with strong water table variations occurring even a few minutes later the begin of rain. A percolation along the water-proof PVC pipes, which were inserted into the ground to contain the probes, was suspected; a layer of bentonite clay was used in order to prevent the water from flowing into the pipes and a lack of effectiveness of such cover was presumed. Owing to a scarce quality of bentonite used in 2006, this waterproofing layer cracked after a few storms which washed the cover away allowing rain and overland flow water to infiltrate into the wells. Thus, only the first five rain events of 2006 field campaign could be considered.

All Spearman rank correlation coefficients reported in Table 15 and Table 16 are significant at 99% for both years considered: this indicates a strong relationship between discharge (marked by the letter “Q” in the table), groundwater (name of piezometric wells in the table) and soil moisture (“sm” in the table) as well as the same strict connection among all single capacitance rods within the site, suggesting that fluctuations occurred with similar temporal and spatial dynamics across the catchment. The negative signs before the correlation coefficients for discharge-groundwater and soil moisture-groundwater comparisons are due to the fact that the difference between the ground surface and the water table, i.e. the depth to the water table from the surface, was recorded. Especially in 2007 dataset, the values of correlation coefficient between discharge and all piezometric wells are very similar to the ones between soil moisture and all piezometric wells: this further confirms the same dynamics which characterize the processes across the whole hillslope independently of the time scale considered. The changes of ρ values with respect to the spatial localization of water level loggers is discussed further in section 5.2.

Table 15: Spearman rank correlation coefficients for the 2006 monitoring period from June 26 to July 10; all values are statistically significant ($p < 0.01$)

Spearman	Q	sm	L2	L3	L4	L5	L6	L7	L8	L10
Q	1									
sm	0.84	1								
L2	-0.62	-0.85	1							
L3	-0.58	-0.83	0.96	1						
L4	-0.55	-0.63	0.81	0.82	1					
L5	-0.59	-0.84	0.96	0.99	0.83	1				
L6	-0.54	-0.61	0.75	0.79	0.79	0.79	1			
L7	-0.59	-0.83	0.96	0.99	0.82	0.99	0.79	1		
L8	-0.83	-0.77	0.64	0.64	0.64	0.67	0.78	0.66	1	
L10	-0.83	-0.83	0.74	0.68	0.55	0.69	0.72	0.69	0.82	1

Table 16: Spearman rank correlation coefficients for the whole 2007 monitoring period; all values are statistically significant ($p < 0.01$) except the one marked with *

Spearman	Q	sm	L1	L2	L3	L4	L5	L6	L7	L8	L10	L11	L12
Q	1												
sm	0.87	1											
L1	-0.30	-0.30	1										
L2	-0.71	-0.73	0.49	1									
L3	-0.58	-0.60	0.52	0.89	1								
L4	-0.77	-0.80	0.54	0.89	0.78	1							
L5	-0.61	-0.64	0.55	0.90	0.91	0.84	1						
L6	-0.69	-0.67	0.45	0.94	0.95	0.88	0.92	1					
L7	-0.74	-0.73	0.57	0.91	0.88	0.92	0.94	0.92	1				
L8	-0.42	-0.29	-0.31	0.24	0.23	0.24	0.12	0.35	0.24	1			
L10	-0.41	-0.44	0.56	0.69	0.72	0.73	0.72	0.72	0.74	0.06	1		
L11	-0.55	-0.57	0.63	0.78	0.75	0.79	0.78	0.79	0.79	0.05*	0.80	1	
L12	-0.24	-0.24	0.29	0.62	0.69	0.52	0.61	0.70	0.53	0.23	0.68	0.64	1

5.2 Water table variations and assessment of the steady state assumption

Owing to the problems described in section 5.1, only five rainstorm events could be used in order to study the water table variations within Rio Larici catchment for the 2006 dataset whereas groundwater response to nineteen rainfalls were analyzed in 2007, for a total of 24 storms. Thus, Figure 44 is presented only for the first year studied, reporting data from the middle of May to the middle of October, 2007: the graph displays the water table fluctuations

recorded by some capacitance probes installed over the hillslope in relation to precipitation and stream discharge (no data are available from the middle of July to the middle of August). First, discharge exhibits a clear response to precipitation, followed by corresponding variations of groundwater. At such seasonal scale, almost a perfect synchrony among peaks is observed; in fact, zooming at a few week scale, a small lag time resulted between peak discharge and maximum rise of water table. Particularly, the delay is more evident for those piezometers installed in the upper part of the site. The frame reporting the legend in Figure 44 displays in brackets, close to the level loggers' name, the distance of each instrument from the head of the creek, where the flow becomes channelled and a clear gully is visible. It is interesting to note that water table recorded by piezometric wells localized further away from the creek, in the area defined as far-stream zone, is definitely deeper than groundwater levels monitored by wells placed in the near-stream zone. This is consistent with field surveys which revealed very wet conditions in the central-lower part of the catchment even during inter-storm periods.

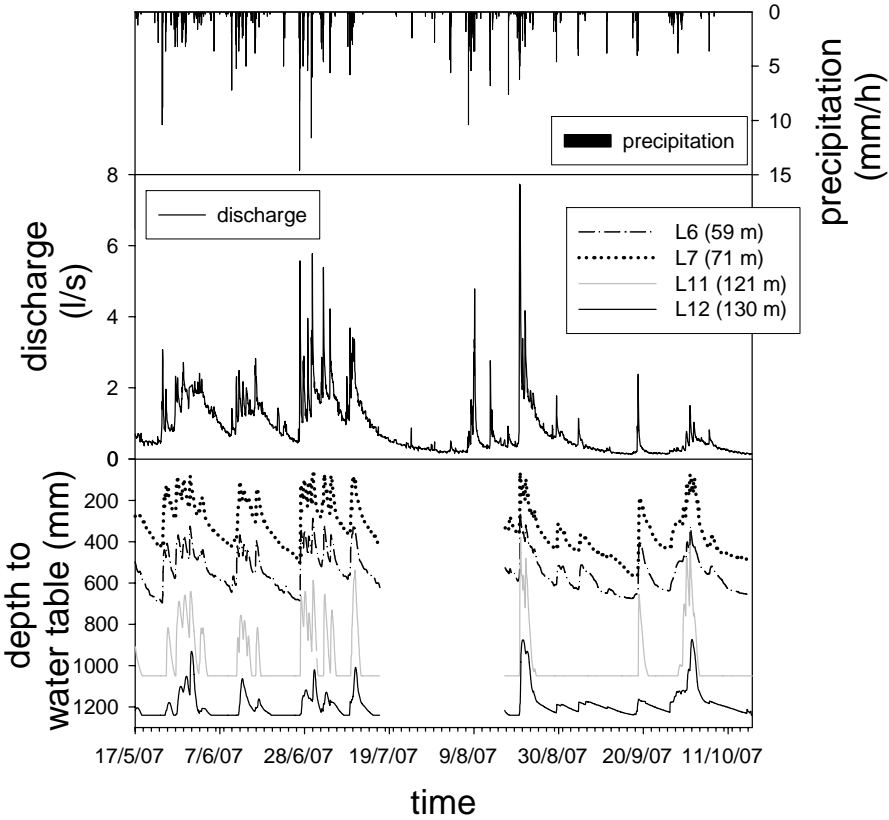


Figure 44: water table level recorded by four piezometric wells within Rio Larici subcatchment in 2007 compared to stream discharge and precipitation. In the frame: distance of each well from the channel head

Seibert et al. (2003) found that in their experimental site in Sweden the groundwater levels closest to the stream were in phase with runoff while areas further away lagged behind the stream flow; furthermore, they noted that the correlation between water table levels and runoff decreased markedly with the distance of the wells from the stream, whereas a high degree of correlation was observed between wells at similar distances from the creek. In our case, all correlations between discharge and groundwater level were positive both in 2006 and in 2007 (see Table 15 and Table 16 in section 5.1) and the various piezometric wells across the site were always positively related to each other. Spearman correlation coefficients between discharge and groundwater were also plotted versus the distance of each well from the channel in order to test the influence of the spatial distribution of level loggers on the relationship between groundwater and runoff (Figure 45). All correlations are above the significance level: in 2007 there is a certain decrease of RMSE with distance which, on the contrary, cannot be observed in the 2006 data set. Thus, unlike Seibert et al. (2003), distance from the creek is not a discriminating factor in partitioning the hillslope in near-stream and far-stream zone; groundwater level in wells close to Rio Larici stream appeared to have temporal dynamics similar to each others and also similar to the wells in the far-stream zone; besides, stream discharge shows a good correlation with water table across the whole hillslope. Although a clear difference in water table depth exists between the near- and the far-stream zone, no significant time lags between water table increase and peak runoff were observed. This suggests an almost synchronous response of the site to precipitation inputs and that a steady state assumption for the entire sub-catchment can be made.

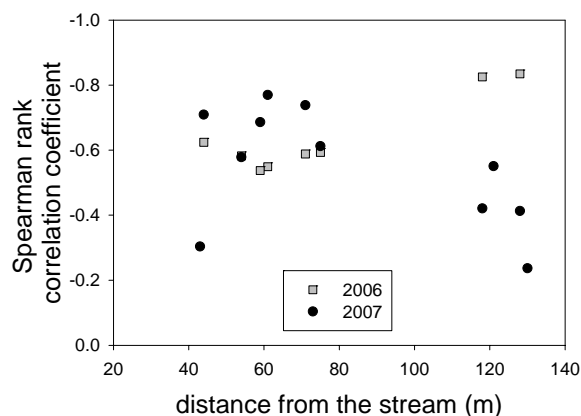


Figure 45: Spearman rank correlation between water table levels and discharge against distance of each piezometric well from the stream

Following Moore and Thompson (1996) and Seibert et al. (2003), in order to assess the goodness of prediction of a model which is based on a steady-state assumption, a reformulation of TOPMODEL was used. According to Beven and Kirkby, (1979), the depth to the water table at location i and time t , $z_{i,t}$, is expressed by equation 16

$$z_{i,t} = \bar{z}_t - \frac{1}{f}(I_i - \bar{I}) \quad (16)$$

where \bar{z}_t is the mean depth in the catchment, f is a parameter governing the rate of decrease of the saturated hydraulic conductivity with depth, I_i is a local soil-topographic index and \bar{I} is its average over the entire catchment area. Moore and Thompson (1996) suggested a rearrangement and a reformulation of equation 16:

$$z_{i,t} = \frac{\bar{I}}{f} - \frac{I_i}{f} + \bar{z}_t \quad (17)$$

$$z_{i,t} = a_0 + b_i + c_t + \varepsilon \quad (18)$$

where a_0 is a constant, b_i represents the location effect, c_t represents the time effect and ε is the random error. In this linear model, three components are sufficient to describe the levels of water table: i) a constant for a given catchment; it depends on the average level of water table; ii) a location effect, which is applied to each location at all piezometric wells and is invariant with time; it depends on the topographical position of each well and other properties (i.e. transmissivity); iii) a time effect, applied to all locations at the same time; it reflects the hydrologic conditions at the sampling time. Equation 18 was fitted to the measured piezometric data by using a least square approach. The linear model for the prediction of water table variations was applied at the rain event scale for five rainfalls in 2006 and nineteen in 2007; groundwater data were available at 15-minute time interval. The analysis of variance for single storms was performed and values of mean squared error (MSE), root mean squared errors (RMSE) and R^2 between modelled and measured data are presented in Table 17.

Table 17: errors and R² values obtained by the analysis of variance for the model $z_{i,t} = a_0 + b_i + c_t + \varepsilon$ for single rainfalls in 2006 and 2007

Storms 2006	MSE (mm ²)	RMSE (mm)	Adjusted R ²
1-06	22	4.7	0.9994
2-06	336	18.3	0.9921
3-06	17	4.1	0.9996
4-06	1159	34.0	0.9780
5-06	735	27.1	0.9842
Storms 2007	MSE (mm ²)	RMSE (mm)	Adjusted R ²
1-07	1770	42.1	0.9832
2-07	1957	44.2	0.9813
3-07	502	22.4	0.9940
4-07	327	18.1	0.9965
5-07	1606	40.1	0.9847
6-07	275	16.6	0.9972
7-07	1175	34.3	0.9892
8-07	4778	69.1	0.9537
9-07	537	23.2	0.9948
10-07	457	21.4	0.9956
11-07	1550	39.4	0.9840
12-07	2788	52.8	0.9763
13-07	1443	38.0	0.9878
14-07	3562	59.7	0.9650
18-07	6873	82.9	0.9275
19-07	529	23.0	0.9919
20-07	518	22.8	0.9948
21-07	444	21.1	0.9953
22-07	3975	63.0	0.9564

Both location and time for the linear model had a significant effect ($p < 0.01$) on the groundwater level $z_{i,t}$ at a certain well i observed at time t for all storms. The model proved to be a good predictor of groundwater height across all catchment; the errors between simulated and observed values are small, ranging from a minimum of 4 mm to a maximum of 8 cm. The degree of variance of groundwater explained by the model is high, varying from 93% to 99%. A closer observation of data revealed that generally lower errors occurred for those rainfalls where water table variations were moderate whereas the departure of modelled values from the measured ones increased for marked water table variations. For instance, the highest value of RMSE resulted for

rainstorm number 18, in 2007 when all piezometers installed over the hillslope (except L9 which never recorded over the two field campaigns) showed considerable fluctuations. The plots depicted in Figure 46 show the relationship between RMSE between simulated and observed values and maximum water content, maximum rise of groundwater and saturated area over the hillslopes . The graphs confirm this finding: when the maximum level of water table, the highest value of soil moisture and the length of active stream network increase, the errors increase too; in other words, the higher the runoff response, the higher the errors of the linear model.

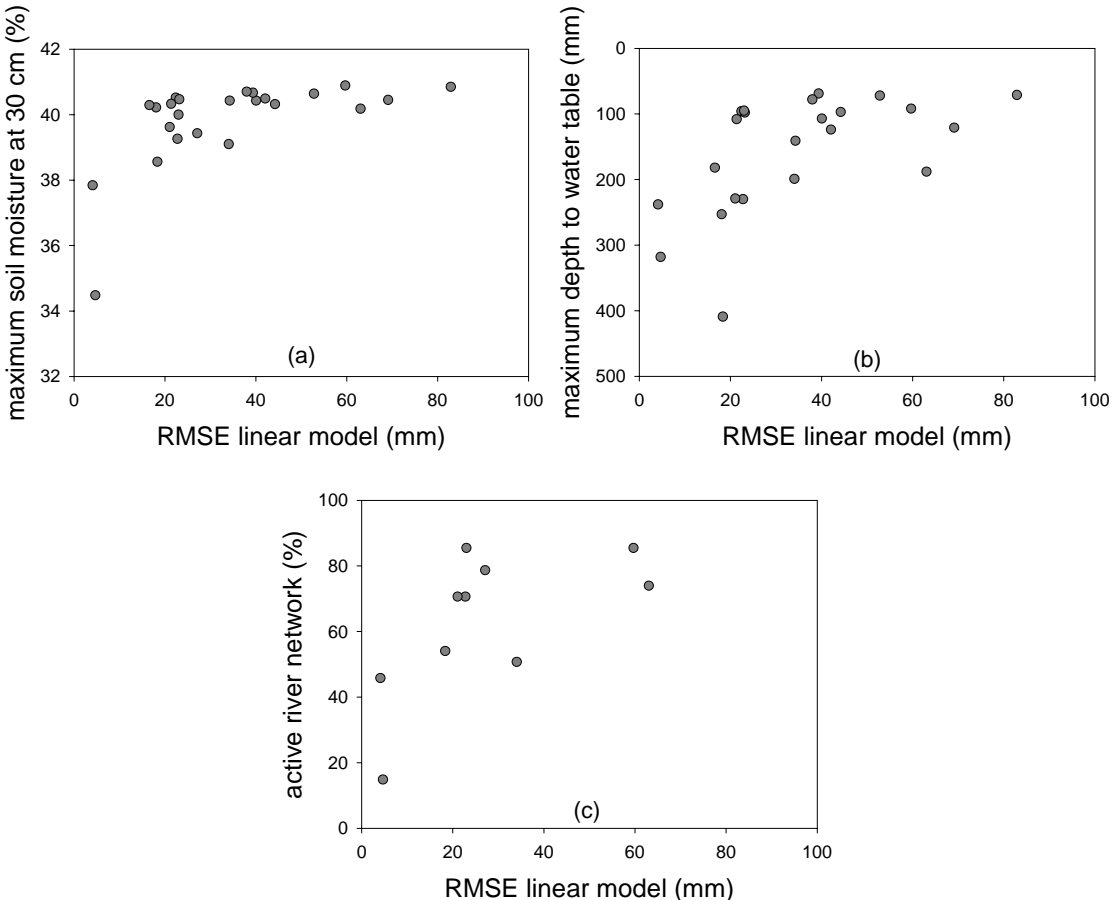


Figure 46: RMSE for the model $z_{i,t} = a_0 + b_i + c_t + \varepsilon$ for each rainfall plotted against maximum value of soil moisture at 0-30 cm depth (a), piezometric peak (b) and active stream network (c)

Were departures between modelled and measured groundwater levels dependent on the spatial localization of piezometric wells across the catchment? Table 18 presents RMSE values for the linear model for each capacitance probe and each storm analyzed in 2006 and 2007. The errors for each well were averaged over the rainfalls and plotted against the distance from the stream (Figure 47): once more, a different behaviour between near- and far-stream zone

Table 18: RMSE for the model $z_{i,t} = a_0 + b_i + c_t + \varepsilon$ for each piezometric well at the rainstorm scale

Wells→	L1	L2	L3	L4	L5	L6	L7	L8	L10	L11	L12
Storms↓											
1-06	-	9.5	2.1	1.4	2.5	4.1	1.9	2.9	4.1	-	-
2-06	-	32.5	9.3	4.9	4.7	17.2	8.6	26.9	6.4	-	-
3-06	-	6.1	2.0	3.3	1.3	3.3	2.6	6.3	3.3	-	-
4-06	-	12.3	6.6	28.6	3.7	17.2	75.5	22.2	23.0	-	-
5-06	-	18.6	3.3	10.6	12.0	16.9	59.3	21.7	14.3	-	-
1-07	30.8	22.3	51.3	10.6	9.6	65.6	61.9	34.2	34.1	36.3	36.3
2-07	37.9	27.5	36.3	7.4	9.8	32.4	32.9	50.2	28.1	96.7	31.3
3-07	15.2	19.2	25.8	4.9	9.5	16.2	23.1	22.2	9.6	35.2	31.3
4-07	12.7	17.5	38.6	6.8	8.4	19.6	5.8	15.8	12.7	12.7	12.7
5-07	44.3	27.4	33.8	9.3	11.7	32.7	56.9	37.9	30.1	57.8	43.5
6-07	6.4	7.5	21.1	3.3	3.3	15.0	5.6	6.5	12.3	36.3	19.2
7-07	37.4	16.4	28.9	4.6	6.4	31.8	33.3	37.4	19.1	65.7	29.4
8-07	58.9	32.3	-	13.1	22.3	71.6	29.3	73.0	59.8	93.9	70.5
9-07	18.3	20.8	-	8.4	14.7	12.7	21.9	19.8	17.1	46.7	14.2
10-07	20.1	8.7	-	8.6	10.4	18.2	21.2	19.6	8.6	29.6	26.7
11-07	18.1	24.3	-	9.6	26.8	18.9	32.7	32.1	14.8	76.9	59.1
12-07	43.1	38.6	-	5.1	16.2	26.7	27.5	51.0	27.0	124.5	30.8
13-07	32.7	18.7	-	4.8	6.4	18.8	35.0	33.1	18.7	83.2	35.6
14-07	34.9	44.5	-	22.3	24.5	29.3	43.7	65.2	61.7	124.0	37.3
18-07	61.9	56.0	35.1	25.2	62.0	21.4	29.4	96.3	91.7	160.0	100.2
19-07	11.5	20.8	11.1	5.3	8.6	7.5	18.7	19.3	14.3	48.0	34.0
20-07	20.8	26.6	31.8	15.7	13.3	15.7	28.6	20.8	20.8	20.8	12.0
21-07	17.6	26.8	41.3	12.0	8.7	15.7	7.8	17.3	17.6	17.6	12.8
22-07	59.9	39.0	75.7	16.8	17.8	35.5	89.2	70.4	50.0	87.0	61.2
Mean RMSE	31.2	23.9	26.7	10.1	13.1	24.0	34.3	33.4	25.0	66.0	36.7

is not evident, the model errors did not increase as function of distance from the creek and the position of piezometers did not seem to influence the model predictions. The highest deviation of simulated water levels from the groundwater measurements is associated to piezometer L11 which is the well that displayed consistently, over time, the greatest variations of water table

levels. On the contrary, the lowest values of mean squared errors were observed for wells L4 and L5 which showed very small variations of water table level over the field campaigns. Thus, the linear model proved to predict accurately the groundwater level in the 3.3 ha wide Rio Larici at the rainstorm scale, without significant differences between the near-stream and the far-stream zone, confirming the goodness of the steady state assumption. Although the overall errors are quite small, the cases where the model showed some inaccuracies were related to conspicuous water table variations.

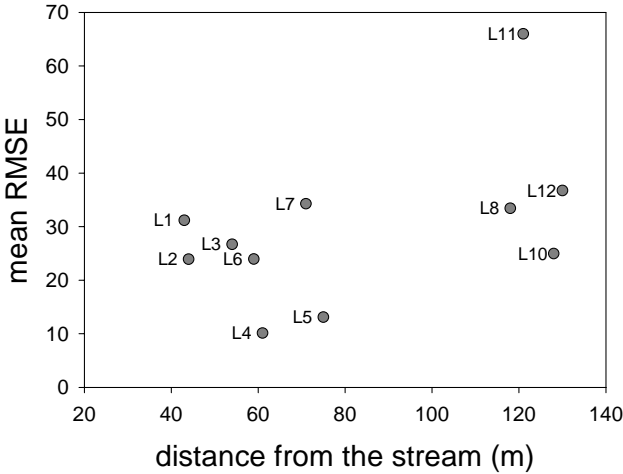


Figure 47: RMSE of every piezometric well averaged over all storms and plotted against the distance from the stream

Two examples of the different predictions in the groundwater level computed by the linear model are presented in Figure 48. The plots depict precipitation, stream runoff and simulated/measured water table variations for two storms with different properties: panel a) displays data from rain event number 19, occurred on August 21, 2007, with total precipitation of 10.4 mm; panel b) shows data from rainfall number 22, occurred on September 18, 2007, with total precipitation of 19.8. Despite the greater amount of rain fell during the second storm, the discharge (both pre-event and peak) was lower: this is due to a long dry period without precipitation (around seven days in a row) that happened just before the storm number 22. The root mean squared errors for the linear model $z_{i,t} = a_0 + b_i + c_t + \varepsilon$ for storms 19-07 and 22-07 are 23 mm and 63 mm, respectively. All the other storms were analyzed but, for the sake of brevity, graphs are not reported here.

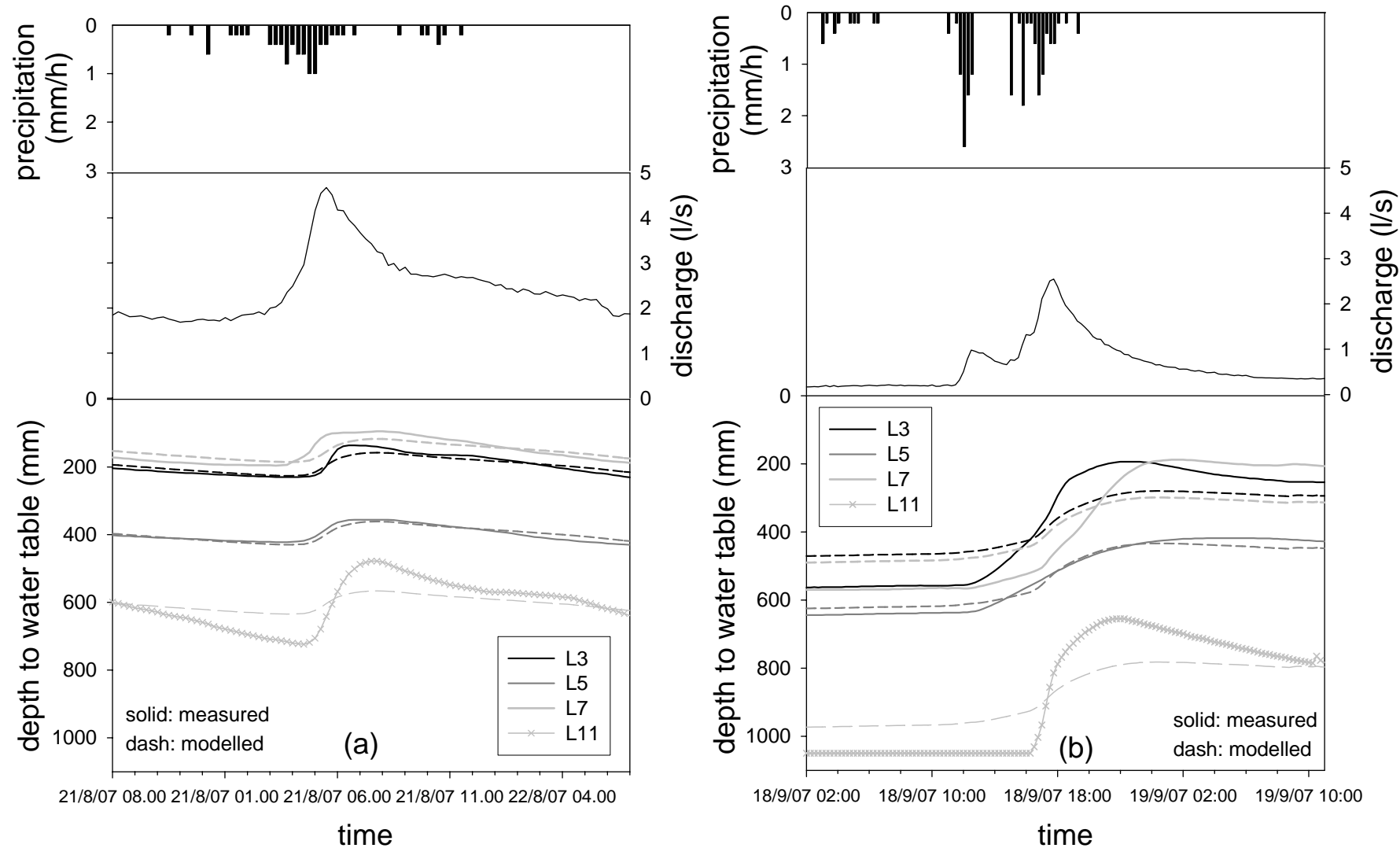


Figure 48: examples of differences between measured and modelled values of water table recorded by four piezometric wells compared to stream discharge for storms number 19-2007 (a) and 22-2007 (b)

Generally, a positive or negative temporal shift did not seem to occur between the peak of simulated water table values and the maximum rise of measured values, instead the two curves tend to increase and decrease at the same time. The departure of modelled groundwater levels from the measured ones is mainly represented by an overestimate of the model before the water table rise and a subsequent underestimate of the peak (see Figure 48, b): indeed, in the dataset, it was much more frequently observed an initial overestimate of the model followed by an underestimate after the maximum rise of water table. In other words, the linear model gives a more smoothed curve respect to the real one. When small rain events occur (see Figure 48, a), the RMSE are generally lower as well as the water table variations; the simulated and measured curves are much nearer to each other, the model still underestimates the piezometric peak, though in a smaller way. Thus, the higher errors of the linear model were always found during (relatively) heavy rains and, in addition, for those piezometric wells that exhibited important ground water fluctuations. Piezometer L11 in Figure 48 provides a good example: the overall variation (greater for the major storm) is more marked compared to the ones of the other capacitance rods; at the same time, the RMSE is noticeably higher for L11 respect to the other wells both for the small storm number 19 (L11 48 mm, L3 11 mm, L5 9 mm, L7 19 mm; RMSE for the total rain event: 23 mm) and for the bigger storm number 22 (L11 87 mm, L3 76 mm, L5 18 mm, L7 89 mm; RMSE for the total rain event: 63 mm). Other examples that confirm this remark can be found by observing Table 18.

The departure between the measured water table levels and the ones predicted by the linear model can be explained by the clear hysteresis effect of the relationship between discharge and groundwater levels at the rainfall scale. Figure 49 depicts four examples of different piezometers for various storms but this phenomenon, more or less marked according to the importance of rainfalls, could be consistently observed in the whole dataset. Myrabø (1997) described a hysteresis effect between runoff and water table in a small catchment in moraine terrain in Norway: he found that the groundwater table was higher during the increasing discharge than during the recession. In our hillslope, we observed an opposite behaviour respect to the one described by Myrabø (1997): in the Rio Larici dataset the hysteretic cycle between discharge and water table is anti-clockwise. Referring to plots of Figure 49, during the rising limb of the hydrograph the groundwater is deep and increases slowly; when the peak

discharge is reached, the piezometric level is still increasing and attains its maximum during the hydrograph recession. This hysteresis effect can be explained by the time lag existing between the start of precipitation and the recharge of groundwater: the delay is due to the quicker generation of runoff during or after a rainfall compared to the infiltration, storage and following flow processes of subsurface water. Thus, owing to such hysteretic non-linear behaviour of water table, the model is not able, for its intrinsic linear nature, to predict accurately the groundwater level during conspicuous water table variations.

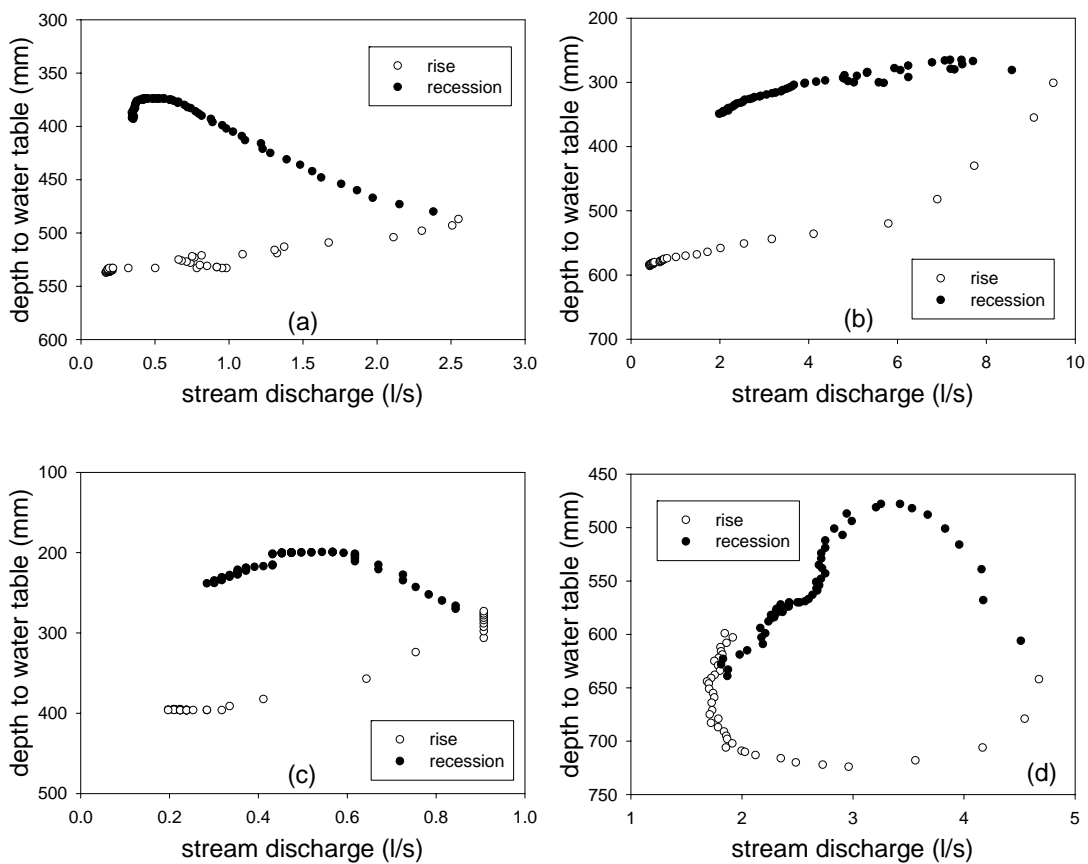


Figure 49: examples of hysteretic behaviour of relationship between water table height and stream discharge at the rainstorm scale: a) L4, storm 22-07; b) L6, storm 18-07; c) L7, storm 5-06; d) L11, storm 19-07

Water table variations and runoff response: concluding remarks

Occurrence of overland flow, stream discharge, soil moisture at 0-30 cm depth and water table variations were monitored in a small alpine subcatchment (3.3 ha) of Rio Vauz basin (1.9 km²) in the Eastern Italian Alps. Rio Larici subcatchment is formed by steep hillslopes in the upper part, a gentle plateau in the central portion where water tends to be stored even during inter-storm periods and a narrow gully where permanent watercourse exists. A binary response of presence/absence of overland flow was obtained by the installation of simple overland flow detectors: they provided information about the extension of the saturated area in the catchment and the development of the ephemeral stream network forming during or after rainfalls. Generation of overland flow was identified in mechanisms of saturation from above and in return flows of water which percolates in the upper part of the hillslope and emerges downstream following preferential flow paths. At the rainfall scale, saturated areas within the sites were positively correlated with peak discharge, the highest level of water table, antecedent soil moisture conditions and the maximum value of water content measured during or immediately after the storm. Strict relationships were also found between runoff coefficient calculated at the rainfall scale and maximum soil moisture, maximum rise of water table and active stream network. Moreover, the highest level of groundwater across the entire hillslope displayed good correlations with pre-event discharge and peak discharge and with antecedent and maximum soil moisture conditions. A positive correlation was also found between stream discharge and water content for the entire monitoring period. All these observations suggest a strong consistency between subsurface and surface runoff, which respond with similar spatial and temporal dynamics to precipitation inputs at the rainstorm scale.

Multiple correlations performed among all water level measurements for 2006 and 2007 dataset were highly significant ($p < 0.01$) across the entire catchment, independently of the topographical position of piezometers: deeper water table levels were found in the far-stream zone respect to the near-stream zone where groundwater is much closer to the surface owing to topographical convergences. However, despite this difference in water height, all piezometric wells across the site were always positively related to each other, no significant time lags were detected in the response and same runoff patterns were found across the hillslope. Thus, the distance from the creek was considered not to be

a discriminating factor in partitioning the site in near-stream and far-stream zone.

The steady state assumption for the whole hillslope was tested by applying a reformulation of Topmodel at the single rainfall scale. The linear model proved to be a fine predictor of the groundwater level with small overall errors between the simulated and measured water table levels (root mean squared errors ranged from a minimum of 4 mm to a maximum of 8 cm). Once more, a different behaviour between near- and far-stream zone was not evident although the major departures between predicted and observed values were found for heavy rainfalls and/or for particularly active piezometric wells. A temporal shift between simulated and observed peaks did not occur but often the model underestimated the maximum rise of water table, especially for significant variations. These deviations were attributed to the hysteresis effect discovered in the relationship between discharge and groundwater at the rainstorm scale: thus, owing to this non linear behaviour, a linear model was not able to predict accurately the groundwater level during important variations.

REFERENCES

- Albertson J. and Montaldo N., 2003: *Temporal dynamics of soil moisture variability: 1. Theoretical basis*. Water Resources Research 39 (10): doi: 10.1029/2002WR001616. issn: 0043-1397
- Beven K., Kirkby M., 1979. *A physically based variable contributing area model of basin hydrology*. Hydrological Sciences Bulletin, 24, 1, 43–69
- Blazkova S., Beven K., Tacheci P., Kulasova A., 2002: *Testing the distributed water table predictions of TOPMODEL (allowing for uncertainty in model calibration): The death of TOPMODEL?* Water Resources Research, 38, 11, 1257, doi:10.1029/2001WR000912, 2002
- Blonquist Jr. J.M., Jones S.B., Robinson D.A., 2005: *A time domain transmission sensor with TDR performance characteristics*. Journal of Hydrology, 314 (2005) 235-245
- Borga M., Dalla Fontana G. and Cazorzi F., 2002a: *Analysis of topographic and climatic control on rainfall-triggered shallow landsliding using a quasi-dynamic wetness index*. Journal of Hydrology, 268(1-4), 56-71
- Borga M., Dalla Fontana G., Gregoretti C. and Marchi L., 2002b: *Assessment of shallow landsliding by using a physically based model of hillslope stability*. Hydrological Processes, 16, 2833-2851
- Bronstert A. and Bárdossy A., 1999: *The role of spatial variability of soil moisture for modelling surface runoff generation at the small catchment scale*. Hydrology and Earth System Sciences, 3(4), 505-516, 1999
- Campbell Scientific, Inc., 2002-2003: *CS616 & CS625 - Water Content Reflectometers -User Guide*. Campbell Scientific, Inc.
- Chandler D.G, Seyfried M., Murdock M- and McNamara J., 2004: *Field Calibration of Water Content Reflectometers*. Soil Sci. Soc. Am. J., vol. 68.
- Choi M. and Jacobs J.M., 2007: *Soil moisture variability of root zone profiles within SMEX02 remote sensing footprints*. Advances in Water Resources. 30, 883-896
- Clow D.W., Schrott L., Webb R., Campbell D.H., Torizzo A. , Dornblaser M., 2003: *Ground water occurrence and contributions to streamflow in an alpine catchment, Colorado Front Range*. Vol. 41, No. 7 –Ground Water – Watershed Issue 2003 (pages 937–950)

- Cosh M.H., Jackson T. J., Bindlish R., Famiglietti J.S. Ryu D., 2005: *Calibration of an impedance probe for estimation of surface soil water content over large regions*. Journal of Hydrology, 311 (2005), 49-58
- Cosh M.H., Jackson T. J., Bindlish R., Prueger J.H., 2003: *Estimation of watershed scale soil moisture from point measurements during SMEX02*. First Interagency Conference on Research in the Watersheds, October 27-30, 2003, Benson, Arizona
- Cosh M.H., Stedinger J.R. and Brutsaert W., 2004: *Variability of surface soil moisture at the watershed scale*. Water Resources Research, 40, W12513
- Delta-T Devices Ltd, 2004: *User manual for the moisture meter type HH2*. Delta-T devices Ltd
- de Jong C., 2005: *The contribution of condensation to the water cycle under high-mountain conditions*. Hydrological Processes, 19 (12), 2419-2435
- Elsenbeer H., Lack A., 1996. *Hydrometric and hydrochemical evidence for fast flowpaths at La Cuenca, Western Amazonia*. Journal of Hydrology 180, 237-250
- Engstrom R., Hope A., Kwon H., Stow D. and Zamolodchikov D., 2005: *Spatial distribution of near surface soil moisture and its relationship to microtopography in the Alaskan Arctic coastal plain*. Nordic Hydrology, 36, 219-234
- Famiglietti J.S., Devereaux J.A., Laymon C.A., Tsegaye T., Houser P.R., Jackson T.J., 1999: *Ground-based investigation of soil moisture variability within remote sensing footprints during the Southern Great Plains 1997 (SGP97) Hydrology Experiment*. Water Resources Research, 35(6), 1839-51
- Fares A., Buss P., Dalton M., El-Kadi A.I., Parson L.R., 2004: *Dual field calibration of capacitance and neutron soil water sensors in a shrinking-swelling clay soil*. Vadose Zone Journal 3:1390-1399
- Gardi L., 2003: *Hydrogeology of the Cordevole catchment*. Free University of Amsterdam, Faculty of Earth and Life Sciences
- Gaskin G.J. and Miller J.D., 1996: *Measurement of soil water content using a simplified impedance measuring technique*. Journal of Agricultural Engineering Research, 63, 153-160
- Godsey S., Elsenbeer H., Stallard R., 2004: *Overland flow generation in two lithologically distinct rainforest catchments*. Journal of Hydrology 295 (2004) 276-290

- Gòmez-Plaza A., Alvarez-Rogel J., Alabaladejo J, Castillo V.M., 2000. *Spatial patterns and temporal stability of soil moisture across a range of scales in a semi-arid environment*. *Hydrological Processes*, 14, 1261–1277
- Gong Y., Cao Q., Sun Z., 2003: *The effects of soil bulk density, clay content and temperature on soil water content measurement using time domain reflectometry*. *Hydrological Processes*, 17, 3601-3614
- Grant L., Seyfried M. and McNamara J., 2004: *Spatial variation and temporal stability of soil water in a snow-dominated, mountain catchment*. *Hydrological Processes*, 18(18), 3493-3511
- Grayson R.B. and Western A.W., 1998: *Towards areal estimation of soil water content from point measurements: time and space stability*. *Journal of Hydrology*, 207 (1998) 68-82
- Grayson R.B., Western A.W., Chiew F.H.S. and Blöschl G., 1997: *Preferred states in spatial soil moisture patterns: local and non local controls*. *Water Resources Research*, 33, 12: 2897-2908, 1997
- Hansson K., Lundin L., 2006: *Water content reflectometer application to construction materials and its relation to Time Domain Reflectometry*. *Vadose Zone Journal*, 5, 459-468
- Herbrard O., Voltz M., Andrieux P., Moussa R., 2006: *Spatio-temporal distribution of soil surface moisture in a heterogeneously farmed Mediterranean catchment*, *Journal of Hydrology*., 329, 110–121, 2006
- Hupet F., Vanclooster M. 2002. *Intraseasonal dynamics of soil moisture variability within a small agricultural maize cropped field*. *Journal of Hydrology* 261, 86–101
- Jacobs J.M., Mohanty B.P., Binayak P. and Hsu E.-C. , 2004: *SMEX02: Field scale variability, time stability and similarity of soil moisture*. *Remote Sens. Environ.* 92:436–446
- Jolánkai G., Rast W., 1999: *The hydrologic cycle and factors affecting the generation, transport and transformation of nonpoint source pollutants*. In: *Assessment and control of nonpoint source pollution of aquatic ecosystems: a practical approach*. UNESCO and The Parthenon Publishing Group, USA
- Jones S.B., Wraith J.M., Or D., 2002: *Time domain reflectometry measurement principles and applications*. *Hydrological Processes* 16, 141–153
- Kachanoski R.G., de Jong E., 1988: *Scale dependence and the temporal stability of spatial patterns of soil water storage*. *Water Resources Research*, 24, 85-91

- Kaleita A.L., Heitman J.L., Logsdon D.D., 2005: *Field calibration of the Theta Probe for Des Moines Lobe soils*. Applied Engineering in Agriculture, 21 (5), 865-870
- Kelleners T. J., Soppe R. W. O., Ayars J. E., Skaggs T. H., 2004: *Calibration of capacitance probe sensors in a saline silty clay soil*. Soil Science Society American Journal, 68:770-778
- Keller AG, 2004: *DCX data logger operating instructions*
- Koster R.D., Dirmeyer P.A., Guo Z., Bonan G., Chan E., Cox P., Gordon C.T., Kanae S., Kowalczyk E., Lawrence D., Liu P., Lu C.-H., Malyshev S., McAvaney B., Mitchell K., Mocko D., Oki T., Oleson K., Pitman A., Sud Y.C., Taylor C. M., Verseghy D., Vasic R., Xue Y. and Yamada T., 2004: *Regions of strong coupling between soil moisture and precipitation*, Science, 305, 1138-1140
- Lamb R, Beven K, Myrabø S. 1997. *Discharge and water-table predictions using a generalized TOPMODEL formulation*. Hydrological Processes 11, 1145-1168
- Lane, L., Hernandez, M., Nichols M., 1997: *Processes controlling sediment yield from watersheds as functions of spatial scale*. Environmental Modelling and Software, 12, 355-369
- Lin H., 2006: *Temporal stability of soil moisture patterns and subsurface preferential flow pathways in the Shale Hills catchment*. Vadose Zone Journal, 5, February 2006
- Looney S.W. and Gullledge T.R., 1985: *Probability plotting positions and goodness of fit for the normal distribution*. The Statistician 34, 297-303
- Martinez-Fernandez J. and Ceballos A., 2003: *Temporal stability in a large-field experiment in Spain*. Soil Science Society of American Journal, 67, 1647-1656
- Martinez-Fernandez J. and Ceballos A., 2005: *Mean soil moisture estimation using temporal stability analysis*. Journal of Hydrology, 2005, 1-11
- Meyles E., Williams A., Ternan L., Dowd J., 2003: *Runoff generation in relation to soil moisture patterns in a small Dartmoor catchment, Southwest England*. Hydrological Processes, 17, 251-264.
- Miller J.D., Gaskin G.J., 1999: *ThetaProbe ML2x - Principles of operation and applications*. Delta-T devices Ltd
- Miller J.D., Gaskin G.J. and Anderson, H., 1997: *From drought to flood: catchment responses revealed using novel soil water probes*. Hydrological Processes 11, 533-541

- Myrabø S. 1997: *Temporal and spatial scale of response area and groundwater variation in till*. Hydrological Processes 11, 1861–1880
- Mohanty B. P. and Skaggs T. H., 2001: *Spatio-temporal evolution and time-stable characteristics of soil moisture within remote sensing footprints with varying soil, slope, and vegetation*. Advances in Water Resources, 24, 1051– 1067
- Molénat J., Gascuel-Oudou C., Davy P., Durand P., 2005: *How to model shallow water-table depth variations: the case of the Kervidy-Naizin catchment, France*. Hydrological Processes, 19, 901–920
- Moore R.D., Thompson J.C., 1996: *Are water table variations in a shallow forest soil consistent with the TOPMODEL concept?* Water Resources Research, 32, 3, 663-669
- Moret D., J.L. arrúe, López M.V., Gracia R., 2006: *A new TDR waveform analysis approach for soil moisture profiling using a single probe*. Journal of Hydrology, 321, 163-172
- Morgan K.T., Parson L.R., Wheaton T.A., Pitts D.J., Obreza T.A., 1999: *Field calibration of a capacitance water content probe in fine sand soils*. Soil Science Society American Journal, 63, 987-989
- Norbiato D. and Borga M., 2007: *Analysis of hysteretic behaviour of a hillslope-storage kinematic wave model for subsurface flow*. Advances in Water Resources, 31, 118-131
- Oldak A., Pachepsky Y., Jackson T.J., Rawls W.J., 2002: *Statistical properties of soil moisture images revisited*. Journal of Hydrology, 255, 12-24
- Pan F., Peters-Lidard C.D. and Sale M.J., 2003: *An analytical method for predicting surface soil moisture from rainfall observations*. Water Resources Research, 39 (11), 1314, doi:10.1029/2003WR002142
- Porporato A., Daly E., Rodríguez-Iturbe I., 2004: *Soil water balance and ecosystem response to climate change*, American Naturalist, 164 (5), 625-633
- Qiu Y., Fu B., Wang J., Chen L., 2001. *Spatial variability of soil moisture content and its relation to environmental indices in a semi-arid gully catchment of the Loess Plateau, China*. Journal of Arid Environments, 49, 723–750
- Raats P.A.C., 2001: *Developments in soil-water physics since the mid 1960s*. Geoderma, 100, 355–387
- Robinson M., Dean T.J., 1993: *Measurement of near surface soil water content using a capacitance probe*. Hydrological Processes, 7, 77-86

- Rodríguez-Iturbe I., Porporato A., 2004: *Ecohydrology of Water-controlled Ecosystems: Soil Moisture and Plant Dynamics*, Cambridge University Press, Cambridge, UK
- Roth K., Schulin R., Flührer H., Attinger W., 1990: *Calibration of Time Domain Reflectometry for water content measurement using a composite dielectric approach*. Water Resources research, 26, 2267-2273
- Ryu D.R. and Famiglietti J.S., 2005: *Characterization of footprint-scale surface soil moisture variability using Gaussian and beta distribution function during the Southern Great Plains 1997 (SGP97) Hydrology Experiment*. Water Resources Research, 41(12):W12433
- Scanlon T.M., Ruffensperger J.P., Hornberger G.M., Clapp R.B., 2000: *Shallow subsurface storm flow in a forested headwater catchment: observation and modelling using a modified TOPMODEL*. Water Resources Research, 36 (9), 2575-2586
- Seibert J, Bishop KH, Nyberg L. 1997. A test of Topmodel's ability to predict spatially distributed groundwater levels. Hydrological Processes 11: 1131-1144
- Seibert J., Bishop B., Rodhe A., McDonnell J.J., 2003: *Groundwater dynamics along a hillslope: a test of the steady state hypothesis*. Water Resources Research, 39, 1, doi:10.1029/2002WR001404
- Serrarens D., MacInture J.L., Hopmans J.W., Bassoi L.H., 2000: *Soil moisture calibration of TDR multilevel probes*. Scientia Agricola, 57, 2, 349-354
- Seyfried M.S., Murdock M.D., 2001: *Response of a new soil water sensor to variable soil, water content, and temperature*. Soil Science Society of America Journal, 65, 28-34
- Shaman J., Stieglitz M., Engel V., Koster R., Stark C., 2002: *Representation of subsurface storm flow and a more responsive water table in a TOPMODEL-based hydrology model*. Water Resources Research, 38, 8, 10.1029/2001WR000636
- Sivapalan M., 2003: *Process complexity at the hillslope scale, process simplicity at the watershed scale: is there a connection?* Hydrological Processes, 17, 1037-1041
- Sklash M.C., Farvolden R.N., 1979. *The role of groundwater in storm runoff*. Journal of Hydrology 43, 45-65
- Spectrum Technologies, Inc., 2003: *Field Scout TDR300 Soil moisture meter. Users's manual*.

- Starks J. P., Heathman G.C., Jackson T.J. and Cosh M.H., 2006: *Temporal stability of soil moisture profile*. Journal of Hydrology, 324 (2006) 400-411
- Stenger R., Barkle G. and Burgess C., 2005: *Laboratory calibrations of water content reflectometers and their in-situ verification*. Australian Journal of Soil Research 43 (5) 607-615
- Svetlitchnyi A.A., Plotnitskiy S.V., Stepovaya O.Y., 2003: *Spatial distribution of soil moisture content within catchments and its modelling on the basis of topographic data*. Journal of Hydrology, 277, 50-60
- Teuling A.J., Uijlenhoet R., Hupet F., van Loon E.E., Troch P.A., 2006: *Estimating spatial mean root-zone soil moisture from point-scale observations*. Hydrological Earth Systems Discussion, 3, 1447-1485, 2006
- Teuling A.J., Troch P.A., 2005: *Improved understanding of soil moisture variability dynamics*. Geophysical Research Letters, 32, L05404, doi:10.1029/2004GL021935
- Thompson J.C, Moore R.D., 1996. *Relations between topography and water-table depth in a shallow forest soil*. Hydrological Processes 10, 1512-1525
- Topp G.C., Davis J.L., Annan A.P., 1980: *Electromagnetic determination of soil water content: measurements in coaxial transmission lines*. Water Resources Research, 16, 574-582
- Topp G.C., Ferre P.A., 2002: *The soil solution phase*, in: Dane, J.H., Topp, G.C. (Eds.), Methods of Soil Analysis, SSSA Books Series, No. 5. Soil Science Society of America, Madison, WI, pp. 417-534
- Troch P. A., Smith J. A., Wood E. F., de Troch F. P. , 1994. *Hydrologic controls of large floods in a small basin: central Appalachian case study*. Journal of Hydrology, 156
- Tromp van Meerveld I., McDonnell J.J., 2005: *Comment to "Spatial correlation of soil moisture in small catchments and its relationship to dominant spatial hydrological processes"*, Journal of Hydrology 286:113-134. Journal of Hydrology, 303, 307-312
- Tromp van Meerveld I., McDonnell J.J., 2006: *On the interrelations between topography, soil depth, soil moisture, transpiration rates and species distribution at the hillslope scale*. Advances in Water Resources, 29 (2006) 293-310
- Tromp van Meerveld I., Peters N.E., McDonnell J.J., 2007: *Effect of bedrock permeability on subsurface stormflow and the water balance of a trenched hillslope at the Panola Mountain Research watershed, Georgia, USA*. Hydrological Processes, 21, 750-769

- Vachaud G., De Silans Passerat A., Balabanis P. and Vauclin M., 1985: *Temporal stability of spatial measured soil water probability density function*. Soil Science Society of American Journal, 49, 822-827
- Van Beusekom M., 2004: *A hydrogeological inventory of the Bacino del Cordevole, northern Italy*. Free University of Amsterdam, Faculty of Earth and Life Sciences
- Van Loon E.E., 2001: *Overland flow: interfacing models with measurements*. PhD thesis, Wageningen University
- Van Wesenbeeck I.J., Kachanoski R.G., 1988: *Spatial and temporal distribution of soil water in the tilled layer under a corn crop*. Soil Science Society of American Journal, 52, 363-368
- Vertessy R., Elsenbeer H., Bessard Y., Lack A.: *Storm runoff generation at La Cuenca*. In Grayson R., Blösch G., 2000: *Spatial pattern in catchment hydrology: observation and modelling*.
- Vogel R.M., 1986: *The probability plot correlation coefficient test for normal, lognormal, and Gumbel distributions*. Water Resources Research., 22:587-90.
- Walker J.P., Willgoose G.R. and Kalma J.D., 2004: *In situ measurement of soil moisture: a comparison of techniques*. Journal of Hydrology, 293 (2004) 85-99
- Weiler M., McDonnell J.J., Tromp-Van Meerveld I., Uchida T., 2005: *Subsurface stormflow*. In Encyclopedia of Hydrological Sciences, edited by M. Anderson, John Wiley and Sons Ltd.
- Western A.W., Duncan M.J., Olszak C., Thompson J., Anderson T., Grayson R.B., Wilson J.D., Young R., 2001: *Calibration of CS615 and TDR instruments for Marhurangi, Tarrawarra and Point Nepean soils*. In : Dowding, C.H., (Ed.), TDR 2001: The Second International Symposium and Workshop on Time Domain Reflectometry for Innovative Geotechnical Applications, Infrastructure Technology Institute at Northwestern University, Evanston, Illinois, pp. 95-108
- Western A.W. and Grayson R.B., 1998: *The Tarrawarra data set: soil moisture patterns, soil characteristics and hydrological flux measurements*. Water Resources Research, 34 (10), 2765-2768, 1998
- Western A.W. and Grayson R.B., 2000: *Soil moisture and runoff processes at Tarrawarra*. In: *Spatial patterns in catchment hydrology: observation and modelling*. Edited by Grayson R. and Blöschl G., 2000, Cambridge University Press

- Western A. W., Grayson R.B., Blöschl G., 2002: *Scaling of soil moisture: a hydrological perspective*. Annual Review of Earth and Planetary Sciences, 30, 181-206.
- Western A. W., Grayson R.B, Blöschl G., Willgoose G.R. and McMahon A., 1999: *Observed spatial organization of soil moisture and its relation to terrain indices*. Water Resources Research, 35, 3
- Western A.W., Seyfried M. S., 2005: *A calibration and temperature correction procedure for the water-content reflectometer*. Hydrological Process. 19, 3785-3793
- Western A. W., Zhou S., Grayson R.B., McMahon T.A., Blöschl G. and Wilson D.J., 2004: *Spatial correlation of soil moisture in small catchments and its relationship to dominant spatial hydrological processes*. Journal of Hydrology, 286 (2004) 113-134
- Wilson J.D., Western A.W., Grayson R.B., 2004: *Identifying and quantifying sources of variability in temporal and spatial soil moisture observations*. Water Resources Research, 40, W02507
- Wilson J. D., Western A.W., Grayson R.B., Berg A.A., Lear M.S., Rodell M., Famiglietti J.S., Wood R.A. and McMahon A.T., 2003: *Spatial distribution of soil moisture over 6 and 30 cm depth, Mahurangi river catchment, New Zealand*. Journal of Hydrology, 276 (2003) 254-274

Web references

www.campbellsci.com: CS625 water content reflectometer

www.delta-t.co.uk: Theta Probe

www.eijkelkamp.com: split tube soil sampler

www.keller-druck.ch: pressure transducer level logger

www.specmeters.com: TDR 300

www.trutrack.com: capacitance level logger

CURRICULUM VITAE

Department of Land and Agro-Forest Environments, University of Padua, Italy
Viale dell' Università 16 – Agripolis, 35020 Legnaro (PD) - Italy
ph.:+39 049 8272700 fax:+39 049 8272686
e-mail: daniele.penna@unipd.it, <http://www.tesaf.unipd.it>

Birthdate February 11th, 1975, Milano, Italy

Education

- 2008 PhD in Environmental Hydrometry, University of Padua, Italy. Thesis: *Soil moisture distribution and runoff response at the hillslope scale: experimental analysis in an alpine environment.*
- 2004 One year master degree in *Hydrogeological hazard assessment and mitigation*, University of Padua, Italy. Project work at Autonomous Province of Bolzano: *Assessment of avalanche hazard and risk in the Martello Valley (BZ – Italian Alps)*. Final evaluation: Pass with *magna cum laude*.
- 2001 B.Sc.+M.Sc. in Natural Sciences, University of Milan, Italy. Thesis: *Picea abies L. Karsten population in the Forni Valley (Stelvio National Park - northern Italy): growth forms and response to recent climate changes*. Final evaluation: 106/110
- 1994 Classical graduation, Lyceum “Omero”, Milano, Italy
- Currently enrolled to *Forest and Environmental Sciences* master degree, University of Padua, Italy

Working and teaching experience

- 2008-present Research assistant, University of Padua, Department of Land and Agro-Forest Environments
- Teaching assistant in *Torrent control and restoration*, B.Sc. Forest and Environmental Sciences, prof. G. Dalla Fontana, University of Padua (academic years 2007-2008 and 2005-2006)
- Thesis supporting supervisor for several students, University of Padua, Faculty of Agriculture, academics years 2006-2007, 2005-2006, 2004-2005.

Research interest

- Experimental hydrology at the hillslope and catchment scale in the alpine environment

- Field surveys and hydrogeological hazard assessment: debris flows and avalanches

Languages

- Italian: native
- English: fluent
- Basic knowledge of Spanish and German

Publications: journals and books

- Penna D., Borga M., Boscolo P., Dalla Fontana G., 2007: *Distribution of soil moisture over different depths in a small alpine basin*. · UNESCO Technical Documents in Hydrology, 81, 117-124
- Penna D., Norbiato D., Borga M., Dalla Fontana G., 2007: *Analisi della stabilità temporale dell'umidità del suolo in un piccolo bacino dolomitico / Temporal stability of surface soil moisture in a small alpine catchment*. In AA.VV. Ricerche ed esperienze di Sistemazioni Idraulico-Forestali (vol 27, 489-502).Nuova Editoriale Bios, Cosenza, Italy. (edited by G.Bischetti)
- Penna D., Borga M., Norbiato D., Dalla Fontana G.: *Distribution of soil moisture over different soil depths for an alpine basin: statistical analysis and assessment of temporal stability*. Journal of Hydrology (submitted)

Publications: conference proceedings and posters

- McDonnell J.J., Hopp L., Mazurkiewicz A., Penna D., Condon P., Okane M., 2007: *Assessing cover system performance: a hillslope hydrology approach*. Mine closure 2007, 16-19 October 2007, Santiago, Chile (poster session and conference proceedings, in press)
- Penna D., Norbiato D., Borga M., Dalla Fontana G., 2007: *Analisi della stabilità temporale dell'umidità del suolo in un piccolo bacino idrografico montano*. Convegno Associazione Italiana Idraulica Agraria "Ricerca ed innovazione nell'idraulica agraria e nelle sistemazioni idraulico-forestali". Milano, 27-28 March 2007 (poster session)
- Penna D., Degli Esposti S., Poscolo P., Borga M., 2006: *Analysis of soil moisture patterns in an alpine basin for various hydrological states*. European Geosciences Union, General Assembly 2006 - Vienna, Austria, 02 - 07 April 2006 (poster session)
- Folladori L., Marian S., Penna D., Saccani A., 1999: *Gli effetti sull'ambiente alpino del riscaldamento climatico posteriore alla piccola età glaciale: il segnale al limite della vegetazione arborea*. VIII convegno glaciologico italiano: "Risposta dei ghiacciai alpini ai cambiamenti climatici". 9-12 settembre 1999 (oral and poster session, conference proceedings)